Development of a Biosensor to Predict Activated Sludge Deflocculation, and the Link Between Chlorination and Potassium Efflux

Robert F. Wimmer

Thesis Submitted to the Faculty of the

Virginia Polytechnic Institute and State University

in partial fulfillment of the requirement for the degree of

MASTER OF SCIENCE

In

Environmental Engineering

Dr. Nancy G. Love, Chair

Dr. Brian J. Love

Dr. John T. Novak

December 21, 2001

Blacksburg, VA

Keywords: glutathione, potassium efflux, activated sludge, chlorine, biosensor, microfluidic, deflocculation, bulking, optode

Development of a Biosensor to Predict Activated Sludge Deflocculation, and the Link Between Chlorination and Potassium Efflux

Robert F. Wimmer

ABSTRACT

In an effort to provide wastewater treatment operators with the capability to be proactive in assessing and solving deflocculation events, this study has tested the components of a biosensor to predict deflocculation and investigated the mechanistic cause of deflocculation relating to chlorination of activated sludge cultures. In order to effectively manage upset events, it is necessary to know the source of an upset and the causative mechanism that the source initiates.

The Glutathione-gated potassium efflux (GGKE) induced activated sludge deflocculation biosensor incorporates novel microtechnology with a whole cell biological element to predict deflocculation from electrophilic sources. This sensor utilizes microfluidic channels to conduct influent wastewater across a biofilm of *Eschericia coli* K-12 and monitors the bacterial response to the influent. The bacterial response, which is efflux of K^+ ion from the cytoplasm, is monitored with a fluorescence-based sensor called an optode. The components of the system satisfy the project requirements, which include minimal expense (both operation and manufacture), on-line capability and minimal maintenance. The research conducted to date demonstrates the ability of the components of the biosensor to fulfill the design requirements. The optode K^+ detector successfully measured an increase in soluble K^+ following the exposure of *E. coli* K-12 to the electrophile N-ethyl malemide. The manufacture of the microfluidic device has been completed and the device has demonstrated the ability to conduct influent under negative pressure across an established biofilm with the optode in place. The establishment of a biofilm under expected hydrodynamic conditions has also been completed. Future research efforts will include integrating the components of the biosensor into a working prototype that will be capable monitoring the reaction of bacteria to the presence of electrophilic compounds in wastewater. Sensors of this nature will provide operators with the early warning necessary to be proactive against toxic upsets rather than reactive.

The knowledge needed to create a biosensor resides in the identification of bacterial response mechanisms that cause upset events in wastewater treatment facilities. The biosensor that has been developed relies on the discovery of the link between electrophile-induced GGKE and activated sludge deflocculation. Research has been concluded, which expands the role of GGKE and activated sludge deflocculation to include chlorine-induced GGKE. Through a series of laboratory-scale reactors, a relationship has been established between chlorine addition to control filamentous bulking, increased soluble K^+ levels and an increase in effluent suspended solids . The results demonstrate that the addition of chlorine to control filamentous bulking may elicit the GGKE mechanism, initiating activated sludge deflocculation, similar to observations of chlorination at full-scale activated sludge wastewater treatment facilities. Establishing a mechanistic cause of deflocculation related to chlorination will permit operators to apply chlorine in a manner that may avoid deflocculation, rather than reacting to deflocculation after it has occurred.

ACKNOWLEDGEMENTS

I would like to thank the National Science Foundation, Grant BES 00-86883, for the financial support to conduct this research.

I wish to thank the members of my advisory committee, Dr. John T. Novak and Dr Brian J. Love for their guidance and assistance throughout my research.

I would like to extend a special thanks to my advisor Dr. Nancy G. Love, without whom I would not have returned to Virginia Tech to continue my education. Dr. Love's dedication to her students and unending desire to see her students grow, both academically and professtionally, has been a source of inspiration and support throughout my studies.

I would like to thank our Laboratory Manager, Julie Petruska, Analytical Chemist, Jody Smiley and Biochemistry Professor and fluorescence microscope expert Dr. Brian Storrie for all of their assistance and guidance in the Laboratory. I would also like to extend my thanks to the National Institute of Standards and Technology (NIST), in particular Dr. Laurie Locasio and Dr. Emmanuel Waddell, for their assistance and hospitality during the research I conducted in Gaithersburg MD. I would also like to acknowledge the work of Felicia Glapion, the undergraduate research assistant who helped me with this work.

Finally, I would like to thank my parents and family for all of their support throughout this process and most importantly my wife and best friend, Lynn, for her support, patience and occasional kick in the rear when necessary throughout these long, challenging years.

Table of Contents

LIST OF FIGURES

List of Tables

Introduction

The current state of design, instrumentation and knowledge of wastewater treatment facilities force operators to be reactive, rather than proactive when challenged with an upset event. This limitation results in decreased efficiency in the treatment process, potential permit violations and an increased workload for operators. In an effort to provide operators with the ability to be proactive when encountering an upset event, the mechanistic knowledge base and the incorporation of this knowledge into advanced instrumentation must be expanded.

Love and Bott (Love, N.G. and Bott C.B. (2000)) reviewed the current state of Upset Early Warning Devices (UEWDs) and found that the majority of the systems available are based on respirometry or the Microtox® toxicity system. These systems will both effectively indicate that an upset event is probable but neither system defines either the **source** or the **cause** of the upset. The differentiation between **source** and **cause** is essential in order to initiate the appropriate preventive or mitigating action. The compound or group of compounds that are responsible for an upset are the **source** of the upset. The **cause** is the mechanism, either the chemical reaction exhibited by the source or the biological and/or biochemical response of bacteria to the source. (Bott C.B. and Love N.G. (Submitted-a))

With the knowledge of the **mechanistic cause** of an impending upset, an operator may take appropriate actions to prevent the upset from adversely affecting the operation of the facility. Bott and Love (submitted a) recently elucidated the mechanistic **cause** of certain deflocculation events. Electrophilic xenobiotic compounds react with bacteria through the glutathione-gated potassium efflux (GGKE) bacterial self defense mechanism, which results in an efflux of K^+ from the bacterial cytoplasm . Bott and Love (submitted a) hypothesized that if GGKE is activated in bacteria residing within activated sludge flocs, then there is a localized increase in K^+ within the floc, which results in a weakening of the floc particle and eventual deflocculation. They subsequently showed that the increase in K^+ in the bulk phase is due to diffusion of K^+ from within the floc, and bulk phase K^+ concentrations are significantly less than concentrations experienced inside the floc (Bott, C.B. and Love, N.G. (Submitted-b)). This newly acquired

knowledge may be incorporated in to a UEWD that will provide an operator with knowledge of both the class of the source compound and the mechanism through which an upset will occur.

Microtechnology

The ability to manufacture devices for a wide variety of application on the micron scale is continually advancing. Many applications of biotechnology are being miniaturized, including PCR, protein separation and blood analysis. The shrinking of the technology reduces the cost associated with analyzing for certain compounds and allows the analysis to take place on site without the need for large and expensive analytical instruments. Many of these devices are based on microfluidic technology, the movement of fluids though micron sized channels. These channels have typically been manufactured in glass and silicon, but more recently a variety of plastic polymers have been used, which are very inexpensive. Numerous methods exist for the fabrication of microscopic channels in plastic, including imprinting (Martynova, L. et al. (1997),Xu, J. et al. (2000)), molding (Duffy, D.C. et al. (1998), Effenhauser, C.S. et al. (1997)) and laser ablation (Roberts, M.A. et al. (1997)).

Biosensors

The utilization of biological elements in sensors to monitor environmental conditions may provide a more powerful and environmentally relevant measurement of environmental conditions. The Microtox® toxicity monitoring systems (Azur Environmental, Inc.) employ a biological element to predict the toxicity of compounds or environmental samples. Attempts have been made to correlate results from Microtox® assays with actual toxicity in receiving waters or other aquatic environments, including activated sludge cultures (Love and Bott 2000). The incorporation of a biological element into environmental sensors makes them more environmentally relevant than classical analytical measurements of contaminants, which do not factor in the interaction of the biological components of the aquatic system with the potential contaminant. Other biological sensors have been developed utilizing the luciferase (*lux*-gene) system of bacteria (Turner, N.L. et al. (2001);Kelly, C.J. et al. (1999)), whereby the bacteria luminescence as metabolism occurs and the intensity of the luminescence decreases as the bacteria are adversely impacted.

The existing biosensors utilized at wastewater treatment facilities (Microtox®, on-line respirometry) may be effective at predicting an **effect** (e.g., loss in respiration potential) during a wastewater treatment upset, but are lacking in the ability to link the **effect** to the **source** or to the **causative mechanism** of the upset event. The development of a biosensor capable of identifying the source and the causative mechanism of an impeding upset will provide operators with the ability to be proactive, rather than reactive in the manner in which they manage the facility.

Chlorine and deflocculation

Chlorine is used to control filamentous bulking in activated sludge wastewater facilities, but it has been observed that deflocculation often follows the extended addition of chlorine (Campbell, H.J. et al. (1985), 1985, Hwang, Y.W. and Tanaka T. (1998), Jenkins et al.(1993)). The **effect** of chlorine addition, deflocculation, is known but the **mechanistic cause** of chlorine induced activated sludge deflocculation is only a matter of speculation.

Hwang et al. (1998) and Jenkins et al. (1993) suggest that the continual addition of chlorine to control filamentous bulking eventually results in the destruction of floc forming bacteria, which promotes deflocculation. Their explanation for chlorine-induced deflocculation is based on microscopic observation of the wastewater, but their hypothesis was not specifically tested. Campbell et al. (1985) also observed activated sludge deflocculation following chlorine addition and suggested that an "overdose" of chlorine was employed. However, they noted that specific oxygen uptake rates did not decrease and that rotifers were still active, both suggesting a healthy microbiological population. This set of observations counters the hypothesis that chlorine addition results in the death of floc forming bacteria and that another **mechanism** may be responsible for the deflocculation that is observed.

Research Hypothesis

GGKE Biosensor

This research will investigate the feasibility of constructing a micro scale biosensor to predict activated sludge deflocculation caused by glutathione gated potassium efflux (GGKE). We suggest that a stable, pure culture bacterial biofilm will efflux potassium when exposed to sub-

lethal concentrations of an electrophilic compound and that this increase in K^+ concentration may be detected with a modification of an existing fluorescent K^+ optode sensor. With the knowledge of the effect of a compound, it will be possible to predict an activated sludge deflocculation event and allow wastewater operators to be proactive in preventing the deflocculation event or mitigating the effects of a deflocculation event.

Chlorine-Induced GGKE

Chlorine possesses the chemical structure and capability to act as an electrophilic compound. It is suggested that the deflocculation observed with chlorine addition for filamentous bulking control is linked to the GGKE activated sludge deflocculation hypothesis. Specifically, we suggest that chlorine acts as an electrophilic compound and activates the GGKE bacterial self defense mechanism, resulting in a localized intrafloc increase in K^+ that weakens sludge flocs and results in deflocculation.

Experimental Objectives

The overall objectives of this research are as follows:

- Study and optimize the components of a prototype biosensor to predict activated sludge deflocculation, utilizing a pure culture bacterial biofilm, microfluidic devices and fluorescent K^+ detection.
- Investigate the relationship between chlorine addition to control filamentous bulking, soluble K^+ concentration and effluent quality to determine if chlorine addition elicits the GGKE bacterial self defense mechanism and initiates activated sludge deflocculation.

The specific results and methods utilized to address these objectives are presented in the chapters of this thesis.

References

Bott C.B. and Love N.G. (Submitted-a) A physiological mechanism for activated sludge deflocculation caused by shock loads of toxic electrophilic chemicals. *Water Environment Research*.

Bott, C.B. and Love, N.G. (Submitted-b) Implicating the glutathione-gated potassium efflux system as a cause of activated sludge deflocculation in response to shock loads of toxic electrophilic chemicals. *Applied and Environmental Research*.

Campbell, H.J., Troe, D., Gray, R., Jenkins, D., and Kirby, C.W. (1985) In-Basin Chlorination for Control of Activated Sludge Bulking in Industrial Waste Treatment Plants. *Procedings of the 40th Industrial Waste Conference* 759-773.

Duffy, D.C., McDonald J.C., Schueller, O.J.A., and Whitesides, G.M. (1998) Rapid prototyping of microfluidic systems in poly(dimethylsiloxane). *Analytical Chemistry* **70** 4974-4984.

Effenhauser, C.S., Bruin, G.J.M., Paulus, A., and Ehrat, M. (1997) Integrated capillary electrophoresis on flexible silicone microdevices: analysis of DNE restriction fragments and detection of single DNA molecules on microchips. *Analytical Chemistry* **69** 3451-3457.

Hwang, Y.W. and Tanaka T. (1998) Control of *Microthrix parvicella* foaming in activated sludge. *Water Research* **5** 1678-1686.

Jenkins, D., Richarad, M.G., and Daigger, G.T. (1993) *Manual on the Causes and Control of Activated Sludge Bulking and Foaming, 2nd Edition*. Lewis Publishers, Inc., Chelsea, Michigan.

Kelly, C.J., Lajoie, C.A., Layton A.C., and Sayler G.S. (1999) Bioluminescent Reporter Bacterium for Toxicity Monitoring in Biological Wastewater Treatment Systems. *Water Environment Research* **71** (131-35).

Love, N. G. and Bott C.B. A Review and Needs Survey of Upset Early Morning Devices. Love. N.G. and Bott C.B. A Review and Needs Survey of Upset Early Morning Devices. 2000. Alexandria, VA, Water Environment Research Foundation.

Martynova, L., Locasio, L.E., Gaitan, M., Kramer, G., Christensen, R.G., and MacCrehan, W.A. (1997) Fabrication of plastic microfluid channels by imprinting methods. *Analytical Chemistry* **69** 4783-4789.

Roberts, M.A., Rossier, J.S., Bercier, P., and Girault (1997) UV laser machined polymer substrates for the development of microdiagnostic systems. *Analytical Chemistry* **69** 2035-2042.

Turner, N.L., Horsburgh, A., Paton, G.I., Killham, K., Meharg, A., Primrose, S., and Strachan, J.C. (2001) A Novel Toxicity Fingerprinting Method for Pollutant Identification with *lux*-Marked Biosensors. *Environmental Toxicology and Chemistry* **20** (11), 2456-2461.

Xu, J., Locasio, L.E., and Lee, C.S. (2000) Room temperature imprinting method for plastic microchannel fabrication. *Analytical Chemistry* **72** 1930-1933.

Chapter 1

Literature Review

During upset conditions at wastewater treatment facilities (e.g. poor BOD/COD removal, reduced nitrification, deflocculation), the ingenuity and quick responses of operators determine the extent to which an upset will affect the efficiency of the wastewater treatment process. The reactive nature of handling upset events at wastewater treatment facilities is due in part to the lack of knowledge regarding the source and the causative mechanisms of upset conditions. The source of an upset may include xenobiotic compounds, elevated concentrations of biotic compounds (NH_3, BOD, solids), mechanical or facility failure (Love, N.G. and Bott C.B. (2000)). The causative mechanism is the chemical, biological, or biochemical response that the system exerts in response to the source of the upset. The causative mechanism is not necessarily an observed upset event, but rather the underlying reason for that observation.

Activated Sludge Upset Events

Upset events in activated sludge wastewater treatment facilities may include; decreased or inhibited BOD/COD removal, foaming, poor settling, increased chlorine demand and bulking (Berthouex, P.M. and Fan Richard (1986)). Berthouex and Fan found these events may be caused by equipment or facility failure, wet weather events, toxic or inhibitory inputs to the facility and human error. In a survey of wastewater treatment plant operators and designers, Love and Bott (2000) found the majority of upset events resulted in decreased BOD/COD removal, ineffective nitrification, deflocculation and non-filamentous bulking. Kelly et al.Kelly, C.J. et al. (1999) discusses the transient nature of many activated sludge upset events. Due to this transient nature the **cause** and **source** of the upset is often never determined and therefore the ability to prevent or mitigate the effects of a future upset is limited by the lack of knowledge.

Glutathione-Gated Potassium Efflux and Activated Sludge Deflocculation

Bott and Love Bott C.B. and Love N.G. (Submitted-a) proposed a **causative mechanism** for activated sludge deflocculation relating to electrophilic compounds (**source**). The glutathione-gated potassium efflux (GGKE) activated sludge deflocculation hypothesis accounts for certain upset events that occur at activated sludge wastewater treatment facilities. The GGKE mechanism (described in depth in the following section) is a bacterial self defense mechanism, which results in the efflux of potassium from a bacterium. In an activated sludge floc, it is believed that this mechanism results in a localized intrafloc increase in potassium (Bott, C.B. and Love, N.G. (Submitted-b)). Novak, Higgins and coworkers Higgins, M.J. and Novak, J.T. (1997b), Higgins, M.J. and Novak, J.T. (1997a)a, Novak, J.T. et al. (1998)) have demonstrated that the ratio of monovalent cations (K^+, NH_3^+, Na^+ and others) to divalent cations (Fe^{2+}, Mg^{2+}, Ca^{2+}) is integral to predicting the strength and stability of floc particles. When the ratio of monovalent to divalent cations increases (e.g. a localized increase in K^+), floc strength decreases, resulting in floc shear and formation of pin floc. Pin floc exhibits poor settling efficiency in secondary clarifies and results in increased effluent suspended solids, a higher effluent chlorine demand for disinfection and, if employed, increased backwash demand on sand filters (Bott, C.B. (2001)).

Bott and Love (submitted a) demonstrated that exposure of activated sludge to certain **source** electrophilic compounds (N-ethyl malemide (NEM), 2,4-chlorodinitrobenzene (CDNB)) resulted in the movement of K^+ from the bacterial cytoplasm to the bulk phase. In experiments utilizing sequencing batch reactors (SBRs), the increase in bulk phase K^+ was followed by an increase in effluent volatile suspended solids (VSS) at the end of the SBR cycle. This work supports the hypothesis that GGKE is the **cause** of deflocculation.

Glutathione-Gated Potassium Efflux

The **cause** of upset events is often the reaction of bacteria to a toxicant (**source**). These reactions are often bacterial self defense mechanisms, which include but are not limited to alteration of the phospholipid bi-layer, preventing deleterious compounds from entering the cytoplasm (Bearden, A.P. et al. (1999))), The GGKE defense mechanism protects bacteria from electrophilic compounds by utilizing reduced glutathione (GSH), the predominant cytoplasmic low molecular

weight thiol compound, to reduce potential oxidative toxins, thereby minimizing their deleterious effects.

Glutathione has been detected in all Gram-negative bacteria tested to date, but GSH is not present in the majority of Gram-positive bacteria (Booth, I.R. et al. (1993)). Ness et al. (Ness, L.S. et al. (1997) have demonstrated that the GGKE system evolved as a method of protecting against methylglyoxal, an electrophilic, potentially toxic by-product of metabolism. Methylglyoxal forms when a bacterium in an electron donor deficient state is exposed suddenly to abundant carbon and the glucose oxidation pathways become overwhelmed (Kalapos, M.P. (1999)). The natural need for an eletrophile protection system has allowed bacteria to adapt to survive exposure to man-made electrophiles, such as NEM and CDNB.

The basis of the GGKE system resides in the ability of bacteria to exert fine control over intracellular K^+ levels. McLaggan et al. (McLaggan, D. et al. (1994) explains that K^+ is the primary cation involved in maintaining osmotic or turgor pressure in the bacteria. The ability of bacteria to adapt to osmotic changes in the environment resides in the ability of bacteria to control intracellular K^+. One method of bacterial control of K^+ is through the Kef B and Kef C K^+/proton antiport channels.

Bakker et al. (Bakker, E.P. et al. (1987) investigated the mechanisms of K^+ efflux from bacteria by studying the events that promote the Kef B and Kef C K^+ transport systems. An important finding of this work is the separation of K^+ transport systems that function in response to alkalinization of the cytoplasm and transport systems responsible for turgor pressure regulation from those that are involved in GGKE. Using mutant bacteria, which did not posses the Kef B and Kef C systems, Bakker demonstrated that these bacteria could still alter potassium levels without the presence of the transport systems in response to alkalinization and turgor pressure shifts, but were not capable of GGKE. Meury et al. (Meury, J. and Kepes, A. (1982) demonstrated that cells deficient in reduced glutathione are unable to maintain cytoplasmic K^+ levels, implying that these compounds act to prevent the Kef B and Kef C K^+/proton antiport channels from opening.

The opening of the Kef B or Kef C channel leads to the efflux of K^+ from the cytoplasm and the subsequent acidification of the cytoplasm by the import of a proton to maintain charge stability. The slight acidification of the cytoplasm (<0.5 pH units) initiates the DNA protective system, which seeks to further protect the DNA from electrophile-induced damage (Ferguson, G.P. et al. (1995)). Bengoechea et al. (Bengoechea, J.A. and Skurnik, M. (2000) found that DNA protection is also induced through K^+ efflux and the subsequent acidification of the cytoplasm in response to cationic antimicrobial peptides. An interesting finding of Ferguson et al. (Ferguson, G.P. et al. (1998) was the effect of bacterial growth state on survivability following an attack by electrophilic compounds. This work demonstrated that stationary-phase bacteria are more resistant than exponential phase cells when faced with electrophilic attack.

Mannervik et al. (Mannervik, B. and Danielson, U.H. (1988) reviewed the structure and activity of glutathione transferases, which facilitate the reaction of electrophiles and glutathione. The review describes the activity of glutathione reductase, the enzyme necessary for the reduction of glutathione following an electrophile attack. Glutathione reductase facilitates the reaction of glutathione disulfide (GSSG), the oxidized form of glutathione, with NADPH and a proton to form two reduced GSH molecules and a $NADP^+$. The requirement for NADPH is critical, in that bacteria must be actively respiring to replenish the NADPH pool in order to ensure the presence of GSH to provide control over the KefB and KefC K^+ efflux channels. Vuilleumier (Vuilleumier, S. (1997) expanded upon the review of Mannervik and introduced evidence for the conservation of GSH and glutathione transferases through bacterial evolution. The conservation of these enzymes and compounds throughout Gram negative bacteria indicates the importance of these pathways to the function and viability of bacteria.

Wastewater Treatment Biosensors

GGKE is hypothesized to be a **mechanistic cause** of deflocculation at wastewater treatment facilities (Bott and Love, submitted a). The ability to translate the knowledge of a **mechanistic cause** into the operator's capability to be proactive resides in the development of advanced biosensors. These biosensors must overcome the limitations of chemical analysis of wastewater, including; expense, time and the uncertain interaction of a potential toxicant with the activated sludge (Kelly, C.J. et al. (1999)).

There are a number of upset early warning devices (UEWDs) currently in use or in the research and development stage. Love and Bott (2000) surveyed the existing devices to determine the strengths and weaknesses of the current technology. The survey included devices such as; on-line respirometry, Microtox®, whole cell sensors and bacterial BOD probes, among other devices. While many of these devices were capable of providing some warning of impending upset to the operator of a facility, the devices were unable to determine the causative agent or the **source** of the upset. Without the ability to determine the causative agent, the operator is left without the necessary knowledge to prevent or mitigate the effect of this causative agent. If the causative agent is identified, a facility has a variety of options available. For example, the influent may be diverted to storage to be bled into the system over time, or appropriate coagulants or polymers may be added to bind the toxicant, making it less bioavailable and, therefore, less of a threat to the operation of the facility.

Several novel biosensors currently in development seek to provide information that is more useful to the operator. A new use of the *lux* (luciferase genes) gene cassette by Kelly et al. (1999) seeks to predict activated sludge deflocculation caused by toxic influents. These researchers isolated bacteria from the mixed liquor and then inserted the *lux* gene into an isolate, creating a genetically engineered microorganism (GEM). This method seeks to use indigenous bacteria to act as the biological element of the biosensor so that typical influent flows that might affect non-indigenous *lux* modified bacteria but not indigenous bacteria will not activate the biosensor. The GEMs are exposed to influent and bioluminescence is measured as an indicator of viability and health. As the bacteria are exposed to toxic influents, the bioluminescence decreases. In a batch test, this technique correlated the decrease in intensity of bioluminescence with a decrease in activated sludge oxygen uptake rate. These researchers also developed a continuous monitoring system, which demonstrated a rapid decrease in signal upon exposure to hydroquinone.

Another new *lux* gene-based biosensor utilizes the bioluminescence intensity of *E. coli* HB101pUCD607 in response to a test compound over time (Turner, N.L. et al. (2001)). The *lux* gene is incorporated into a general function gene and decreases in luminescence as the bacteria is

adversely affected by toxicants. The profile is then incorporated into a computer algorithm, allowing identification of the compound upon future exposure. This very novel work may allow operators to determine what the causative agent is and then take appropriate action. This new biosensor also seeks to differentiate between bioavailable and total toxicant load, since it is only the bioavailable fraction that will impact an activated sludge system, and only the bioavailable fraction will interact with the *lux*–encoded bacteria.

A novel biosensor is discussed in Chapter 2 that is designed to provide operators with the ability to be proactive when challenged with shock event that activate the GGKE system in activated sludge cultures. The components of the biosensor include a microfluidic device, a pure culture bacterial biofilm and a fluorescent K^+ sensor. Each component possesses characteristics that offered challenges when they were integrated into a single functional sensor, yet each has great potential. The components of microfluidic biosensors are reviewed next.

Microfluidic Devices

Microtechnology is a burgeoning field of research and development, one aspect of which is the construction of numerous microfluidic devices that incorporate extremely small channels (< than 40μm) in width. It is also possible to construct pumps, diverters, loops and other standard fluid control devices on the micro scale (Wilding, P. et al. (1994)). The majority of the early devices were constructed in pieces of ceramic; they functioned very well but were very expensive to construct due to the cost of ceramic. Microfluidics may also be constructed in a variety of plastics and have been created through imprinting processes (Xu, J. et al. (2000),Martynova, L. et al. (1997)) and by researchers at the National Institute of Standards and Technology (NIST) through the use of laser ablation, which produces devices that are easy to manufacture and inexpensive to produce. Ongoing research has also investigated methods of pumping fluids through microfluidic devices through use of electrical potential differences, gravity flow and negative pressure. Others have also investigated methods of determining flow rate and mixing conditions inside of microchannels (Ross, D. et al. (2001)). The ability to provide laminar flow in laser ablated microchannels has been investigated by Waddell et al. (Waddell. E. et al. (Submitted), who determined that the type of plastic, the material (different gases or liquids)

through which the laser passes during ablation and post-ablation treatment (sonication, alcohol rinsing) all affect the surface conditions of a micro channel.

Potassium Measurement Devices

Potassium may be measured through a number of well-established analytical processes. Standard Methods (1998) suggest the use of atomic absorption spectrometry, inductively coupled plasma emission spectrometry or ion chromatography for measurement of K^+. These methods are well documented and standardized but require expensive equipment, analytical laboratory space and are time and labor intensive. Ion selective electrodes are manufactured by numerous companies (e.g., Fisher and Orion) and allow on-line measurements of K^+, but these probes are large in comparison to microfluidic devices. Additionally, experience in our laboratory indicates that K^+-selective ion selective electrodes are not sufficiently robust to function continuously in mixed liquor or under field conditions.

Shortreed et al. (Shortreed, M.R. et al. (1997) investigated the use of fluorescent materials, compiled into an optode, for the measurement of soluble K^+. This method employs competitive cation exchange between a chromoionophore, which fluoresces inversely to the degree of protonation, and an ionophore, which selectively competes for K^+ ions. These compounds are combined with lipophilic additives, which provide a net negative charge to force the chromoionophore and ionophore to maintain charge neutrality within the poly(vinyl chloride) (PVC) film in which the components reside. Shortreed has demonstrated the ability of this optode film to accurately determine the soluble K^+ concentration within the ranges observed in human blood and cytosolic levels.

Bacterial Attachment and Biofilm Formation

The steps and factors, which influence bacterial attachment, have been investigated by many researchers. Busscher et al. (Busscher, H.J. et al. (1990) proposed a series of steps that bacteria undergo as a biofilm forms. Bacteria are transported to a surface through gravity, diffusion or convection. As a bacterium approaches a surface, a series of forces interact with the cell, beginning with van-der Waals forces. As the bacterium continues to approach, electrostatic repulsive forces will interact with the cell. Bussher et al. (1990) suggest that localized positive charges on bacteria will interact with a negatively charged surface to mediate attachment. A

layer of interfacial water exists, which provides a barrier between the bacterium and the surface. Busscher et al. (1990) suggest that hydrophobic groups on the bacterial surface disperse the water molecules, allowing attachment to proceed.

Absolom et al. (Absolom, D.R. et al. (1983) has proposed a thermodynamic approach to predict bacterial attachment and biofilm formation. The approach suggests that at equilibrium, the free energy at a surface will be minimized; therefore, if a bacterial surface and attachment surface both reduce the free energy at a surface, attachment will be favored. However, in a review of research on biofilm attachment, Morra and Cassinelli (Morra, M. and Cassinelli, C. (1997) found that the thermodynamic theory (surface free energy) of bacterial attachment had numerous inconsistencies and that the method of bacterial attachment still has more unknowns than knowns.

van Loosdrecht et al. (van Loosdrecht, M.C.M. et al. (1987a) investigated bacterial hydrophobicity and the influence of the bacterial cell surface to attachment of polystyrene. This work found that bacterial hydrophobicity increased in association with bacterial attachment, a finding supported by Cunliffe et al. (Cunliffe, D. et al. (1999). van Loosdrecht et al. (van Loosdrecht, M.C.M. et al. (1987b) also found that the hydrophobicity of the bacteria increased as the growth rate of the bacteria increased, suggesting that bacterial growth state will have an effect on bacterial attachment. Cowell et al. Cowell, B.A. et al. (1999) found that nutrient limitations affected the hydrophobicity of the bacterial surface. As the ratio of carbon to nitrogen was increased, *Pseudomonas aeruginosa* cell surface hydrophobicity increased, as did bacterial attachment to a contact lens, the surface under investigation.

The substratum surface hydrophobicity will also affect attachment, as demonstrated by Cunliffe et al. (1999) who demonstrated that a hydrophilic surface yielded less bacterial attachment. The substratum may be altered in order to prevent bacterial attachment as Onyiriuka et al. Onyiriuka, E.C. et al. (1991) have investigated by treatmenting polystyrene with an oxygen plasma surface modification, which results in creation of a hydrophilic surface. Interestingly, Onyiriuka et al. (1991) also found that rinsing with water removed the oxidized species from the polystyrene surface, decreasing the hydrophilicity of the surface.

There are numerous methods for determining the surface characteristics of a bacterium. van Loosdrecht et al. (1987a) studied the surface conditions using contact angle measurements. Tylewska et al. (Tylewska, S. et al. (1988) used hydrophilic and hydrophobic resin beads to determine the surface properties of bacteria while investigating the attachment of *P. aeruginosa* to glass and plastic. The zeta potential method has also been employed by van Loosdrecht (1987b), while investigating bacterial attachment. The bacterial attachment to hydrocarbon (BATH) assay is a modification of the octanol-water partitioning coefficient protocol and has been reviewed by van der Mei et al. (van der Mei, H.C. et al. (1991).

Pembrey et al. (Pembrey, R.S. et al. (1999) investigated the effects of bacterial preparation on the validity of many of the bacterial surface measurement techniques that are currently employed. This work found that air-drying or freeze-drying, produced cells that were no longer viable and had modified surface properties. Centrifugation greatly modified cell surface properties, especially those determined by zeta potential. The suspension of bacteria in hydrocarbon for the BATH test significantly changed the cell surface properties of the bacteria studied. The investigation also found that resuspension of bacteria in solutions of different conductivity than the original growth medium greatly affected the cell surface properties. The observation is also supported by Fletcher Fletcher, M. (1990), who reviewed many of the surface characteristic assays and found that every method has its limitations and is subject to potential distortions. Fletcher (1990) found that the most reliable method for measuring bacterial attachment was direct measurement to a surface, and proposed a measurement device. This device consists of small glass bottle with an influent and effluent glass tube fitted into the cap of the glass bottle. The test surface resides at the bottom of the glass bottle and the bottle is filled with the test medium. At the end of the attachment period, the test medium is flushed out and the surface is analyzed.

Picioreanu et al. (Picioreanu, C. et al. (2001)) conducted an investigation of the effect of hydrodynamic conditions on biofilm formation. Their study demonstrated that biofilms that form under steady state flow conditions exhibit less biomass sloughing and more stable biofilms. The work also found that increased bacterial growth rates promote abrupt biomass loss.

Rijnaarts et al. (Rijnaarts, H.H.M. et al. (1993) found that the attachment of bacteria to Teflon and glass surfaces is much greater during flowing conditions rather than static batch systems. This study suggests that bacterial transport to the surface is greatly affected by convection, and diffusion interactions are minimal.

Activated Sludge Bulking and Foaming

The development of a biosensor to predict activated sludge deflocculation is built on the mechanistic knowledge developed by Bott and Love (submitted a). It is necessary to continue to investigate the mechanisms that may be the cause of activated sludge upset events, so that operators are provided with the tools to be proactive when dealing with potential upset conditions. The link between activated sludge deflocculation and chlorination to control filamentous bulking is present, but the mechanism to explain the link has not been investigated to date.

Jenkins et al. (1993) have investigated and reviewed incidences of bulking and foaming in activated sludge. They have found that overgrowth of filamentous bacteria cause the majority of activated sludge bulking events. These filamentous bacteria become overabundant due to shifts in the operation or activity of an activated sludge wastewater treatment facility. Examples of these shifts include: changes in dissolved oxygen concentrations, changes in F:M ratios, or presence of sulfur-based compounds in the influent. When filaments become overabundant, they produce a bulking sludge, which prevents floc particles from settling and compacting in secondary clarifiers. Jenkins et al. (1993) have described the potential effects of bulking sludge, which include solids loss from secondary clarifiers and a reduced ability to control sludge age due to a decrease in sludge storage volume in secondary clarifiers. They have also reviewed numerous case studies describing the operating conditions and bacterial consortia that occur during activated sludge bulking.

Activated sludge foaming may occur due to an overgrowth of hydrophobic filamentous bacteria or the presence of surfactants in the influent. In severe cases of foaming, stable foam may persist

and flow over the sides of the aeration tank, or degrade effluent characteristics as the foam carries over to the secondary clarifiers.

Control of Foaming and Bulking

Jenkins et al. (1993) have presented several methods of controlling activated sludge bulking. These include: installation of selector zones to influence the composition of the bacterial population and prevent the overgrowth of filaments; modification of operating conditions to minimize proliferation of filamentous bacteria; and addition of chemicals to selectively kill filamentous bacteria. These processes have been broadly studied (e.g.,Hwang, Y.W. and Tanaka T. (1998);Campbell, H.J. et al. (1985)).

Jenkins et al. (1993) recommends application rates and points for the addition of hydrogen peroxide or chlorine, either as HOCl, chlorine gas or chlorine dioxide. Many case studies are presented where disinfection successfully killed filaments and improved both sludge volume index measurements and plant operation. Hwang & Tanaka (1998) investigated the use of bactericidal cationic polymers, HOCl and cationic polymers to control foaming. The investigation found that the cationic polymers with bactericidal action were very effective at selectively killing the filamentous bacteria and promoting improved settling with the polymer.

Ramirez et al. (Ramirez, G.W. et al. (2000) investigated how chlorination of activated sludge controlled filamentous growthusing the BacLight® bacterial stain from Molecular Probes®. The study showed that chlorine was effective at selectively killing filamentous bacteria and improving SVI measurements. The research also demonstrated a method of monitoring activated sludge bacterial viability with the BacLight® stain and fluorescent microscopy.

Hwang & Tanaka (1998) and Jenkins et al. (1993) noted that increasing concentrations of and prolonged doses of chlorine in activated sludge systems eventually led to a decrease in floc strength and stability, which led to deflocculation. These deflocculation events resulted in an increase in both effluent solids and effluent chlorine demand. Both research groups suggested that deflocculation occurs because over-chlorination leads to the death of floc forming bacteria along with the filamentous bacteria; however, neither group investigated this hypothesis further.

The study presented in this thesis suggests that bacterial stress response mechanisms may be at least partly responsible for deflocculation events observed with prolonged or overdosed chlorination.

Chlorine and Bacterial Self-Defense Systems

The observation that deflocculation occurs following chlorine addition indicates that a bacterial process or mechanism is occurring which is the **cause** of the deflocculation. In order to elucidate the mechanism, the properties of chlorine must be investigated. Chlorine is probably the most widely used disinfectant worldwide (Dukan, S. et al. (1999)), but the mechanism of bactericidal action and the existence of bacterial defense mechanisms are still under investigation. McDonnell et al. (Mcdonnell and Russell (1999) reviewed many disinfectants and their properties and suggested that chlorine exhibits bactericidal control by targeting DNA synthesis. This would suggest that chlorine is bacteriostatic, which means it prevents further bacterial growth, as opposed to bactericidal, which means it is lethal to active bacteria. Pietersen et al. (Pietersen, B. et al. (1996) studied the response of *E. coli* to HOCl and concluded that HOCl is bacteriostatic after observing the recovery of bacteria exposed to HOCl following a lag period.

A bacteriostatic compound will affect the ability of a bacterium to divide or to effectively respire. Barrette et al. (Barrette Jr., W.C. et al. (1989) investigated the effect of HOCl on bacterial ATP production and demonstrated that *E. coli* exposed to HOCl had a reduced ability to produce ATP due to a disruption in the adenylate system and a net reduction in the adenylate energy charge. The inability of bacteria to maintain effective respiration following HOCl attack may negatively impact its ability to reduce GSSG to GSH following exposure to oxidants, which impacts the cell's ability to protect itself from subsequent oxidative attack. Barrette and coworkers suggest that sulfhydryl groups may be the targets of HOCl attack, which includes glutathione. Venkobachar et al. (Venkobachar, C. et al. (1977) suggested that HOCl acts as an uncoupler of the electron transport chain, which is consistent with the work of Barrette et al. (1989).

Daly et al. (Daly, B. et al. (1998) investigated the effect of HOCl on an established biofilm, and showed that the rate at which cells sloughed decreased from steady state values following

exposure of the biofilm to HOCl. After HOCl was removed from the influent, and after a lag period, the rate of cell sloughing returned to steady state values. This result further supports the notion that HOCl is bacteriostatic and not always bactericidal, suggesting that bacteria have a means of protecting themselves from the popular oxidant. Sommer et al. (Sommer, P. et al. (1999) found that the age of the biofilm affected the ability of the biofilm to withstand HOCl attack. As the biofilm aged, the biofilm was more resistant to HOCl and this resistance was found to be independent of the biofilm structure.

It should be noted that the majority of the studies reviewed here involved pure culture systems exposed to HOCl, and the oxidative challenge occurred in buffered solutions with minimal carbon (energy) loads. Such an experimental setup permits the majority of the chlorine to interact with cells rather than oxidizing carbon in the media, which is what would occur in a mixed liquor sample. Therefore, the extension of pure culture results to activated sludge cultures must consider that the actual chlorine concentration experienced at exposure is greater in pure culture studies than in activated sludge studies for the same chlorine dose.

Chlorine may elicit the GGKE bacterial self defense mechanism and the work of Hibberd et al. (Hibberd, K.A. et al. (1978) provides a basis for this hypothesis. Hibberd and coworkers investigated the interaction of diamide , a strong oxidizing disinfectant, with glutathione in *E. coli*. They found that diamide exhibited bacteriostatic effects, similar to HOCl, and did not alter the ratio of reduced glutathione to oxidized glutathione. Diamide did react with the glutathione and formed protein-glutathione mixed disulfides, an indication that the GGKE system may be activated. Although diamide is chemically distinct from HOCl, it does act as a strong oxidizer and the interaction of diamide with glutathione points to the possibility that chlorine will also interact with glutathione. This study did not investigate potassium efflux as this portion of the self-defense mechanism had yet to be deduced.

Dukan et al. (Dukan, S. et al. (1999) investigated the influence of dimolecular oxygen exposure following HOCl challenge and concluded that HOCl is bacteriostatic at low concentrations, but is bactericidal if bacteria are exposed to oxygen following chlorine exposure. This may be due to the observed increase in free iron following HOCl exposure, which can lead to the formation

of hydroxyl radicals via the Fenton reaction. Dukan and coworkers also observed a decrease in glucose 6 phosphate dehydrogenase (G6PD) activity, which is consistent with the notion that HOCl-exposed bacteria are unable to effectively respire. They also noted a drop in cytoplasmic glutathione, which suggests that the GGKE mechanism is affected by HOCl exposure. The subsequent lethality of oxygen following HOCl challenge appears to occur because HOCl depletes the supply of free radical scavengers in bacteria, thereby allowing oxygen to exert lethal free radical damage.

Laplace et al. (Laplace, J.-M. et al. (1997) investigated the effect of HOCl upon *Enterococcus faecalis*and demonstrated that the culture did not develop resistance to HOCl, as demonstrated by repeated exposure. They also found that stationary phase bacteria were more resistant to HOCl than exponential phase bacteria. Although Laplace and coworkers did not investigate the relationship with glutathione, the stationary phase resistance is similar to results demonstrating an increased GGKE response in stationary phase bacteria (Ferguson, G.P. et al. (1998). Rowe et al. (Rowe, M.T. and Kirk, R. (1999) further support the idea that stationary bacteria are more resistant to insult in a study demonstrating that stationary bacteria subjected to decreased pH are more likely to survive subsequent heat stress.

Chesney et al. (Chesney, J.A. et al. (1996) investigated the relationship between bacterial glutathione and HOCl. Using a mutant strain of *E. coli* that is unable to produce glutathione, they studied the ability of *E. coli* to survive HOCl challenges with and without glutathione. The results indicated that glutathione provides bacteria with a protective mechanism against HOCl, as the bacteria without glutathione exhibited an increased rate of cell death compared to wild type *E. coli.* Chesney and coworkers also challenged *E. coli* with chloramines and found results similar to those observed with HOCl. They did not monitor K^+ during the HOCl exposure experiments, which prevents direct implication of the GGKE self defense mechanism.

Bacteria will attempt to protect their viability when exposed to chlorine. The protective mechanisms that they employ have yet to be fully determined, but the literature suggests that the GGKE bacterial self defense mechanism is probably involved. Regardless of which mechanism bacteria employ, it is hypothesized that the mechanism will have an effect on activated sludge

following exposure to chlorine. If the protective stress response mechanism(s) employed by bacteria can be determined, then the information will provide treatment plant operators with the mechanistic knowledge needed to be proactive when adding chlorine to control filamentous bulking. The third chapter of this thesis addresses the hypothesis that GGKE plays a role in the deflocculation process effect observed when mixed liquors are chlorinated.

References

(1998) *Standard Methods for the Examination of Water and Wastewater*. APHA, AWWA, WEF, Washington DC.

Absolom, D.R., Lamberti, F.V., Policova, Z., Zingg, W., van Oss, C.J., and Neumann, A.W. (1983) Surface Thermodynamics of Bacterial Adhesion. *Applied and Environmental Microbiology* **46** (1), 90-97.

Bakker, E.P., Booth, I.R., Dinnbier, U., Epstein, W., and Gajewska, A. (1987) Evidence for Multiple K^+ Export Systems in *Eschericia coli*. *Journal of Bacteriology* **169** (8), 3743-3749. Notes: NGL PC 2450

Barrette Jr., W.C., Hannum, D.M., Wheeler, W.D., and Hurst, J.K. (1989) General Mechanism for the Bacterial Toxicity of Hypochlorous Acid: Abolition of ATP Production. *Biochemistry* **28** 9172-9178.

Bearden, A.P., Sinks G.D., Vaes, W.H.J., Ramos, E.U., Hermens, J.L.M., and Schultz, T.W. (1999) Bioavailability, Biodegredation, and Acclimation of *Tetrahymena pyriformis* to 1-Octanol. *Ecotoxicology and Environmental Safety* **44** 86-91.

Bengoechea, J.A. and Skurnik, M. (2000) Temperature-regulated efflux pump/potassium antiporter system mediates resistance to cationic antimicrobial peptides in *Yersinia*. *Molecular Microbiology* **37** (1), 67-80.

Berthouex, P.M. and Fan Richard (1986) Evaluation of treatment plant performance: causes, frequency, and duration of upsets. *Jounal of Water Polluction Control Federation* **58** (5), 368-375.

Booth, I.R., Douglas, R.M., Ferguson, G.P., Lamb, A.J., Munro, A.W., and Ritchie, G.Y. (1993) K^+ efflux systems. In: Bakker, E.P. (ed), pp. 291-308, CRC Press, Baco Raton.

Bott, C. B. ELUCIDATING THE ROLE OF TOXIN-INDUCED MICROBIAL STRESS RESPONSES IN BIOLOGICAL WASTEWATER TREATMENT PROCESS UPSET. 2001. Virginia Polytechnic Institute and State University.

Bott C.B. and Love N.G. (Submitted-a) A physiological mechanism for activated sludge deflocculation caused by shock loads of toxic electrophilic chemicals. *Water Environment Research*.

Bott, C.B. and Love, N.G. (Submitted-b) Implicating the glutathione-gated potassium efflux system as a cause of activated sludge deflocculation in response to shock loads of toxic electrophilic chemicals. *Applied and Environmental Research*.

Busscher, H.J., Sjollema, J., and van der Mei, H.C. (1990) Relative Importance of Surface Free Energy as a Measure of Hydrophobicity in Bacterial Adhesion to Solid Surfaces. In: pp. 335-359, American Society for Microbiology, Washington DC.

Campbell, H.J., Troe, D., Gray, R., Jenkins, D., and Kirby, C.W. (1985) In-Basin Chlorination for Control of Activated Sludge Bulking in Industrial Waste Treatment Plants. *Procedings of the 40th Industrial Waste Conference* 759-773.

Chesney, J.A., Eaton, J.W., and Mahoney Jr., J.R. (1996) Bacterial glutathione: a sacrificial defense against chlorine compounds. *Journal of Bacteriology* **178** (7), 2131-2135.

Cowell, B.A., Willcox, M.D.P., and Schneider, R.P. (1999) Effect of nutrient limitation on adhesion characteristics of *Pseudomonas aeruginosa*. *Journal of Applied Microbiology* **86** 944-954.

Cunliffe, D., Smart C.A., Alexander C., and Vulfson, E.N. (1999) Bacterial Adhesion at Synthetic Surfaces. *Applied and Environmental Microbiology* **65** (11), 4995-5002.

Daly, B., Betts, W.B., Brown, A.P., and O'Neill, J.G. (1998) Bacterial loss from biofilms exposed to free chlorine. *Microbios* **96** 1-21.

Duffy, D.C., McDonald J.C., Schueller, O.J.A., and Whitesides, G.M. (1998) Rapid prototyping of microfluidic systems in poly(dimethylsiloxane). *Analytical Chemistry* **70** 4974-4984.

Dukan, S., Belkin, S., and Touati, D. (1999) Reactive Oxygen Species are Partially Involved in the Bacteriocidal Action of Hypochlorous Acid. *Archives of Biochemistry and Biophysics* **367** (2), 311-316.

Effenhauser, C.S., Bruin, G.J.M., Paulus, A., and Ehrat, M. (1997) Integrated capillary electrophoresis on flexible silicone microdevices: analysis of DNE restriction fragments and detection of single DNA molecules on microchips. *Analytical Chemistry* **69** 3451-3457.

Ferguson, G.P., Creighton, R.I., Nikolaev, Y., and Booth, I.R. (1998) Importance of RpoS and Dps in survival of exposure of both exponential- and stationary-phase *Escherichia coli* cells to the electrophile *N*-Ethylmaleimide. *Journal of Bacteriology* **180** (5), 1030-1036.

Ferguson, G.P., McLaggan, D., and Booth, I.R. (1995) Potassium channel activation by gluthione-S-conjugates in *Escherichia coli*: protection against methylglyoxal is mediated by cytoplasmic acidification. *Molecular Microbiology* **17** (6), 1025-1033.

Fletcher, M. (1990) Methods for Studying Adhesion and Attachment to Surfaces. *Methods in Microbiology* **22** (251-283).

Hibberd, K.A., Berget, P.B., Warner, H.R., and Fuchs, J.A. (1978) Role of Glutathione in

Reversing the Deleterious Effects of a Thiol-Oxidizing Agent in *Escherichia coli*. *Journal of Bacteriology* **133** (3), 1150-1155.
Notes: NGL PC # 5290

Higgins, M.J. and Novak, J.T. (1997a) Dewatering and settling of activated sludges: The case for using cation analysis. *Water Environment Research* **69** (2), 225-232.

Higgins, M.J. and Novak, J.T. (1997b) The effect of cations on the settling and dewatering of activated sludges: Laboratory results. *Water Environment Research* **69** (2), 215-224.

Hwang, Y.W. and Tanaka T. (1998) Control of *Microthrix parvicella* foaming in activated sludge. *Water Research* **5** 1678-1686.

Jenkins, D., Richarad, M.G., and Daigger, G.T. (1993) *Manual on the Causes and Control of Activated Sludge Bulking and Foaming, 2nd Edition*. Lewis Publishers, Inc., Chelsea, Michigan.

Kalapos, M.P. (1999) Methylglyoxal in living organisms chemistry, biochemistry, toxicology and biological implications. *Toxicology Letters* **110** 145-175.

Kelly, C.J., Lajoie, C.A., Layton A.C., and Sayler G.S. (1999) Bioluminescent Reporter Bacterium for Toxicity Monitoring in Biological Wastewater Treatment Systems. *Water Environment Research* **71** (131-35).

Laplace, J.-M., Thuault, M., Hartke, A., Boutibonnes, P., and Auffray, Y. (1997) Sodium Hypochlorite Stress in *Enterococcus faecalis*: Influence of Antecedent Growth Conditions and Induced Proteins. *Current Microbiology* **34** 284-289.

Love, N. G. and Bott C.B. A Review and Needs Survey of Upset Early Morning Devices. Love. N.G. and Bott C.B. A Review and Needs Survey of Upset Early Morning Devices. 2000. Alexandria, VA, Water Environment Research Foundation.

Mannervik, B. and Danielson, U.H. (1988) Glutathione Trasferases - Structure and Catalytic Activity. *CRC Critical Reviews in Biochemistry* **23** (3), 283-337.
Notes: NGL PC 3800

Martynova, L., Locasio, L.E., Gaitan, M., Kramer, G., Christensen, R.G., and MacCrehan, W.A. (1997) Fabrication of plastic microfluid channels by imprinting methods. *Analytical Chemistry* **69** 4783-4789.

Mcdonnell and Russell (1999) Antiseptics and disinfectants: activity, action and resistance. *Clinical Microbiology Reviews* **12** (1), 147-177.

McLaggan, D., Naprstek, J., Buurman, E.T., and Epstein, W. (1994) Interdependence of K^+ and Glutamate Accumulation during Osmotic Adaption of *Escherichia coli*. *The Journal of Biological Chemistry* **269** (3), 1911-1917.
Notes: NGL PC # 2720

Meury, J. and Kepes, A. (1982) Glutathione and the gated potassium channels of *Escherichia*

coli. *EMBO Journal* **1** 339-343.

Morra, M. and Cassinelli, C. (1997) Bacterial adhesion to polymer surfaces: A critical review of surface thermodynamic approaches. *Journal of Biomaterial Science Polymer Edition* **9** (1), 55-74.

Ness, L.S., Ferguson, G.P., Nikolaev, Y., and Booth, I.R. (1997) Survival of *Escherichia coli* cells exposed to iodoacetate and chlorodinitrobenzene is independent of the glutathione-gated K^+ efflux systems KefB and KefC. *Applied and Environmental Microbiology* **63** (10), 4083-4086.

Novak, J.T., Love, N.G., Smith, M.L., and Wheeler, E.R. (1998) The effect of cationic salt addition on the settling and dewatering properties of an industrial activated sludge. *Water Environment research* **70** (5), 984-996.

Onyiriuka, E.C., Hersh, L.S., and Hertl, W. (1991) Solubilization of Corona Discharge- and Plasma- Treated Polystyrene. *Journal of Colloid and Interface Science* **144** (1), 98-102.

Pembrey, R.S., Marshal, K.C., and Schneider, R.P. (1999) Cell Surface Analysis Techniques:What Do Cell Preparation Protocols Do to Cell Surface Properties. *Applied and Environmental Microbiology* **65** (7), 2877-2894.

Picioreanu, C., van Loosdrecht, M.C.M., and Heijnen, J.J. (2001) Two-Dimensional Model of Biofilm Detachment Caused by Internal Stress from Liquid Flow. *Biotechnology and Bioengineering* **72** (2), 205-218.

Pietersen, B., Brözel, V., and Cloete, T. (1996) The response of *Escherichia coli* K12 upon exposure to hypochlorous acid and hydrogen peroxide. *Water SA* **22** (1), 43-48.

Ramirez, G.W., Alonso, J.L., Villanueva, A., Guardino, R., Basiero, J.A., Bernecer, I., and Morenilla, J. (2000) A Rapid, Direct Method for Assessing Chlorine Effect on Filamentous Bacteria in Activated Sludge. *Water Research* **34** (15), 3894-3898.

Rijnaarts, H.H.M., Norde, W., Bouwer, E.J., Lyklema, J., and Zehnder, A.J.B. (1993) Bacterial Adhesion under Static and Dynamic Conditions. *Applied and Environmental Microbiology* **59** (10), 3255-3265.

Roberts, M.A., Rossier, J.S., Bercier, P., and Girault (1997) UV laser machined polymer substrates for the development of microdiagnostic systems. *Analytical Chemistry* **69** 2035-2042.

Ross, D., Johnson, T.J., and Locascio, L.E. (2001) Imaging of Electroosmotic Flow in Plastic Microchannels. *Analytical Chemistry* **73** 2509-2515.

Rowe, M.T. and Kirk, R. (1999) An investigation into the phenomenon of cross-protection in *Eschericia coli* 0157:H7. *Food Microbiology* **16** 157-164.

Shortreed, M.R., Dourado Sunil, and Kopelman, R. (1997) Development of a fluorescent optical potassium-selective ion selector with ratiometric response for intracellular applications. *Sensors and Actuators Part B* **38-39** 8-12.

Sommer, P., Martin-Rouas, C., and Mettler, E. (1999) Influence of the adherent population level on biofilm population, structure and resistance to chlorination. *Food Microbiology* **16** 503-515.

Turner, N.L., Horsburgh, A., Paton, G.I., Killham, K., Meharg, A., Primrose, S., and Strachan, J.C. (2001) A Novel Toxicity Fingerprinting Method for Pollutant Identification with *lux*-Marked Biosensors. *Environmental Toxicology and Chemistry* **20** (11), 2456-2461.

Tylewska, S., Hryniewicz, W., Kostrzynska, M., and Izdebska-Szymona, K. (1988) Factors Influencing the Adhesive Properties of *Pseudomonas aeruginosa*. *ACTA Microbiologica Polonica* **37** (2), 183-190.

van der Mei, H.C., Rosenberg, M., and Busscher, H.J. (1991) Microbial Cell Suface Analysis. In: pp. 263-283.

van Loosdrecht, M.C.M., Lyklema, J., Norde, W., Schraa, G., and Zehnder, A.J.B. (1987a) Electrophoretic Mobility and Hydrophobicity as a Measure To Predict the Initial Steps of Bacterial Adhesion. *Applied and Environmental Microbiology* **53** (8), 1898-1901.

van Loosdrecht, M.C.M., Lyklema, J., Norde, W., Schraa, G., and Zehnder, A.J.B. (1987b) The Role of Bacterial Cell Wall Hydrophobicity in Adhesion. *Applied and Environmental Microbiology* **53** (8), 1893-1897.

Venkobachar, C., Iyengar, L., and Rao, A.V.S.P. (1977) Mechanism of Disinfection:Effects of Chlorine on Cell Membrane Functions. *Water Research* **11** 727-729.

Vuilleumier, S. (1997) Bacterial Glutathione *S*-Transferases: What are they Good for? *Journal of Bacteriology* **179** (5), 1431-1441.
Notes: NGL PC 3410

Waddell. E., Locasio, L.E., and Kramer, G. (Submitted) UV Laser Micromachining of Polymers for Microfluidic Applications. *Journal of the Association of Laboratory Automation*.

Wilding, P., Pfahler, J., Bau, H.H., Zemel, J.N., and Kricka, L.J. (1994) Manipulation and flow of biological-fluids in straight channels micromachined in silicon. *Clinical Chemistry* **40** (1), 43-47.

Xu, J., Locasio, L.E., and Lee, C.S. (2000) Room temperature imprinting method for plastic microchannel fabrication. *Analytical Chemistry* **72** 1930-1933.

Chapter 2

Development of a Biosensor to Predict Activated Sludge Deflocculation

Formatted to be submitted to Biosensors and Bioelectronics

Abstract

The components of a biosensor to predict activated sludge deflocculation caused by the glutathione gated potassium efflux system have been investigated and optimized. When combined in an operating prototype these components will monitor the K^+ concentration of influent wastewater as it passes over a pure culture bacterial biofilm. The sensor will make use of microfluidic technologies and a fluorescent potassium detection system to create a biosensor that is inexpensive, easy to operate and able to withstand the challenges of the wastewater treatment environment.

1. Introduction

Domestic sewage is most often treated through the activated sludge biological treatment system. This process is capable of removing soluble and particulate carbon, nitrogen and in some cases phosphorus from domestic sewage. The removal of these contaminants protects receiving waters, oceans, rivers and lakes from eutrophication and contamination. The process relies on the biological conversion of soluble and particulate contaminants into biomass, by a diverse group of bacteria. At the end of the conversion process, the bacteria must be separated from the wastewater so that an effluent with minimal particles, carbon and nutrients will be discharged. The most common method of bacterial removal is gravity settling.

The bacteria that are formed during the activated sludge processform flocs, which are complex structures composed of flocculant bacteria, filamentous bacteria, exopolymeric substances and an assortment of inert particles, cations and anions. Ideally, the floc particles should be more dense than water so that they settle by gravity when placed into a quiescent environment. The bacteria are separated from the liquid effluent through gravity settling, and remove the majority of residual particulate contaminants along with them. A breakdown in the gravity settling process results in the transfer of contaminants to receiving streams and the loss of treatment efficiency at the wastewater treatment facility.

Deflocculation is an upset event that leads to the disaggregation of flocs and a breakdown in the gravity settling process. It can when interbacterial links in floc particles weaken. Deflocculation could result in the release of colloidal material, particulate organic carbon and the formation of smaller floc particles called pin floc. Colloidal material and pin floc do not settle well in the gravity-settling phase of the biological treatment process and, therefore, may significantly impact downstream treatment steps (e.g., disinfection, filtration) and the receiving water.

Deflocculation and other treatment process upset events are an important issue at wastewater treatment facilities (Love and Bott, 2000). In many instances, these events are transient and the facility operators do not know that an upset has occurred until the event has concluded . During upset events, the **source** of the upset is often never determined and operators are forced to be reactive, attempting to repair the symptoms of the upset and not the causative agent. In recent years, new technologies have emerged to provide a warning to operators of an impending upset.

These systems, primarily based around on-line respirometry and the Microtox® bioassay, are capable of detecting toxic inputs into a wastewater treatment system (Love and Bott 2000). While these systems are capable of providing a warning to operators, the warning is non-specific in that it does not identify the **source** of the upset, but only indicates that a challenge is present. Without the knowledge of the causative agent entering a facility, operators may only take general precautionary measures that may or may not prevent the eventual **effect** (deflocculation, reduced organic carbon or nutrient removal) from occurring.

Bott and Love (submitted a) have recently presented data supporting a hypothesis linking a bacterial mechanism with toxin-induced deflocculation. Their hypothesis states that electrophilic compounds entering wastewater treatment facilities will activate the glutathione-gated potassium efflux (GGKE) bacterial self defense mechanism. This mechanism is present in all Gram negative bacteria studied to date (Booth et al., 1993), and involves the interaction of an electrophilic compound with glutathione, the predominate low molecular weight cellular thiol. This reaction initiates a chain of events starting with the activation of K^+/proton antiport channels, which pump K^+ from the cytoplasm to the bulk liquid phase. The corresponding import of a proton results in the acidification of the cytoplasm, which serves to protect DNA from electrophilic attack (Ferguson et al., 1998). When this immediate (i.e., a matter of seconds) reaction occurs within activated sludge flocs, Bott and Love (submitted b) hypothesized that this results in localized changes in the monovalent to divalent cation (M:D) ratio within floc particles. This alteration in the M: D ratio weakens floc particles and results in deflocculation, as demonstrated by the work of Novak and coworkers (Higgins and Novak, 1997a, Higgins and

Novak, 1997b, Novak et al., 1998). Bott and Love (submitted a) have suggested that the GGKE mechanism is the **causative** process resulting from the electrophilic toxicant.

In an effort to provide wastewater treatment operators with an early warning of impending electrophilic (**source**) shock, we propose a novel biosensor, which detects potassium efflux (**cause)** from bacteria exposed to the source, and predicts deflocculation (**effect)**. One unique aspect of this sensor is that it predicts both **source** and **effect** by detecting the causative action. With the advent of novel microtechnologies, it is possible to combine the mechanistic knowledge presented by Bott and Love (submitted a, submitted b), with a bacterial biofilm that is integratedwith low cost components to form a biosensor. This biosensoris depicted schematically in figure 1.

The backbone of the biosensor is a microfluidic device. These devices conduct fluid through microscopic channels that are etched or molded into a variety of materials. The initial microfluidic devices were constructed from glass and silicon. In an effort to minimize the cost of the biosensor, the cost of the material into which the channel is placed should be minimized. There are a variety of plastic substrates that satisfy this requirement and provide other benefits, such as being resistant to corrosion. Numerous methods exist for fabricating microscopic channels in plastics, including imprinting (Martynova et al. 1997, Xu et al. 2000), molding (Duffy et al. 1998, Effenhauser et al. 1997) and laser ablation (Roberts et al. 1997). The channels for the biosensor constructed for this study were created by laser ablation, based on methods developed by Waddell et al. (submitted). A pure Gram negative culture was immobilized along the surface of the channel. Finally, the biosensor was designed to detect

changes in soluble K^+ concentration caused by GGKE as the influent passed the bacterial biofilm. A fluorescent chromoionophore-ionophore optode, proposed by Shortreed et al. (1997) to measure cytosolic and blood levels of K^+, was adapted for use with the biosensor to monitor changes in wastewater K^+ levels.

The specific research objectives for this project were to:

1. determine how the physiological growth state of bacterial cells influence cell immobilization,
2. determine surface chemical and structural features that enhance immobilization of whole bacterial cells to target polymeric substrata,
3. construct prototype microfluidic optode biosensors in collaboration with National Institute of Standards and Technology (NIST) researchers that are capable of detecting changes in K^+ associated with the GGKE response using the microfluidic device, and
4. produce an inexpensive, low maintenance, on-line device that is simple to operate.

2. Experimental

2.1. Culture and Growth Media

Escherichia coli K-12, ATCC # 23282 was purchased from ATCC (Manassas, Virginia) and grown in Luria-Bertani (LB) media (Atlas, 1997). The culture was streaked on solid LB media (1.5% agar) to ensure culture purity and for short-term storage. All subsequent cultures of *E. coli* K-12 were inoculated from the solid media and were handled using aseptic techniques. For all experiments, *E. coli* K-12 was cultured in LB, M9 mineral medium with 2.0 g/L D-glucose (designated M9 and includes glucose, unless specifically stated) ((1997)), or M9 with limited nitrogen (M9LN). M9LN contained 3.3 mM NH_4Cl, which is 0.18 times the amount present in M9 and provides a 20:1 C: N (molar) ratio, the M9LN substituted NaH_2PO_4 for KH_2PO_4 to

regulate the K^+ concentration as experimental conditions required, this was accomplished by altering the amount of 1M KCl added to the media. All chemicals were purchased from Fisher Scientific (Atlanta, GA). Cultures were grown at ambient temperature (approximately 23°C) on stir plates. Optical density was measured at 580 nm with a spectrophotometer (Spectronic 20, Thermo Electron Corp., Waltham, MA) to determine growth curves for *E. coli* K-12 on each of the three media (Appendix 1).

2.2. Plastic Coupons and Surface Modifications

Three materials were tested for bacterial attachment efficiency; polyethylene terephthalate glycol (PETG), polycarbonate (PC), and acrylic (AC) (McMaster-Carr Supply Company, Dayton, NJ). Flat plastic coupons measuring 1" x 2" x ¼" were treated in two different March Instruments Plasmod units at frequencies of 13.56 MHz and 50W. The samples were loaded into the plasma chamber after which the vacuum was applied. The chamber was evacuated to a pressure of less than 0.1 Torr after which the chamber was filled with gas (either ammonia or oxygen) to a pressure of 0.2 Torr. The electrodes were then biased to create a radio frequency plasma between them. Samples were exposed to the plasma for 5 minutes. The plasma was then turned off and the samples were evacuated for 5 to 10 minutes to remove any remaining metastable species or secondary reactions with air. The coupons were removed from the chamber and used in the bacterial attachment experiments.

2.3. Bacterial Attachment Experiments

Bacterial attachment experiments were conducted in two phases to determine (1) which growth state was most favorable for cell attachment, and (2) how surface modifications to the plastic

coupons affected cell attachment. For the first experiment, *E. coli* K-12 was cultured in 1 L of LB media to early log, late log, or stationary growth phase. The bacterial culture was pumped into a 295 ml glass amber bottle, which was sealed with a rubber stopper at 18 ml/min so that the fluid circulated back out the top of the bottle. The fluid was returned to the culture media vessel where aeration was provided, then returned to the amber bottle in a closed flow-through manner. Flow in the glass bottle was determined by calculation to be laminar (Re = 10). This vessel was a modification of a rinsing vessel described by Fletcher (1990). Rectangular PC coupons (no surface treatment), three per bottle, were placed inside the glass bottles with their shortest end resting on the bottom of the bottle. The coupons were stabilized in the bottle by placing 1 inch of 1" OD Tygon tubing into the center of the base of the bottle. This design also prevented the plastic coupons from contacting one another. The culture was allowed to flow through the bottle for 3 hours and 40 minutes. After this phase, the influent was replaced with glucose-free M9 media, which was pumped through the assembly for 1 hour and 40 minutes to remove any bacteria in the bulk phase. The protocol was repeated as described above with new coupons for each medium (M9 with glucose, and M9LN with glucose) with a 1 hour 40 minute glucose-free M9 bottle rinse in-between. Each experimental condition was tested in triplicate.

The LIVE/DEAD® BacLight™ bacterial viability system (Molecular Probes, Inc., Eugene, Oregon) was used to assess the number of viable *E. coli* K-12 cells that attached to the plastic samples. This system uses two fluorescent nucleic acid stains; the SYTO® 9 (green) stain penetrates the bacterial cytoplasmic membrane under all conditions, while propidium iodide (red) can enter the cell and stain the nucleic acid only if the integrity of the membrane has been compromised. Therefore, bacteria with intact membranes fluoresce green, and lysed or "dead"

cells fluoresce red. The stain was prepared with 3 µl of SYTO® 9 and 3 µl of propidium iodide in 994 µl of deionized water immediately before being applied to the plastic coupons. Using tweezers, the plastic coupons were slowly (over the course of 30 seconds) removed from the liquid phase and placed onto a paper towel. The side of the plastic in contact with the paper towel was dried and cleaned with a Kim-wipe. The opposite side of the plastic was treated with15 µl of the Live/Dead® stain mixture, and a glass coverslip were attached to the plastic by applying nail polish around the edges. The plastic coupons were incubated in the dark for 15 minutes, and then were viewed with a Zeiss Axiovert S1D0TV epifluorescence microscope (Carl Zeiss, Inc., Thornwood, New York) at 630x magnification and a shutter speed of 4 ms/frame. To observe viable (green) cells, a 480 + 20 nm excitation filter, a 505 nm long-pass dichroic mirror, and a 535 + 25 nm emission filter was used. To observe nonviable or damaged (red) cells, a 545 + 15 nm excitation filter, a 570 nm long-pass dichroic mirror, and a 610 + 37 nm emission filter were used. Black and white images of the plastic coupons with attached bacteria were obtained using a computer-controlled charge-coupled device (CCD). The number of cells of green or red fluorescence was quantified using PC-based *Scion Image* release beta 4b (Fredrick, MD). The number of green versus red cells was quantified in at least 3 fields for each color to determine relative densities of viable cells. For the second phase, bacterial attachment experiments were repeated using *E. coli* K-12 cultured in LB media to the late log growth phase and the three different polymer surfaces, with and without surface treatment. The experimental protocol described above for phase 1 experiments was used.

2.4. Construction of Microfluidic Devices

Microfluidic channels were constructed in plastic substrates using a laser ablation system (LMT-4000 Laser Micromachining System, Potomac Photonics, Inc., Lanham, MD) which was equipped with a KrF pulsed (7 ns) excimer (248 nm) laser and an Aerotech Unidex 500 PC-based motion controller (Pittsburgh, PA). It was possible to control the repetition rate of the laser from single shot to 200 Hz using a motorized stage with ± 1-micron repeatability. The micromachining system was equipped with real time live video software that enabled visualization during channel fabrication. The test devices were created under a nitrogen gas environment with a laser fluence of 1200 mJ/cm^2. The pressure of the gas exiting the nozzle was controlled with a gas regulator and was approximately 20 psi. Plastic microfluidic devices were constructed from, PETG (DSM Engineering Plastic Products, Sheffield, MA), PC (McMaster-Carr Supply Company, Dayton, NJ) or poly (vinylchloride) (PVC) (McMaster-Carr Supply Company, Dayton, NJ). After cutting the plastic into 25 mm by 76 mm rectangles, channels were constructed into the plastic with the laser ablation system to make the base for the microfluidic device (see Figure 2). After ablation, the microfluidic base pieces were sonicated in a 50/50 (v/v) solution of ethanol/water, and dried under a stream of N_2 gas. The samples were stored in Petri dishes until used.

2.5. Fluorescence Detection System

The fluorescent K^+ selective detection film, referred to as a cocktail, was constructed in a tetrahydrofuran (THF) solvent in accordance with the methods for optode film I outlined in Shortreed et al. (1997). The optode consists of a chromoionophore, which is ideally hydrogen ion selective, an ionophore which is K^+ selective and lipophilic additives, which carry a negative

charge. These constituents reside in a PVC film and maintain charge neutrality. The lipophilic additives force the ionophore and the chromoionophore to compete for a positive charge to counter the lipophilic additive. As the K^+ concentration increases surrounding the film the ionophore binds more K^+ forcing the chromoionophore to deprotonate. The ionophore decreases in fluorescent intensity as the degree of K^+ ions bound increases. The chromoionophore increases in fluorescent intensity as the degree of protonation decreases. A drop of the cocktail (approximately 0.2 µl) was placed onto polyester lamination film (# 8567K12 McMaster-Carr, Dayton, N.J.) and the THF solvent was allowed to evaporate, creating a PVC film containing the potassium detection ionophore-chromoionophore couple. The film served as a lid for the microfluidic device, and was sealed in place using heat/pressure lamination at 73°C for 15 minutes with 900 lbs of force applied (Model 2925 Hot Press, Carver Laboratory Equipment Wabash IN with a CN 76000 Omega Thermocontroller, Stamford, CN). The laminate film and PETG were placed between two sheets of tedlar film, which were in turn placed between two 6" by 6" steel plates (1/4" thick) so that the detection film lay over the microfluidic channel (see Figure 1). Polyester was used for the film because other materials (polycarbonate, PDMA, acetate film, 3M® mailing tape, PMMA) were shown to interfere significantly with the performance of the optode (data not shown). Fluorescence of the chromoionophore was detected using a Zeiss Axiovert S1D0TV epifluorescence microscope (CarlZeiss, Inc., Thornwood, New York) using a band pass filter set (excitation HQ545/30, dichroic mirror Q570LP, emission HQ 610/75 Chroma, Brattleboro, VT). Black and white images of the optode were obtained using a computer-controlled charge-coupled device (CCD). The intensity of the optode was quantified using PC-based *Scion Image* release beta 4b (Fredrick, MD). This method differs from that of Shortreed et al. (1997) who used a ratiometric approach to quantifying K^+. As the

chromoionophore fluorescence peak increases (decreased degree of protonation) the ionophore fluorescence peak decreases (increased K^+ ion binding). Shortreed et al. (1997) used the ratio of these peaks to determine the K^+ concentration.

The optode was calibrated and tested for sensitivity by flowing 50 µl of 20 mM HEPES buffer (Fisher, Atlanta GA.), pH 6.96, with AA K^+ standard (SP351-100, Fisher, Atlanta GA) added to provide a calibration range of 1 mg/L K^+ to 30 mg/L K^+, past a 3 cm x 3 cm piece of polyester laminate onto which a drop of the cocktail was placed. The laminate was attached to a glass microscope slide (lab marking tape, Fisher, Atlanta GA) so that the standard moved between the glass slide and the optode attached to the polyester laminate. The glass slide was marked with 0.5 cm x 0.5 cm grid to ensure that the optode was always placed in the same location for analysis. The calibration standard was wicked past the optode with a Kim-Wipe; 20mM HEPES buffer without K^+ was passed over the optode between standards.

In order to eliminate potential fluorescent interference, each compound to be tested was exposed to the same fluorescent excitation energy as the optode was. Neither, typical wastewater influent, NEM, M9LN media or HEPES buffer demonstrated any fluorescent emission following exposure (data not shown)

2.6. GGKE batch experiment

A batch culture of *E. coli* was grown in LB media to late log phase (OD 1.5) and then centrifuged at 11,300xg for 25 min at 10°C. The supernatant was discarded and the pellet was resuspended in 400 ml of aseptically prepared 40% strength M9LN (prepared from 5x M9LN

stocks, see section 2.1,), pH 6.60 with 20 mg/L K^+,(from 1M KCl M9LN stock), similar to section 2.1. The M9LN was utilized to provide a lower initial K^+ concentration than LB media, and to keep K^+ concentrations within the linear range of the optode. M9LN media also provided multiple cations (e.g. Mg^{2+}, Na^+, Ca^{2+}) that may compete with K^+ for the cation exchange sites on the ionophore. The resuspended culture was incubated for 1 hour on a stir-plate at ambient temperature (24°C), and then transferred into 150 ml beakers (in 110 ml aliquots) with stir bars. Samples were taken at time 0, 1 min and 20 minutes post exposure, immediately centrifuged (5 min at 13,000xg), filtered though a 0.45 μm nitrocellulose filter (Fisher, Atlanta GA) and stored at 4°C for future analysis for K^+. Three samples were treated with either 10 mg/L N-ethyl malemide (NEM) (Sigma, St. Louis, MO), 50 mg/L NEM or nothing (negative control). The samples were analyzed for K^+ by both atomic absorbance (AA) spectrometry (APHA, 1998) with a Perkin-Elmer 5100 PC AA spectrometer (Norwalk, CT) and with the optode. For AA spectrometry analysis, samples were diluted with a 2% HNO_3 (V:V) (concentrated HNO_3 Fisher, Atlanta, GA) solution that contained 10% cesium chloride solution (V:V). Cesium chloride solution was prepared with 6.35 g of CsCl (Alfa Aesar, Ward Hill, MA) and brought to 500 ml with 0.5% (V:V) HNO_3. The cesium chloride was needed to counter the potential interference of sodium ions with the K^+ ions that were analyzed by AA spectrometry. In a preliminary experiment, K^+ standards were spiked with NaCl to match Na levels found in the M9LN media. There was no difference between the AA spectrometry determined K^+ concentration of the standards with and without Na (data not shown). The optode measurements were conducted as was previously described for developing a standard curve.

2.7. Establishment of the biofilm

The biofilm was established in the channel by pumping late log phase *E. coli* K-12, cultured in LB media, through the channel at 1 µl/min for 8 hours. The *E. coli* K-12 was drawn into a 250µl gas tight syringe (Hamilton, Reno, NV) and placed onto a KD Scientific model 200 syringe pump (New Hope, PA). The needle of the syringe was placed inside of a 0.3 m length of B3603 Tygon tubing (Cole Parmer, Vernon Hill, IL). The opposite end of the tubing was placed into a 20 mm x 50 mm piece of poly (dimethyl siloxane) (PDMS) (Sylgard 184 Elastomer Kit, Fisher, Atlanta GA) so that the open end was exposed. The end of the tubing was placed over one end of the channel that was not covered by the polyester laminate and sealed in place with adhesive caulk (Macklanburg-Duncan, Oklahoma City, OK). The PDMS was attached to the PETG channel coupon with clamps. A series of experiments were performed in which the culture was pumped through the channel for varied lengths of time. The biofilm was analyzed with acridine orange stain. The stain was prepared by adding 100 mg of acridine orange (BP116-10 Fisher, Atlanta GA) to 10 ml of ethanol (Fisher Atlanta GA). One (1) ml of the stain was added to 10 ml of 20 mM HEPES buffer, pH 6.96. This solution was passed through the channel, in the same direction as the bacteria were pumped through, by placing 50 µl of stain solution onto one end of the channel and putting the other end of the channel under negative pressure (-20 mm Hg) for 10 sec. The stain was allowed to react for 1 min before a 50 µl drop of HEPES buffer was placed onto the end of the channel and passed through the channel with negative pressure to rinse residual unbound stain. The stained coupon was analyzed using a Zeiss Axioplane fluorescence microscope (Carl Zeiss, Inc., Thornwood, New York) with a yellow GFP filter set (HQ 500/20, Q515LP, D535/30, Chroma, Brattleboro, VT). The fluorescence image was characterized using

HiPic 32 version 5.0.1 imaging software (Hamamats Photonis Deustchland, Bridgewater, N.J.). The images were captured at 43 msec per frame.

3. Results and discussion

3.1. Selection of bacteria

In an effort to create a controlled environment for the analysis and validation of the GGKE biosensor, the decision was made to create a pure culture biofilm for the sensor. It is possible to establish a biofilm with samples of mixed liquor or influent from an activated sludge wastewater treatment facility, but this would have introduced another set of variables into the matrix. *E. coli* K-12 has been used extensively to elucidate the GGKE mechanism (Booth et al. 1993, Fergusson et al. 1999) and, therefore, is an obvious choice for the biosensor. The majority of organisms cultured in activated sludge are Gram negative and therefore possess the GGKE mechanism, which suggests that the use of *E. coli* K-12 as a surrogate will be acceptable. It is recognized that bacteria present in the influent wastewater may colonize the biosensor, but we expect that the established *E. coli* biofilm will resist colonization for some time, especially if filtered wastewater is used. If the influent colonization results in fouling of the biofilm or clogging of the channel, the microfluidic portion or the device may be replaced. Use of plastic components suggests that the cost associated with the disposable biosensor element would be low cost.

3.2. Effect of Bacterial Growth State on Cell Attachment

The literature suggests that as the hydrophilicity of a substratum decreases (Cunliffe et al., 1999) the probability of bacterial attachment increases. The measurement of substratum surface

hydrophobicity and bacterial cell surface hydrophobicity was pursued using a contact angle approach during preliminary investigations (data not shown). However, due to significant data scatter and recent literature reports which demonstrated that the techniques used to measure cell surface hydrophobicity often alter the cell surface hydrophobicity being measured (Pembrey et al., 1999), it was concluded that the contact angle data did not adequately predict the optimal substratum for bacterial attachment. Therefore, a direct measurement of bacterial attachment to the substratum (LIVE/DEAD® experiments presented here) was used to provide the most accurate assessment of bacteria-substratum compatibility.

The results from the bacterial growth state and culture media experiment are depicted in Figure 3. The graph displays the number of viable bacteria attached to the surface of the polycarbonate and the percentage of the total bacteria attached to the surface that are viable, as defined by the Live/Dead® assay. Each growth medium exhibited attachment of the greatest percentage of viable bacteria at different points along the growth curve. These results are tempered by the high degree of variability associated with each of the growth states and media. The LB media-grown late log phase culture of *E. coli* K-12 exhibited elevated levels of attachment and a high percentage of viable cells that were attached. While it is impossible to make any definitive conclusions from the data in Figure 3, it was possible to select the late log growth state with LB media as an adequate growth condition for the remainder of the attachment experiments. This is further supported by the work of van Loosdrecht et al. (1987a) who suggest that the bacterial cell surface is more hydrophobic, and therefore has a greater propensity for attachment to a substratum, during the logarithmic growth phase. This agrees with the observations of the bacterial attachment in early and late log for both LB media and M9LN. The change in bacterial

attachment properties throughout the cell growth profile may be due to changes in the subunits that form the exocellular layer of the bacterial cells or changes in the proteins associated with the bacteria (Fletcher, 1990). It may also be due to the formation of exopolymeric substances by the bacteria as the bacterial population becomes concentrated and the culture matures. The results of the growth state and media comparison, in conjunction with the short time frame necessary to establish a dense culture of *E. coli* K-12 (<24 hours) with LB media, support the decision to use LB media and the late log growth state throughout the substratum selection experiments.

3.3. Effect of Polymeric Material and Surface Treatment on Cell Attachment

The number of viable bacteria attached to the plastic coupons varied with surface treatment and material, with O_2 plasma and PETG showing better cell attachment on average (Figure 4). O_2 plasma treatment also showed better average cell attachment for PC over untreated and NH_3 treated coupons, although the effect was not as significant as it was for PETG. For PC and PETG, NH_3 plasma treatment actually resulted in poorer cell attachment relative to the untreated controls. The ease of initial attachment of bacteria is essential to the formation of a stable biofilm that will be able to withstand the shear stresses associated with continuous flow through the system under typical operational conditions (Picioreanu et al., 2000). It is hypothesized (Picioreanu et al., 2000) that the initial development of a biofilm occurs with the attachment of bacteria in valleys or troughs of a surface and the bacteria then multiply to form patches of biofilm. This suggests that both the surface roughness and the initial attachment of bacteria will be essential to the development of a strong and stable biofilm.

3.4. K^+ Sensor Response

The polyester film used to immobilize the K^+ detection optode did not interfere with its performance (data not shown). The preliminary studies also investigated the stability of the optode film in response to the heat it encounters during lamination (73°C for 15 minutes). There was no decline in activity (either fluorescence intensity or rate of reaction), after heating (data not shown).

There were significant challenges associated with modifying the optode developed for cytosolic and blood K^+ measurements to wastewater K^+ measurements. Shortreed et al. (1997) used a spectrograph to calculate K^+ concentrations using a ratiometric approach. In development of this biosensor, band pass fluorescent intensity was used to determine K^+ concentration, based on a standard curve of fluorescent intensity relative to K^+ concentration, (see section 2.5). The advantage of the ratiometric approach to analyzing the optode's response is that photobleaching effects are minimized as the ratio of peak intensity is utilized as opposed to absolute band pass fluorescent intensity. Figure 5 depicts the fluorescent intensity of the optode on polyester film as it was exposed to continuous excitation emissions. Significant photobleaching was observed during the initial exposure, with fluorescent intensity decreasing at a stable but slow rate after 25 minutes. This observation led to the conclusion that all optodes must be prebleached for 35 minutes in order to minimize the effect of photobleaching on subsequent K^+ measurements.

K^+ concentrations in domestic wastewater are typically on the order of 0.2 mM (Bott and Love submitted a). It is preferable that the optode produce a response that may be characterized mathematically, such as a linear response. Figure 6 depicts the standard curve established for the

optode film deposited onto the polyester laminate. The curve is linear over the typical K^+ range for wastewater and the range of the fluorescent response is broad enough that a 3 mg/L K^+ (0.08 mM) change (typical of the GGKE response in activated sludge) will be detected by the optode.

3.5. GGKE batch experiment

The standard curve in Figure 6 was determined with HEPES buffered standards at pH 6.96. It was necessary to determine the response of the optode to K^+ shifts in a complex matrix with multiple cations present (e.g. Mg, Ca, Na). The batch NEM shock experiment was conducted to determine if *E. coli* K-12 would exhibit the GGKE response and create an increase in K^+ that could be detected with the sensor. The dose of NEM, 10 mg/L, is well below the IC_{50} as determined by Bott and Love (submitted a). Therefore the response of the bacteria to NEM constitutes a GGKE response and not a cell lysis event.

Figure 7 depicts the K^+ concentration for the shocked culture of *E. coli* K-12 over the time course of the experiment. The 2.9 mg/L increase in soluble K^+, as determined by atomic absorbance spectrometry is typical of a GGKE response to an electrophile (Booth et al., 1993). The K^+ measured by AA was used to compare an established (APHA, 2000) K^+ analysis method that is believed to be accurate with the optode results. The optode-determined K^+ concentrations were consistently lower than the AA measurements, but the relative rise in the K^+ concentration between time 0 and 20 min after NEM exposure was similar for both. An explanation for the lower K^+ values detected with the optode relates to the pH of the batch experiment (pH 6.60), which has a 0.141 mM greater proton concentration than the standard curve (pH 6.96). As described earlier (section 2.5) the optode fluoresces due to the degree of protonation of the

chromoionophore and is therefore also responsive to pH shifts. The difference in the K^+ concentration value between the AA and the optode methods at the 20 min data point is 0.11 mM (a similar difference was observed with the other data points). Since one K^+ molecule displaces one proton in the optode system 78% (0.11 mM K^+ /0.141 mM H^+) of the discrepancy between the two techniques may be attributed to the difference in pH between the standard curve and test medium.

This potential lack of accuracy may not be a significant limitation to the biosensor. It is most important that the biosensor be capable of detecting relative shifts in the K^+ concentration in the sample. When a GGKE event occurs there will be a sudden spike in K^+ concentration and this will be the event that triggers the biosensor alarm. In an attempt to mitigate the effects of pH, the prototype biosensor will be constructed with two optodes, one placed before the established biofilm and the other after the biofilm. This arrangement should allow for precise relative changes in K^+ to be detected while eliminating pH effects by comparing the response of the two optodes. The impact of the pH-based discrepancy can also be minimized by calibrating the optode with a standard solution poised at the pH of the influent sample. Bott (2001) found that buffering in domestic wastewater prevented significant changes in pH during an efflux event;, therefore, during a GGKE event the first optode K^+ value should remain constant, while the second optode will register the increase in K^+ produced by the biofilm as the electrophilic compound passes over the biofilm.

3.6. Establishment of biofilm in channel

Figure 8 depicts the progression of biofilm formation in the microfluidic channel as the culture flows through the channel. While the theories predicting bacterial attachment are still in flux (Morra, M. and Cassinelli, C., 1997), it is accepted that biofilm establishment progresses with time. This is demonstrated by the lack of any stained bacterial cells in the 4 hour picture and the limited number of dispersed, attached cells depicted in the 6 hour picture. In fact, the streaking in the 6 hour picture indicates that the bacteria were not attached at all but continued to move through the channel. Once bacteria attached to the surface, they formed pockets of cells, which spread and also gathered other cells as they passed through the channel. This growth pattern is demonstrated in the 8 hour picture. A flow through method was used to initiate biofilm formation in the microfluidic channel because of the work of Picioreanu et al. (2000), who demonstrated that biofilms that are established under hydrodynamic conditions similar to those under which they will be continuously exposed exhibit lower rates of sloughing. Stable biofilm formation is important to biosensor longevity because it will limit the chance that the channel will become clogged by pieces of biofilm. Additionally, it was not feasible to establish the biofilm in the channel using a method similar to the bacterial attachment experiments used to evaluate surface properties, because the subsequent attachment of the polyester laminate lid with the hot press would result in the heat induced destruction of the biofilm. Therefore, the biofilm had to be established in channel after the laminate was in place.

4. Conclusions

The components of a novel biosensor to predict GGKE induced activated sludge deflocculation have been investigate and optimized. The optimal growth state and growth media for the

bacterial component of the biosensor have been established. The optode has demonstrated the ability to quantify the K^+ change associated with the GGKE mechanism and the microfluidic backbone has been constructed and lined with a biofilm of *E. coli* K-12. As the project continues, the components will be assembled into an operating biosensor, which will sample the influent stream of a wastewater treatment facility on a continuous basis. The development of a compact fluorescent detection system is ongoing and will allow the inexpensive microfluidic device and optode components of the biosensor to be quickly and easily replaced as channel or optode becomes fouled or unresponsive.

The combination of biological mechanistic knowledge with microtechnology will allow wastewater treatment facility operators to become proactive in dealing with disruptive toxicants. The ability to be proactive will protect both the treatment process and receiving waters, and will reduce the economic impact of upset events at wastewater treatment facilities.

ACKNOWLEDGEMENTS

Authors and their affiliations are: R. F. Wimmer and N. G. Love*, Department of Civil and Environmental Engineering, Virginia Tech (*corresponding author); A. Suggs and B. J. Love, Department of Materials Science and Engineering, Virginia Tech, Blacksburg, VA. E. Waddell and L. Locascio, Analytical Chemistry Division, Chemical and Science Technology Laboratory,National Institute of Standards and Technology (NIST), Gaithersburg, Maryland 20899-8394; S. L. R. Barker, Veridian Pacific-Sierra Research, Charlottesville, VA 22902. We are grateful for the funding for this work, which was provided by the National Science Foundation, Grant BES 00-86883.

References

Atlas, R.M. (1997) *Handbook of Microbiological Media, 2nd Edition*. CRC Press, Boca Raton, FL.

Booth, I.R., Douglas, R.M., Ferguson, G.P., Lamb, A.J., Munro, A.W., and Ritchie, G.Y. (1993) K^+ efflux systems. In: Bakker, E.P. (ed), pp. 291-308, CRC Press, Baco Raton.

Bott, C. B. ELUCIDATING THE ROLE OF TOXIN-INDUCED MICROBIAL STRESS RESPONSES IN BIOLOGICAL WASTEWATER TREATMENT PROCESS UPSET. 2001. Virginia Polytechnic Institute and State University.

Bott C.B. and Love N.G. (Submitted-a) A physiological mechanism for activated sludge deflocculation caused by shock loads of toxic electrophilic chemicals. *Water Environment Research*.

Bott, C.B. and Love, N.G. (Submitted-b) Implicating the glutathione-gated potassium efflux system as a cause of activated sludge deflocculation in response to shock loads of toxic electrophilic chemicals. *Applied and Environmental Research*.

Busscher, H.J., Sjollema, J., and van der Mei, H.C. (1990) Relative Importance of Surface Free Energy as a Measure of Hydrophobicity in Bacterial Adhesion to Solid Surfaces. In: pp. 335-359, American Society for Microbiology, Washington DC.

Cunliffe, D., Smart C.A., Alexander C., and Vulfson, E.N. (1999) Bacterial Adhesion at Synthetic Surfaces. *Applied and Environmental Microbiology* **65** (11), 4995-5002.

Duffy, D.C., McDonald J.C., Schueller, O.J.A., and Whitesides, G.M. (1998) Rapid prototyping of microfluidic systems in poly(dimethylsiloxane). *Analytical Chemistry* **70** 4974-4984.

Effenhauser, C.S., Bruin, G.J.M., Paulus, A., and Ehrat, M. (1997) Integrated capillary electrophoresis on flexible silicone microdevices: analysis of DNE restriction fragments and detection of single DNA molecules on microchips. *Analytical Chemistry* **69** 3451-3457.

Ferguson, G.P., Creighton, R.I., Nikolaev, Y., and Booth, I.R. (1998) Importance of RpoS and Dps in survival of exposure of both exponential- and stationary-phase *Escherichia coli* cells to the electrophile *N*-Ethylmaleimide. *Journal of Bacteriology* **180** (5), 1030-1036.

Fletcher, M. (1990) Methods for Studying Adhesion and Attachment to Surfaces. *Methods in Microbiology* **22** (251-283).

Higgins, M.J. and Novak, J.T. (1997a) Dewatering and settling of activated sludges: The case for using cation analysis. *Water Environment Research* **69** (2), 225-232.

Higgins, M.J. and Novak, J.T. (1997b) The effect of cations on the settling and dewatering of activated sludges: Laboratory results. *Water Environment Research* **69** (2), 215-224.

Love, N. G. and Bott C.B. A Review and Needs Survey of Upset Early Morning Devices. Love.

N.G. and Bott C.B. A Review and Needs Survey of Upset Early Morning Devices. 2000. Alexandria, VA, Water Environment Research Foundation.

Martynova, L., Locasio, L.E., Gaitan, M., Kramer, G., Christensen, R.G., and MacCrehan, W.A. (1997) Fabrication of plastic microfluid channels by imprinting methods. *Analytical Chemistry* **69** 4783-4789.

Morra, M. and Cassinelli, C. (1997) Bacterial adhesion to polymer surfaces: A critical review of surface thermodynamic approaches. *Journal of Biomaterial Science Polymer Edition* **9** (1), 55-74.

Novak, J.T., Love, N.G., Smith, M.L., and Wheeler, E.R. (1998) The effect of cationic salt addition on the settling and dewatering properties of an industrial activated sludge. *Water Environment research* **70** (5), 984-996.

Pembrey, R.S., Marshal, K.C., and Schneider, R.P. (1999) Cell Surface Analysis Techniques:What Do Cell Preparation Protocols Do to Cell Surface Properties. *Applied and Environmental Microbiology* **65** (7), 2877-2894.

Picioreanu, C., van Loosdrecht, M.C.M., and Heijnen, J.J. (2001) Two-Dimensional Model of Biofilm Detachment Caused by Internal Stress from Liquid Flow. *Biotechnology and Bioengineering* **72** (2), 205-218.

Roberts, M.A., Rossier, J.S., Bercier, P., and Girault (1997) UV laser machined polymer substrates for the development of microdiagnostic systems. *Analytical Chemistry* **69** 2035-2042.

Shortreed, M.R., Dourado Sunil, and Kopelman, R. (1997) Development of a fluorescent optical potassium-selective ion selector with ratiometric response for intracellular applications. *Sensors and Actuators Part B* **38-39** 8-12.

van Loosdrecht, M.C.M., Lyklema, J., Norde, W., Schraa, G., and Zehnder, A.J.B. (1987a) Electrophoretic Mobility and Hydrophobicity as a Measure To Predict the Initial Steps of Bacterial Adhesion. *Applied and Environmental Microbiology* **53** (8), 1898-1901.

Waddell. E., Locasio, L.E., and Kramer, G. (Submitted) UV Laser Micromachining of Polymers for Microfluidic Applications. *Journal of the Association of Laboratory Automation*.

Xu, J., Locasio, L.E., and Lee, C.S. (2000) Room temperature imprinting method for plastic microchannel fabrication. *Analytical Chemistry* **72** 1930-1933.

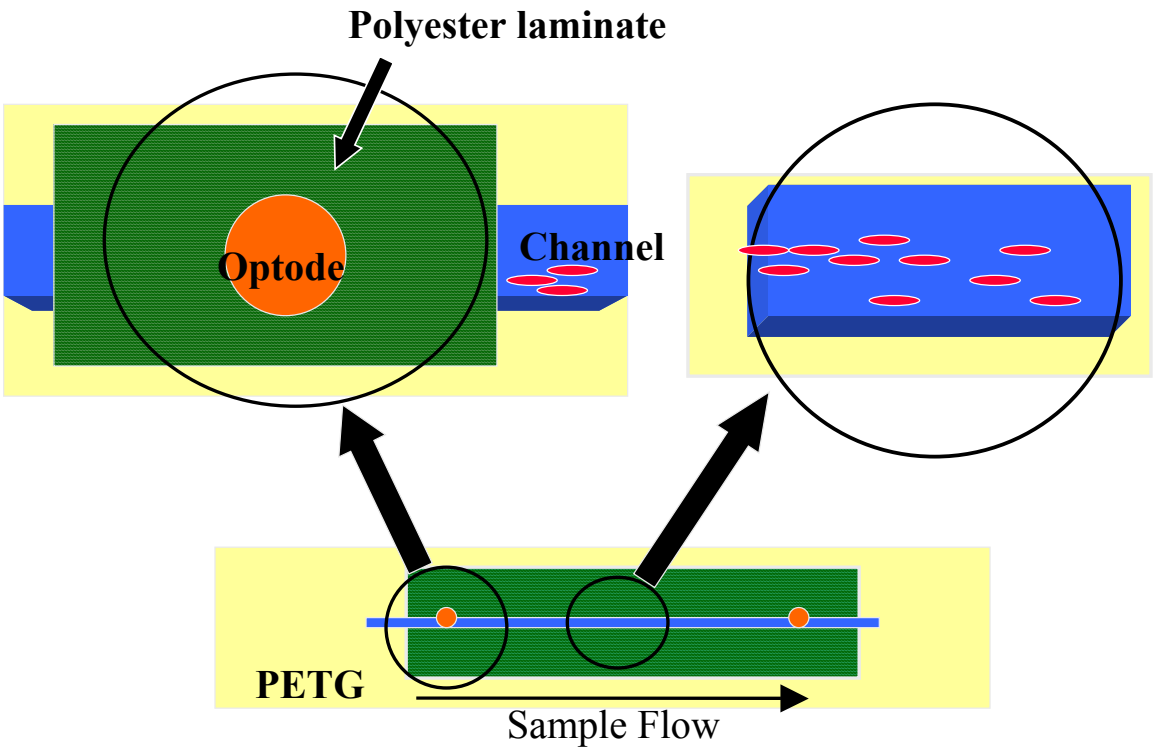

Figure 1-1. Schematic of microfluidic device concept. Device consists of PETG basesubstrate, channel where cell immobilization occurs, and both upstream and downstream K^+ optodes to measure K^+ differential (upstream and downstream of immobilized bacteria) for a given wastewater sample.

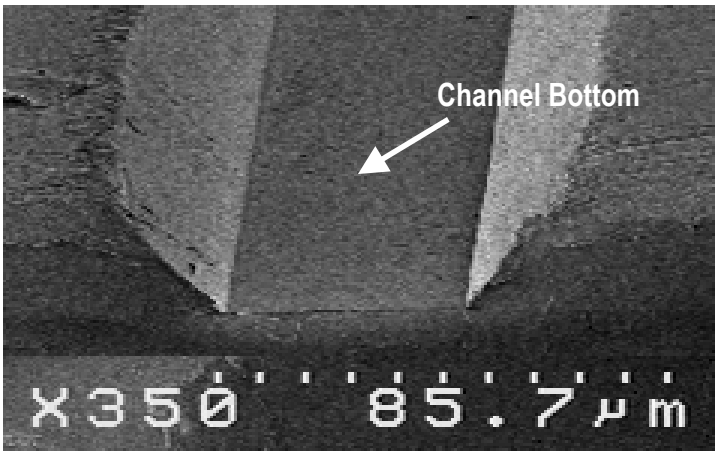

Figure 1-2. Electromicrograph of a laser etched microfluidic channel constructed by NIST (Barker et al. (2000).

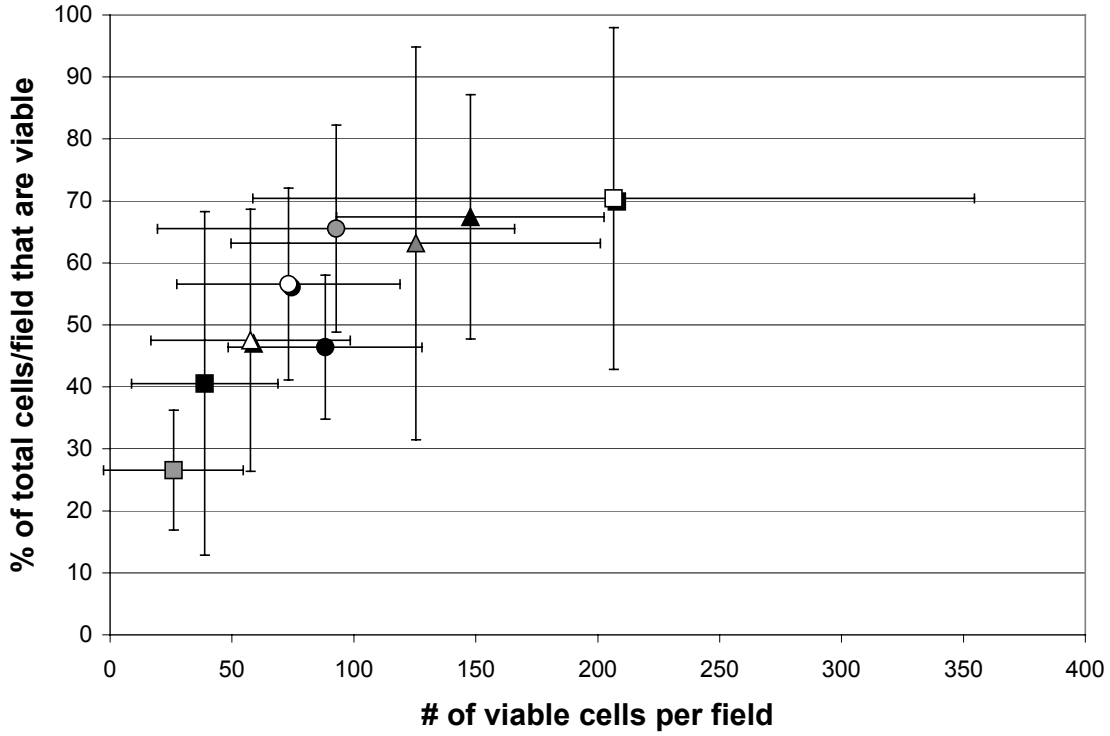

Figure 1-3. Results of bacterial attachment to polycarbonate with various media and growth states. Growth state is represented by fill color: early log= black, late log= grey, stationary= white. Media is represented by symbols: LB= circles, M9= squares, M9LN= triangles. Error bars represent one standard deviation.

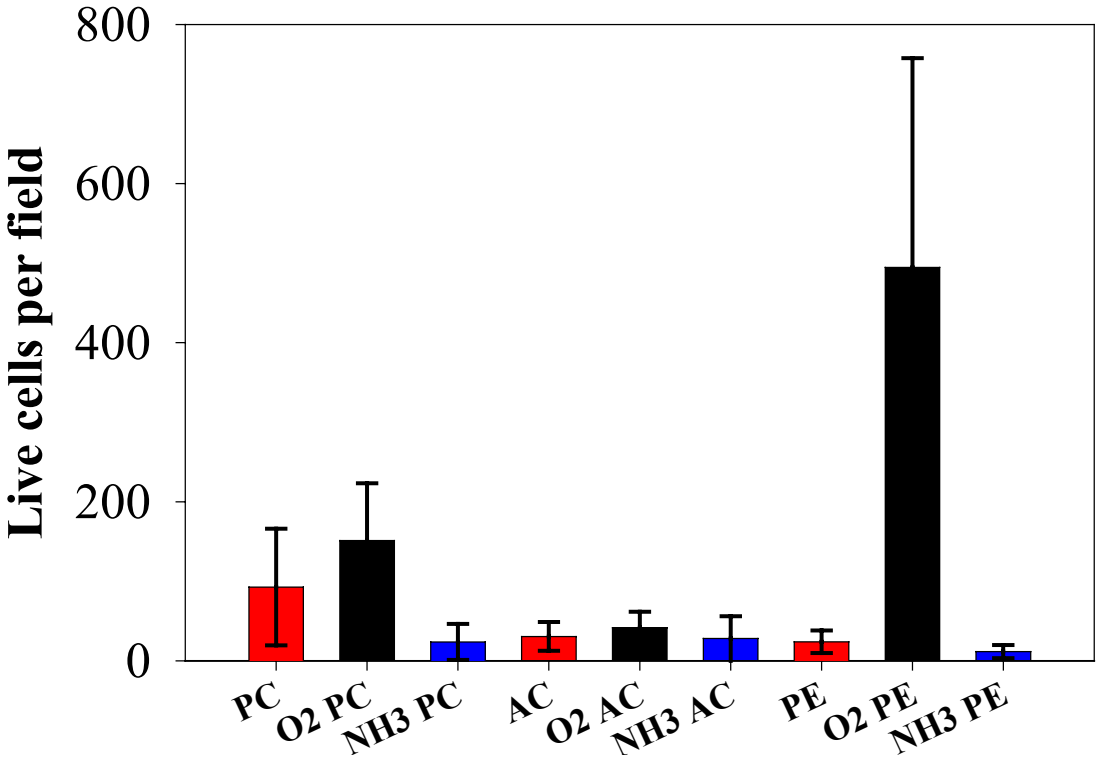

Figure 1-4. Number of bacteria per field, as detected with the LIVE/DEAD® BacLight® bacterial viability system. PC is polycarbonate, AC is acetate, PE is polyethylene terephthalate glycol, O2 indicates oxygen plasma surface treatment, NH3 indicates ammonia plasma surface treatment. Error bars signify one standard deviation.

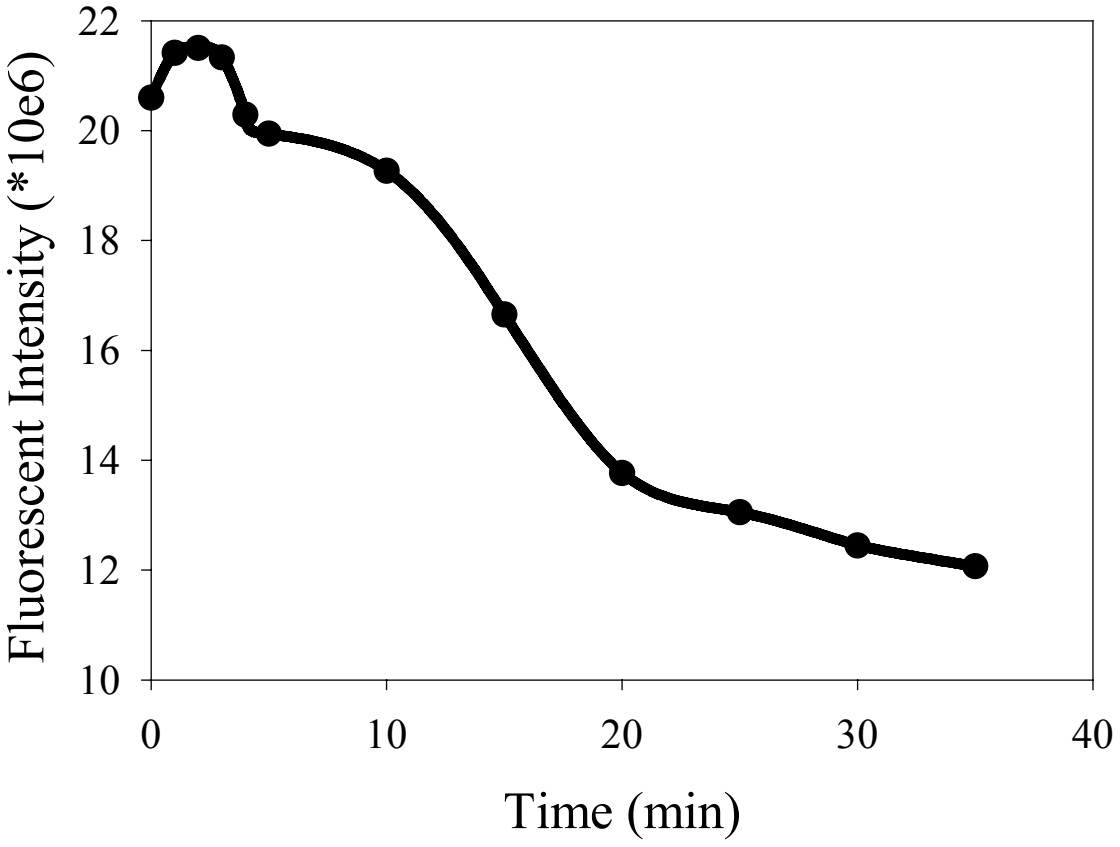

Figure 1-5 Fluorescent intensity of optode exposed to continuous excitation emission during 35 minutes of exposure.

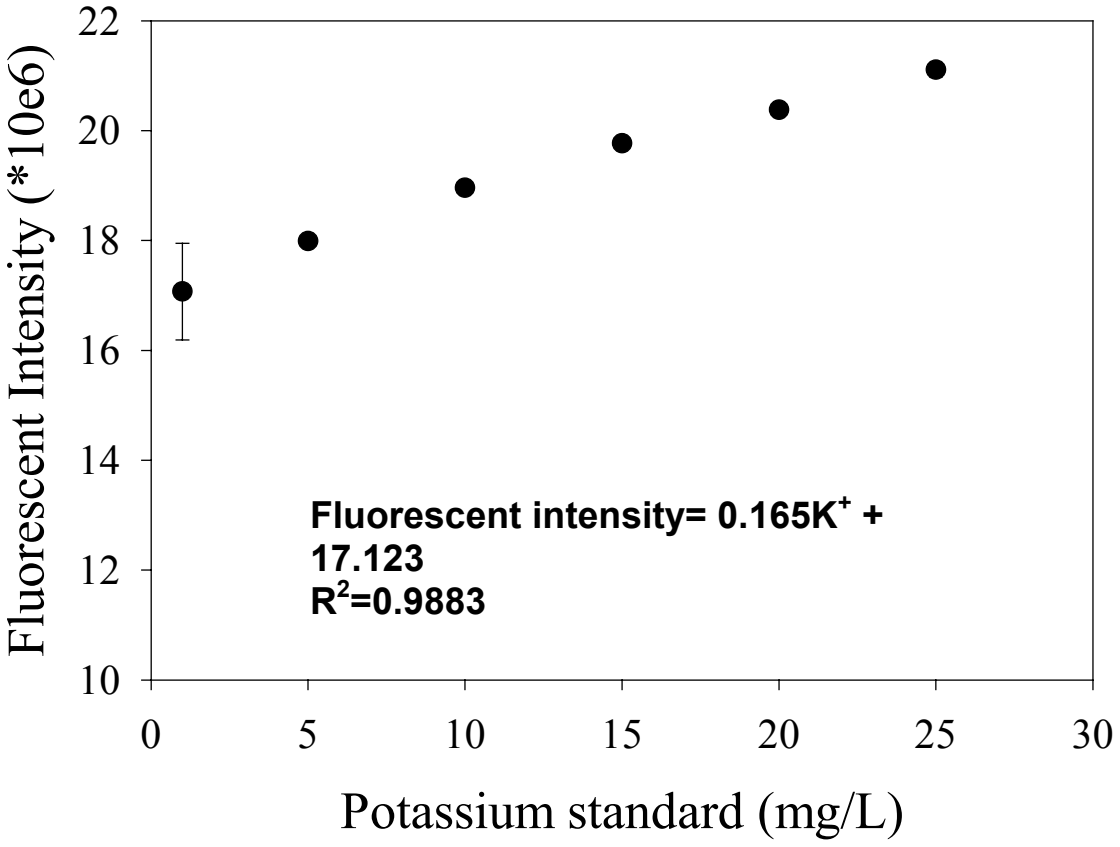

Figure 1-6 Standard curve of optode on polyester film. Error bars represent one standard deviation.

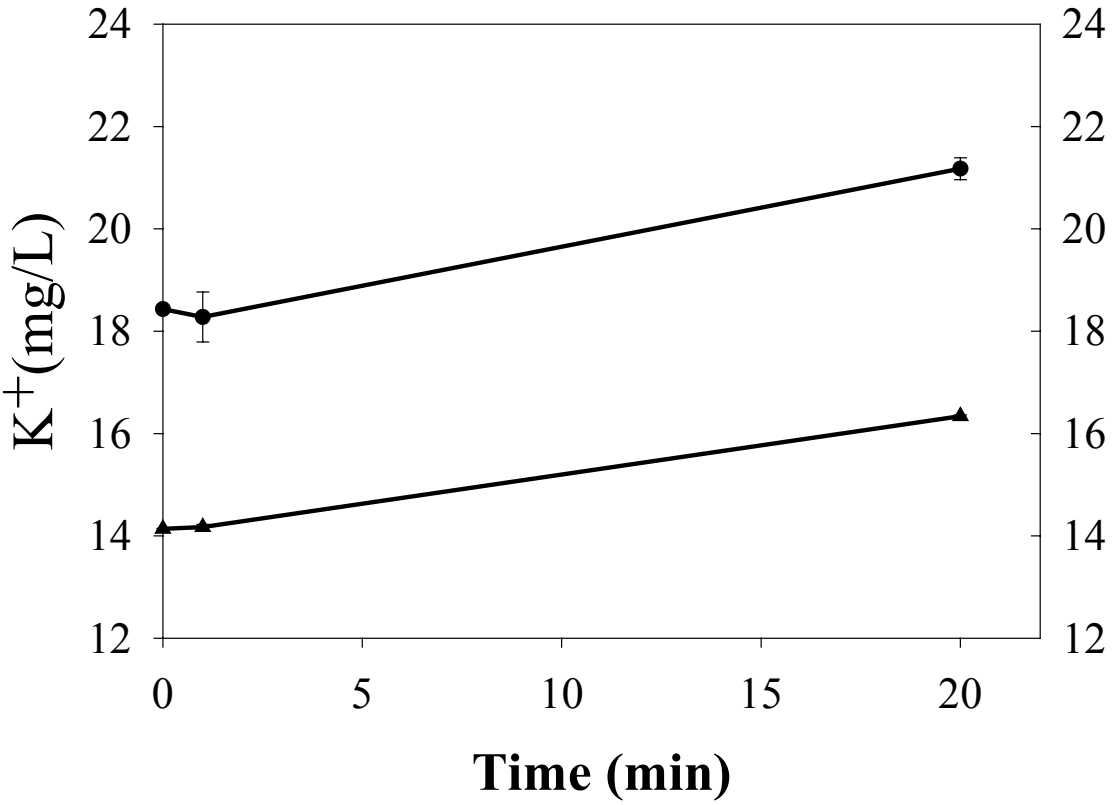

Figure 1-7 K^+ concentration of *E. coli* culture challenged with 10 mg/L NEM. NEM was added immediately after the time 0 data point. Circles represent K^+ concentration determined by AA spectrometry. Triangles represent K^+ concentration determined by the optode. Error bars represent one standard deviation.

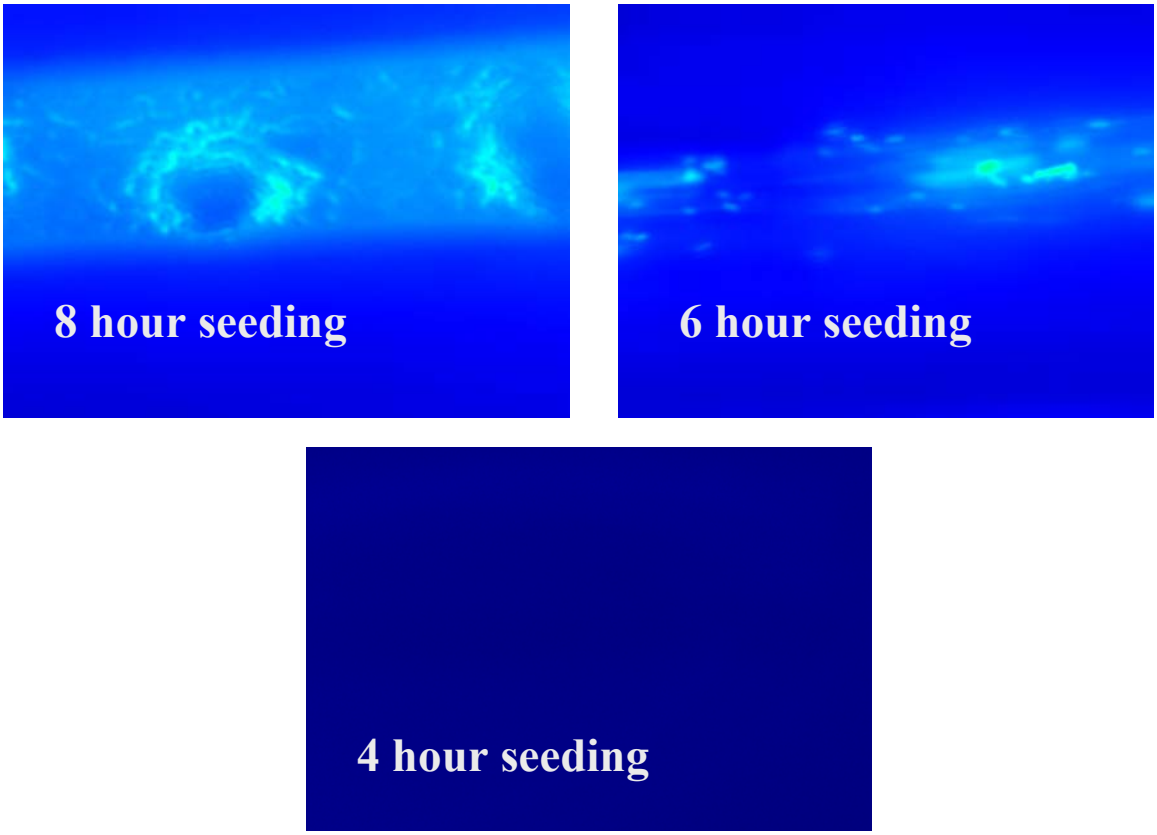

Figure 8 The progressive formation of a biofilm in a microfluidic channel, with cells stained with acridine orange, (lighter colored regions in the 6 and 8 hour pictures).

Chapter 3

Activated Sludge Deflocculation in Response to Chlorine Addition: The Potassium Connection.

Submitted to Water Environment Research January 3, 2002

ABSTRACT

Chlorination is often used to control filamentous bulking in activated sludge systems. A series of laboratory-scale reactor experiments showed that soluble potassium concentrations increased in the bulk liquid phase of mixed liquors that were exposed to chlorine, relative to unchlorinated controls. Effluent turbidity and TSS from settled mixed liquor increased in direct relation to the chlorine mass load. The point of chlorine addition relative to primary effluent addition did not influence the degree of potassium efflux. The results implicate the glutathione-gated potassium efflux (GGKE) bacterial stress response as a mechanism contributing to increased effluent turbidity associated with chlorination of mixed liquor. Potassium may be a useful parameter to monitor when determining chlorine mass doses that should be used controlling filaments while minimizing effluent deterioration.

Keywords: oxidative stress, bulking control, protective stress response

Introduction

It is well documented that activated sludge wastewater treatment systems are prone to bulking caused by an overgrowth of filamentous organisms (e.g., (1993),Lakay, M.T. et al. (1999),Madoni, P. et al. (2000),Thompson, G. et al. (2001). Filamentous bulking may result in loss of solids due to an elevated sludge blanket in the clarifier, or the formation of a stable foam in the aeration basin. In all cases the overgrowth of filaments creates an increased workload for operators and threatens the well-being of the treatment process as well as the downstream environment. A range of approaches have been used to control filamentous bulking, including modifying process operating conditions, modifying reactor and/or clarifier configuration, rectifying wastewater nutrient deficiencies, and using chemical oxidants (such as chlorine gas, hypochlorite salt (bleach), or ozone) to selectively kill filamentous microorganisms (1993).

Of the chemical oxidants used for control of filamentous bulking, chlorine has been found to be the most effective and cost competitive Saayman, G.B. et al. (1998). Jenkins et al. (1993) have established guidelines for how to add chlorine for these purposes. The guidelines identify appropriate addition points and chlorine mass dosage rates (kg $Cl_2/10^3$ kg MLSS-day), which have been found to be most effective at killing filaments while minimizing the impact on floc forming bacteria. It has been suggested that chlorine is most effective if it is rapidly mixed in the RAS line. Wherever chlorination occurs, it should be added so that: the chlorine is well dispersed; extremely high concentrations of chlorine that might kill non-filamentous bacteria are avoided; the biomass is exposed to chlorine multiple times per day; and reactions between chlorine and residual soluble chemicals are minimized to avoid quenching the available chlorine (1993),Neethling, J.B. et al. (1985).

In many cases, the addition of chlorine eventually leads to poor effluent turbidity due to activated sludge deflocculation. Campbell et al. Campbell, H.J. et al. (1985) noted that effluent

turbidity increased as chlorine mass loadings increased at three full-scale industrial wastewater treatment plants that encountered filamentous bulking. Jenkins et al. (1993) reported high turbidity episodes associated with relatively high chlorine mass doses (8 to 16 kg $Cl_2/10^3$ kg MLSS-day) that were applied to the first stage of a two stage activated sludge system in California. The high turbidity was often correlated with the presence of fine effluent particles, and microscopic observations suggested that significant cell lysis of both filamentous and floc-forming bacteria occurred. Recently, Ramirez et al. Ramirez, G.W. et al. (2000) used the BacLight® LIVE/DEAD stain to determine the impact of chlorination on viability of floc-forming versus filamentous bacteria. After 3 days exposure at a chlorine mass dose of 4 mg Cl_2/g MLVSS-day, they determined that 72% of the biomass was viable; however, this number decreased to less than 20% within 9 days at mass doses of up to 8 mg Cl_2/g MLVSS-day. The implications of high effluent turbidity include increased effluent chemical oxygen demand, increased chlorine demand in disinfection contact tanks or decreased effectiveness of UV disinfection systems, and increased backwashing frequency if tertiary filtration is employed.

The tripeptide glutathione (N-(N-L-γ-glutamyl-L-cysteinyl)glycine) is a common low molecular weight thiol that protects cells from strong oxidizing chemicals. It is found in the cytoplasms of both eukaryotic and prokaryotic organisms, and constitutes up to 95% of the LMW thiols found in Gram negative bacteria Apontoweil, P. and Berends, W. (1975),Fahey, R.C. et al. (1978),Tietze, F. (1969). Reduced glutathione (GSH) acts as a sacrificial nucleophile that reacts with oxidants, thereby preventing oxidative damage to critical intracellular macromolecules Carmel-Harel, O. and Storz, G. (2000). Additionally, oxidized glutathione activates cellular events, which further protect bacteria from sustaining oxidative damage. In the case of some electrophilic organic chemicals, glutathione and the electrophile react to form a

glutathione-electrophile conjugate, which initiates the efflux of potassium ions from the cytoplasm through potassium-specific efflux channels Ferguson, G.P. et al. (1993).

The reaction between glutathione and hypochlorous acid appears to be an important component in understanding chlorine-induced death of bacteria. Unlike the reaction between glutathione and electrophilic organics, both reduced and oxidized forms of glutathione have been shown to protect *Escherichia coli* from damage due to chlorine disinfection Chesney, J.A. et al. (1996). When glutathione-containing *E. coli* cultures were exposed to highly oxygenated or starved conditions, they demonstrated a greater resistance to hypochlorous acid stress then glutathione-deficient mutants Saby, S. et al. (1999). In a later study, Dukan et al. Dukan, S. et al. (1999) showed that relatively low concentrations of HOCl (< 1 mg/L as Cl_2) caused significant reductions in the concentration of reduced glutathione (GSH) and the activities of glucose-6-phosphate dehydrogenase and hydroperoxidase I, which indicated that antioxidant defenses were significantly impacted by HOCl. Barrette et al. Barrette Jr., W.C. et al. (1989) demonstrated that HOCl reduced *E. coli*'s ability to produce ATP due to a disruption in the adenylate system. They found that HOCl did not damage the plasma membrane, but suggested that sulfhydryl groups (which include glutathione) may be the targets of HOCl attack. The inability of bacteria to maintain effective respiration following HOCl attack may negatively impact their ability to reduce oxidized glutathione to GSH following exposure to oxidants, which impacts the cell's ability to protect itself from subsequent oxidative attack. Collectively, these results indicate the importance of glutathione in protecting cells from chlorination-induced stress.

Bott and Love Bott C.B. and Love N.G. (Submitted a) hypothesized that activated sludge will deflocculate in the presence of electrophilic Carmel-Harel, O. and Storz, G. (2000) chemicals due to activation of the glutathione-gated potassium efflux (GGKE) process, a

bacterial protective self-defense mechanism. This mechanism is activated when electrophilic compounds react with and oxidize glutathione Elmore M.J. et al. (1990). It is believed that the electrophile-activated efflux of potassium in activated sludge bacteria results in a localized shift in the monovalent to divalent cation ratio within flocs Bott, C.B. and Love, N.G. (Submitted b). Higgins, Novak and coworkers have demonstrated the importance of the monovalent to divalent cation ratio in achieving stable flocs Higgins, M.J. and Novak, J.T. (1997a),Higgins, M.J. and Novak, J.T. (1997b),Novak, J.T. et al. (1998). As the concentration of monovalent cations increases relative to the concentration of multivalent cations, flocs become less stable and are subject to deflocculation.

Previous studies showed that the oxidant diamide induced rapid potassium efflux from bacterial cells Hibberd, K.A. et al. (1978) and GGKE was implicated Elmore M.J. et al. (1990). Others exposed both wild type and glutathione-deficient *E. coli* strains to hypochlorous acid and chloramines and showed that glutathione played a role in protecting the cells from oxidative stress Chesney, J.A. et al. (1996),Saby, S. et al. (1999); however, potassium was not monitored during these studies and the GGKE self defense mechanism was not directly implicated as a protective mechanism against disinfectant-induced death.

The control of filaments with chlorine is a useful practice for operators facing filamentous bulking conditions. While it is recognized that the addition of chlorine may yield a turbid effluent, the reason it occurs is still a matter of speculation. Here, it is hypothesized that chlorinated disinfectants will oxidize cytoplasmic glutathione in activated sludge bacteria and cause GGKE to occur, thereby increasing the M:D cation ratio in flocs and causing high effluent turbidity due to weakened floc structure. The results of lab-scale experiments to test this hypothesis are presented.

Material and Methods

Mixed Liquor and Primary Effluent**.** Mixed liquor and primary effluent were gathered from two local publicly-owned treatment works (POTWs) early in the morning on the day experiments were conducted. The Blacksburg/VPI Regional Wastewater Treatment Facility treats primarily domestic wastewater and is designated POTW #1; the Peppers Ferry Regional Wastewater Treatment Facility receives 40% industrial wastewater and is POTW #2. Both facilities incorporate nitrification, and neither facility was chlorinating at the time samples were collected. Primary effluent was collected from either the weir of the primary clarifier or a junction box downstream of primary clarifiers and upstream of the aeration basins, while mixed liquor was gathered from one aeration basin at each site. Primary effluent and mixed liquor were kept separate for sequencing batch reactor (SBR) experiments. For batch experiments, 4 gallons of mixed liquor were mixed with 1 gallon of primary effluent at the POTW. All field samples were immediately returned to the lab (within 20 minutes of collection) and were either stored at 4°C prior to use (primary effluent for SBR experiments) or kept at room temperature while being continuously aerated (mixed liquor for SBR and batch experiments). Experiments were begun immediately after returning to the lab.

Batch Experiments**.** The impact of HOCl mass loading on potassium efflux and effluent turbidity from settled mixed liquor was determined using a series of batch experiments with samples from POTW # 1. For each batch assay, mixed liquor (1.5 L) was put into a 2 L beaker, mixed with a stir bar and aerated with an air stone and aquarium pump. After 5 minutes of

mixing and aeration, the reactors were challenged with various concentrations of sodium hypochlorite (NaOCl) and allowed to mix for 20 minutes. After 20 minutes the reactors were sampled for soluble K^+ and then were allowed to settle for 20 minutes. The supernatant was measured for turbidity. An unchallenged control reactor was also operator in the same manner. All batch assays were conducted in duplicate.

An independent set of batch experiments were performed in which NaCl was added instead of NaOCl to achieve Na^+ concentrations equal to those added in the chlorine-challenged batch reactors (5 to 12 mM) to determine if the effect being measured was independent of the increase in Na^+ concentration. Batch experiments were conducted in the same manner as for the NaOCl-challenged experiments.

SBR Experiments**.** A series of SBRs were used for time profile experiments to evaluate factors that influence K^+ efflux during NaOCl challenge. Experiments were conducted using mixed liquors from both POTWs. The reactors were constructed from 4 L glass beakers. Aeration was provided by air stones and an aquarium pump. Mixing was provided with a paddle (Rainbird , Richmond, VA) rotated at 103 rpm with an overhead motor. Mixed liquor (3.5 L) was added to each reactor at the beginning of the experiment, and was allowed to mix and aerate for 1 to 2 hours prior to starting experiments to ensure both the removal of any readily available soluble constituents that could constitute chlorine demand, and complete nitrification to minimize chloramine formation. A 60 ml sample was removed for MLSS/MLVSS analysis before aeration and mixing were turned off and a 30 min settling period occurred. At the end of the settling period, 1 L of supernatant was removed and analyzed for effluent VSS ("before challenge" samples). The aeration and stirring were restarted, and a sample was removed 1 minute later for

K^+ analysis. Challenged reactors were shocked by addition of NaOCl at loadings of 4, 8 or 10 mg NaOCl as CL_2/g MLVSS (the test compound) or N-ethyl malemide (NEM) at 50 mg/L (positive control for GGKE, as demonstrated for pure Bakker, E.P. and Mangerich, W.E. ,Booth, I.R. et al. (1985),Meury, J. et al. (1980) and activated sludge Bott C.B. and Love N.G. (Submitted a)cultures). One reactor was not chemically challenged (control). Since the test compound was added to settled, thickened mixed liquor before primary effluent was added, the electrophilic shock event mimicked chemical addition to a return activated sludge (RAS) line, as is often practiced at full-scale treatment plants (1993). In one series of experiments (designated Challenge I), the reactors were sampled intensely following chemical addition while being mixed for 30 minutes before 1 L of primary effluent was added, and sampling continued until the end of the react phase. In a second series of experiments (designated Challenge II), samples were removed for K^+ analysis 1 minute after the challenge, followed by immediate addition of 1 L of primary effluent and continued sampling at designated time intervals for the remainder of the reaction phase. The reactors were allowed to mix for 4 hours after the addition of primary effluent for both Challenge I and Challenge II. A MLSS/MLVSS sample was collected just prior to when aeration and mixing were turned off. The biomass was allowed to settle for 30 minutes after which 1 L of the supernatant was removed for VSS analysis ("after challenge" effluent samples).

It was necessary to investigate the effect of turgor pressure changes due to addition of primary effluent on the observed K^+ efflux response. Both mixed liquor and influent were gathered from POTW #1 and allowed to equilibrate to ambient temperature. Samples (200 mL) of primary effluent and mixed liquor were measured for conductivity in duplicate. A series of SBR reactors were operated similar to the reactors used in the NaOCl challenge experiments.

After allowing the reactors to settle for 30 minutes, the supernatant was removed and the reactors were allowed to mix. Samples for conductivity measurements were immediately removed and measured. A second set of measurements were performed 5 minutes after the start of aeration. The reactors were then challenged with NaOCl (4 and 8 mg NaOCl as Cl_2 /g MLVSS), or left unchallended (control) and samples were removed immediately for conductivity measurements. Ten (10) minutes after challenge, 1 L of primary effluent was added to the reactors and a sample was removed immediately for another conductivity measurement.

Specific Oxygen Uptake Rate**.** Specific oxygen uptake rate (SOUR) tests were performed by removing 540 ml of mixed liquor from SBR reactors 1 hour after NaOCl challenge (Challenge I experiment). The samples were immediately placed into 300 ml BOD bottles that contained 30 ml of filtered (AH-34 filter, Fisher, Atlanta, GA) primary effluent. A dissolved oxygen (DO) probe (Orion 97-08-99, Beverly MA) was immediately inserted into the BOD bottle and the DO concentration was recorded using a computerized data acquisition system (LabView version 6.0, National Instruments, Austin, TX). The slope of the oxygen concentration was determined using the slope function of Excel (Microsoft, Redmond WA.). This value was normalized to the MLVSS to obtain mg O_2 uptake/min-g MLVSS. Analysis of variance was performed on data using Excel 2000.

Chemical Analyses**.** Analyses for TSS/VSS (method 2540 D and E), COD (method 5220 C) and DPD residual chlorine (method 4500-Cl F) were conducted according to Standard Methods (1998). Turbidity was measured by removing 60 ml of supernatant after mixed liquor settling. The samples were analyzed with a digital turbidimeter (Orbeco-Hellige, Farmingdale, NY).

Conductivity was measured with a YSI Model 32 Conductance meter and probe (Yellow Springs Instrument Co. Inc., Yellow Springs, OH).

Samples for cation (Na^+, NH_3^+, K^+, Mg^{2+}, Ca^{2+}) analysis were immediately centrifuged for 1 min at 4750xg, and the supernatant was filtered through a 0.45 µm nitrocellulose syringe filter and immediately frozen (-10°C). Samples were thawed, mixed and analyzed by ion chromatography on a Dionex DX-120 ion chromatograph (IC) with a CS12 IonPac Column, a CSRS ultra suppressor, and an eluent of 20 mM methanesulfonic acid at flow rate of 1.0 mL/min. Alternatively, potassium was analyzed by atomic absorbance (AA) spectrometry as per Standard Methods (1998). For this procedure, samples were diluted with a solution containing 2% HNO_3 (V:V) and 10% cesium chloride (V:V) stock solution (6.35 g of CsCl (Alfa Aesar, Ward Hill, MA) brought to 500 ml with 0.5% (V:V) HNO_3). Cesium chloride is needed to counter the potential interference of sodium ions with the potassium ions that are analyzed by AA spectrometry. In a preliminary experiment, K^+ standards were spiked with NaCl to match sodium levels found in the mixed liquor plus additional sodium, which would be added with NaOCl. There was no difference between the AA spectrometry determined K^+ concentration for the standards with and without sodium (data not shown).

A series of samples were removed from Challenge I and II experiments conducted with POTW# 1 mixed liquor to complete a K^+ mass balance according to the protocol used by Bott and Love Bott C.B. and Love N.G. (Submitted a). A slight modification was implemented whereby 0.45 µm Supor filters were used instead of 0.20 µm filters for filtering acid digested samples.

Chemicals**.** All chemicals used for these experiments were analytical grade or better and were purchased from Fisher Scientific (Atlanta, GA), except for sodium hypochlorite (NaOCl). NaOCl was used to conduct chlorine challenges and was prepared fresh for each reactor experiment. Ten (10) ml of bleach (6% NaOCl by weight, Clorox, Oakland Ca) was combined with nanopure water to provide 1 L of stock solution. All glassware used for NaOCl preparation and storage was acid washed in 10% HNO_3 (V:V), rinsed 3 times with nanopure water, soaked in 20% (V:V) bleach for 30 minutes, and rinsed 4 times with nanopure water. The NaOCl stock solution was analyzed for chlorine concentration (mg/L as Cl_2) according to the DPD chlorine method (1998).

Results and Discussion

Batch Experiments**.** Batch experiments showed that mixed liquor challenged with NaOCl responded in a manner consistent with a GGKE-induced activated sludge deflocculation event. As shown in Figure 1, bulk phase soluble K^+ and settled supernatant turbidity both increased with NaOCl mass doses, particularly as they increase above 6 mg Cl_2/g MLVSS. This result is consistent with the notion put forth by Bott and Love Bott, C.B. and Love, N.G. (Submitted b),Bott C.B. and Love N.G. (Submitted a)that electrophilic chemicals activate the GGKE stress protection mechanism in activated sludge bacteria, causing a rapid and intense increase in the intrafloc concentration of K^+, which is subsequently detected as a subtle increase in K^+ in the bulk liquid. Additionally, the data suggest that the stability and strength of the floc diminishes as the soluble K^+ increases, leading to further deflocculation. This is demonstrated by the increase in effluent turbidity, which increases in relation to the magnitude of the NaOCl challenge. The chlorine mass doses that yielded the most dramatic turbidity increases (greater than 6 mg Cl_2/g

MLVSS) are within the range of those used in the field, but are on the high side (1993). These results are consistent with experiences where higher chlorine doses were used to combat filamentous bacteria that were heavily integrated inside of flocs, and corresponded with higher effluent turbidity consisting of fine particles Campbell, H.J. et al. (1985). Similarly, Neethling et al. Neethling, J.B. et al. (1985) noted that effluents from chlorinated activated sludge facilities deteriorated, as measured by soluble COD, even when exposed to what would be considered typical chlorine concentrations. They suggested that some of the increase in COD was probably due to the presence of fine particles that passed through the filter.

Use of NaOCl as a chlorinating agent in these experiments did not influence the results of the experiments by introducing Na^+. The hypothesis that measured increases in soluble K^+ indicates weakened floc structure is based on the notion that increases in the monovalent to divalent cation ratio inside of mixed liquor flocs weaken cationic bridges between negatively charged ligands Higgins, M.J. and Novak, J.T. (1997a),Higgins, M.J. and Novak, J.T. (1997b),Novak, J.T. et al. (1998). When NaOCl was used as the chlorinating agent, up to 258 mg/L Na^+ (11 mM) was added into the solution of batch experiments. Addition of this concentration of Na^+ as NaCl did not increase supernatant turbidity in the mixed liquor (average 11 ntu) compared to an untreated control reactor (average 30 ntu). These results were as expected, since the change in Na^+ imposed by addition of NaOCl changed the M:D ratio from 2.6 to 2.8, which is much less than that needed to impose a significant change in effluent turbidity in both domestic and industrial mixed liquors Higgins, M.J. and Novak, J.T. (1997b),Novak, J.T. et al. (1998). However, Novak et al. Novak, J.T. et al. (1998) reported that 10 mM sodium decreased the effluent turbidity but increase the capillary suction time (an indicator of biomass dewaterability) for an industrial mixed liquor.

SBR Experiments**.** The results from Challenge I experiments support the observation from the batch experiments that NaOCl addition results in K^+ efflux and increased turbidity due to deflocculation, but only at higher chlorine mass doses. Figure 2 depicts the soluble K^+ concentration for three challenged SBR reactors and the corresponding control over the time course of the experiment for both POTWs. For POTW #1, the 8 mg NaOCl as Cl_2/g MLVSS challenge caused an increase in soluble K^+ of over 2 mg/L within the first 5 minutes of exposure, whereas the 4 mg NaOCl as Cl_2/g MLVSS dosage did not cause a significant increase in K^+ beyond that observed with the control (Figure 2A). For POTW #2, both the 4 and 10 mg NaOCl as Cl_2/g MLVSS challenge experiments caused a soluble K^+ increase of 1.5 and 2 mg/L within 10 and 5 minutes, respectively (Figure 2B). The elevated K^+ levels eventually decreased to levels measured in the control reactor for the lower chlorine dosed system but remained elevated throughout most of the reaction cycle for the higher chlorine dosed systems. The NEM-challenged reactors were positive controls, because NEM is a known GGKE activator. Although the increase in soluble K^+ in the NaOCl-stressed SBRs was not as great as in the NEM-stressed SBRs, a noticeable efflux occurred in both sets immediately after shock relative to the control and suggests that a similar bacterial mechanism is responsible.

Since primary effluent was not added until 30 minutes after the NaOCl shock, it is unlikely that chloramines were formed during the experiments presented in Figure 2. The pH in the POTW #1 mixed liquor was 7.48 while POTW #2 was 7.08. The pK_a for the HOCl/OCl couple is 7.5. Therefore, approximately 50% of the disinfectant would have existed as OCl^- for POTW #1 whereas most of the disinfectant would have existed as HOCl for POTW #2. HOCl is the more potent oxidant of the couple McDonnell, G.K. and Russell, A.D. (1999), and the results

are consistent with the notion that a stronger oxidant was present during the POTW #2 experiments (greater K^+ efflux at similar chlorine mass doses relative to POTW #1).

Mass balances on soluble K^+ were performed around the point when primary effluent was added for the experiments shown in Figure 2. The increases or decreases in K^+ concentration observed for the first point after adding primary effluent were within 5% of what was theoretically expected based on pure dilution or concentration of K^+, except for the 4 mg Cl_2/g MLVSS case for POTW #2. The measured increase in K^+ after adding primary effluent in this case cannot be easily explained, because addition of primary effluent should have decreased K^+ through dilution because the primary effluent K^+ concentration was lower than that in the challenged reactor. Nevertheless, a distinct but subtle K^+ efflux was observed, on average, for this experiment.

NaOCl-induced K^+ efflux from mixed liquor was not influenced by the presence of readily biodegradable substrate. Figure 3 show results from experiments where the SBRs were challenged with 8 or 10 mg NaOCl as Cl_2/g MLVSS 30 minutes before addition of primary effluent (Challenge I, repeat of data from Figure 2) and immediately before addition of primary effluent (Challenge II). K^+ efflux occurred immediately following NaOCl challenge in both cases. Additionally, the degree of efflux was not consistently greater for either scenario when data from both POTWs were considered. Neethling et al. Neethling, J.B. et al. (1985) showed that the free chlorine residual decreased rapidly within the first 60 seconds of being in contact with mixed liquor containing less than 1 mg/L NH_3-N, presumably because it reacted with cells as well as with other compounds in the bulk phase of the mixed liquor. During the Challenge II experiment, primary effluent was added approximately 30 seconds after NaOCl was added. Therefore, it is possible that some chloramines formed during this experiment, but a significant

amount of free chlorine probably reacted before the primary effluent was added. For the Challenge I experiment, it is likely that the bulk liquid chlorine residual decreased significantly by the time primary effluent was added 30 minutes later, and it is unlikely that any chloramines formed.

Effluent VSS concentrations for the Challenge I and II SBRs increased as the magnitude of K^+ effluxed increased, as shown in Table 1. These results are consistent with the batch study results presented earlier, and the work of Bott and Love Bott C.B. and Love N.G. (Submitted a). Additionally, the results correspond with the notion that as more K^+ is released into the floc, the intrafloc M:D ratio would increase and cause a greater disturbance of divalent cation bridging; therefore, a greater decrease in the floc strength would result and yield increased effluent suspended solids Novak, J.T. et al. (1998). Ultimately, the results show that a single dose of chlorine at mass doses considered to be typical of the range applied to return activated sludge caused a significant increase in effluent VSS, which correlated with measurable increases in soluble potassium.

Figure 4 shows a mass balance conducted on an SBR experiment using mixed liquor from POTW #1. K^+ moved from the floc-associated fraction of the mixed liquor samples to the bulk phase immediately after NaOCl was added to the reactor. The calculated total averages 95 $\pm$ 4 % of an independently measured total, showing that a mass balance on potassium was obtained. These data show that potassium moved from mixed liquor flocs to the bulk liquid immediately after chlorine challenge, which is consistent with what would happen if GGKE were activated. Bott and Love Bott, C.B. and Love, N.G. (Submitted b) showed that electrophile-movement of K^+ from cells into the floc created a localized intrafloc increase in monovalent potassium concentration to levels known to cause deflocculation.

K^+ is the primary ion responsible for the regulation of turgor pressure in bacteria McLaggan, D. et al. (1994). As exocellular osmolarity increases, bacteria import K^+ into the cytoplasm to counteract the increased external osmotic pressure upon the cell membrane. As the osmotic pressure outside the cell decreases, K^+ is released from the cell to maintain equilibrium. Addition of NaOCl caused a 6% increase in conductivity and the addition of primary effluent resulted in a 5% increase in conductivity. Collectively, these solution additions caused an increase in bulk phase osmolarity that could induce the bacteria to import K^+ ions in order to maintain balanced turgor pressure. The observation that the bacteria are effluxing K^+ from the cell instead implies that the requirement to protect the bacteria from oxidative attack controls the net flux of K^+ rather than the requirement to maintain cell turgor. Bakker et al. Bakker, E.P. et al. (1987) have demonstrated that the channels that bacteria use for GGKE are separate from those related to K^+ import/export for turgor maintenance. The measured increase in osmolarity suggests that the bacteria may be effluxing even more K^+ than is ultimately measured, because the mechanism of cell turgor regulation may be importing K^+ at the same time. Therefore, it is possible that the osmolarity of mixed liquors will impact the degree of deflocculation associated with chlorine challenge, because it would be based on the net amount of K^+ that ultimately is effluxed.

It has been suggested that deflocculation associated with chlorination may be due to cell lysis from an overdose of chlorine, which affects not only the filamentous bacteria but also the floc forming bacteria Hwang, Y.W. and Tanaka T. (1998),(1993). There are two pieces of evidence in this study, which suggest that cell lysis is not primarily responsible for the deflocculation that was observed. First, mixed liquor SOUR did not change as chlorine dosage increased from 0 to 10 mg Cl_2/g MLVSS for biomass collected from POTW #1 ($F_{calculated}$=1.8,

$F_{critical}$=5.1, α=0.05), or from 0 to 8 mg Cl_2/g MLVSS for biomass collected from POTW #2 ($F_{calculated}$=2.1, $F_{critical}$=6.4, α=0.05). The SOUR for the 10 mg Cl_2/g MLVSS dose for POTW #2 was actually significantly higher than for the other treatments ($F_{calculated}$=10.6, $F_{critical}$=5.1, α=0.05). The reason for this is unclear but is not consistent with what would happen if cell lysis were occurring to a significant degree. This indicates that the organisms are still respiring fully and that there has been minimal to no lysis of the chlorine-exposed mixed liquor. Second, the concentrations of Ca^{2+} and Mg^{2+} in the bulk liquid phase of the challenged reactors did not change following addition of NaOCl (data not shown). If cell lysis were to have occurred it would be expected that the other cations present in the cytoplasm would be detected in the bulk phase as well, but this was not the case. In summary, there is no evidence supporting the notion that significant lysis was occurring in the experimental reactors, and the K^+ increases observed in the bulk liquid phase appear to be due to a controlled release of K^+, as would be the case for GGKE.

The SBR experiments demonstrated that a single chlorination challenge could induce deflocculation. Although it is possible to observe immediate increases in effluent turbidity when high chlorine doses are used (1993), the operators at POTW #2 said that they often observed high turbidity due to chlorination after approximately one sludge age had passed McCutcheon, L. (2001). Chlorine mass dose is typically used as the basis for determining the average daily chlorine load to a treatment system; however, it is the chlorine residual concentration that bacteria are exposed to which actually controls the degree of killing McDonnell, G.K. and Russell, A.D. (1999),Pietersen, B. et al. (1996). To minimize the degree to which floc-forming bacteria are lysed and to minimize the chlorine concentration at which the biomass inventory is exposed, it has been recommended that daily mass doses be applied multiple times over the

course of a day rather than in a single application (1993),Neethling, J.B. et al. (1985). During the SBR experiments conducted on POTW #1 mixed liquor, the effective dose of chlorine at the time and point of contact was calculated to be 18, 33 and 34 mg/L as Cl_2 for the 4 mg Cl_2/g MLVSS-day (Challenge I), 8 mg Cl_2/g MLVSS-day (Challenge I) and 8 mg Cl_2/g MLVSS-day (Challenge II) experiments, respectively. During the SBR experiments conducted on POTW #2 mixed liquor, the effective dose of chlorine at the time and point of contact was calculated to be 18, 17 and 17 mg/L as Cl_2 for the 4 mg Cl_2/g MLVSS-day (Challenge I), 10 mg Cl_2/g MLVSS-day (Challenge I) and 10 mg Cl_2/g MLVSS-day (Challenge II) experiments, respectively. These concentrations are not excessive and are within the range of concentrations that have been shown to be effective at controlling low DO filaments Neethling, J.B. et al. (1985). However, they are well above concentrations known to be inhibitory in *E. coli* K12 pure cultures Pietersen, B. et al. (1996). Nevertheless, the data show that high effluent turbidity can be experienced after one application at chlorine mass loads and concentrations that may be applied at full-scale facilities, and that this turbidity may be caused, at least in part, by the GGKE mechanism.

It has been widely speculated that a primary mechanism of antibacterial action by HOCl is due to reaction with cytoplasmic thiol groups that are commonly found in protective oxidative stress molecules, like glutathione, and selected enzymes Chesney, J.A. et al. (1996),McDonnell, G.K. and Russell, A.D. (1999),Saby, S. et al. (1999). It is also known that exposure to HOCl affects the ability of bacteria to produce ATP Barrette Jr., W.C. et al. (1989). Finally, while it appears that the GGKE mechanism does not rely upon *de novo* protein synthesis or energy to function Elmore M.J. et al. (1990),Meury, J. et al. (1980),Meury, J. and Robin, A. (1990), reduction of oxidized glutathione to GSH requires glutathione reductase and NADPH Carmel-Harel, O. and Storz, G. (2000),Mannervik, B. and Danielson, U.H. (1988). The requirement for

NADPH is critical, in that bacteria must be actively respiring (producing ATP) to replenish the NADPH pool in order to ensure the presence of GSH to provide control over the K^+ efflux channels. Therefore, it is conceivable that chlorine exposure both reduces the adenylate energy charge in bacteria and reduces the cytoplasmic pool of GSH. Without the ability to produce sufficient NADPH, the bacteria would be unable to reduce sufficient pools of oxidized glutathione back to GSH. Over time, subsequent exposure to chlorine would ultimately deplete the GSH pool in biomass and the bacteria (floc formers and filaments, alike) would be unable to protect themselves from oxidative and electrophilic attack. Under this scenario, accelerated cell death would occur upon subsequent exposure to chlorine, and K^+ efflux would decrease with time. Further studies should be conducted to evaluate this hypothesis.

Conclusions

The results presented here demonstrate that a correlation exists between NaOCl challenge, increased soluble phase K^+ concentration, and increased effluent VSS in chlorinated mixed liquors. This correlation is consistent with the work of Bott and Love Bott, C.B. and Love, N.G. (Submitted b),Bott C.B. and Love N.G. (Submitted a) and suggests that the GGKE activated sludge deflocculation mechanism contributes to the increases in turbidity that are often observed with chlorinated mixed liquors. One possible application of this information is to monitor potassium with an ion selective electrode as part of a jar test where a range of chlorine mass doses are applied to mixed liquor; that dosage which minimizes potassium efflux is likely to minimize deterioration in effluent quality during chlorination. Additional studies are recommended to determine the relationship between K^+ release, glutathione levels, chlorination dosage, and effectiveness on controlling filaments during long term experiments.

Acknowledgements

The authors would like to acknowledge the gracious support of: the staff at the Blacksburg/VPI Wastewater Treatment Facility; the staff at the Peppers Ferry Regional Wastewater Treatment Facility; and Felicia Glapion, Julie Petruska and Jody Smiley for analytical and laboratory support.

Bibliography

APHA, AWWA, and WEF (1998) *Standard methods for the examination of water and wastewater, 20th Edition.* United Book Press, Inc., Baltimore, MD.

Apontoweil, P. and Berends, W. (1975) Glutathione biosynthesis in *Escherichia coli* K-12: properties of the enzymes and regulation. *Biochimica et Biophysica Acta,* **399** (1), 1-9.

Bakker, E.P. and Mangerich, W.E. (1982) N-ethylmaleimide induces K^+-H^+ antiport activity in *Escherichia coli* K-12. *FEBS Letters,* **140** (21), 177-180.

Bakker, E.P., Booth, I.R., Dinnbier, U., Epstein, W., and Gajewska, A. (1987) Evidence for multiple K^+ export systems in *Eschericia coli*. *Journal of Bacteriology,* **169** (8), 3743-3749.

Barrette Jr., W.C., Hannum, D.M., Wheeler, W.D., and Hurst, J.K. (1989) General mechanism for the bacterial toxicity of hypochlorous acid: abolition of ATP production. *Biochemistry,* **28** 9172-9178.

Booth, I.R., Epstein, W., Giffard, P.M., and Rowland, G.C. (1985) Roles of *trkB* and *trkC* gene products of *Escherichia coli* in K^+ transport. *Biochimie,* **67** (1), 83-90.

Bott C.B. and Love N.G. (Submitted a) A physiological mechanism for activated sludge deflocculation caused by shock loads of toxic electrophilic chemicals. *Water Environment Research*.

Bott, C.B. and Love, N.G. (Submitted b) Implicating the glutathione-gated potassium efflux system as a cause of activated sludge deflocculation in response to shock loads of toxic electrophilic chemicals. *Applied and Environmental Microbiology*.

Campbell, H.J., Troe, D., Gray, R., Jenkins, D., and Kirby, C.W. (1985) In-basin chlorination for control of activated sludge bulking in industrial waste treatment plants. *Proceedings of the 40th Industrial Waste Conference*, Lafayette, IN, 759-773.

Carmel-Harel, O. and Storz, G. (2000) Roles of the glutathione- and thioredoxin-dependent reduction systems in the *Escherichia coli* and S*accharomyces Cerevisiae* responses to oxidative stress. *Annu. Rev. Microbiol,*. **54** 439-461.

Chesney, J.A., Eaton, J.W., and Mahoney Jr., J.R. (1996) Bacterial glutathione: a sacrificial defense against chlorine compounds. *Journal of Bacteriology,* **178** (7), 2131-2135.

Dukan, S., Belkin, S., and Touati, D. (1999) Reactive oxygen species are partially involved in the bacteriocidal action of hypochlorous acid. *Archives of Biochemistry and Biophysics,* **367** (2), 311-316.

Elmore M.J., Lamb A.J., Ritchie G.Y., Douglas R.M., Munro A., Gajewska A., and I.R. Booth (1990) Activation of potassium efflux from *Escherichia coli* by glutathione metabolites. *Molecular Microbiology,* **4** (3), 405-412.

Fahey, R.C., Brown, W.C., Adams, W.B., and Worsham, M.B. (1978) Occurrence of glutathione in bacteria. *Journal of Bacteriology,* **133** (3), 1126-1129.

Ferguson, G.P., Munro, A.W., Douglas, R.M., McLaggan, D., and Booth Ian R. (1993) Activation of potassium channels during metabolite detoxification in *Escherichia coli*. *Molecular Microbiology,* **9** (6), 1297-1303.

Hibberd, K.A., Berget, P.B., Warner, H.R., and Fuchs, J.A. (1978) Role of glutathione in reversing the deleterious effects of a thiol-oxidizing agent in *Escherichia coli*. *Journal of Bacteriology,* **133** (3), 1150-1155.

Higgins, M.J. and Novak, J.T. (1997a) The effect of cations on the settling and dewatering of activated sludges: laboratory results. *Water Environment Research,* **69** (2), 215-224.

Higgins, M.J. and Novak, J.T. (1997b) Dewatering and settling of activated sludges: the case for using cation analysis. *Water Environment Research,* **69** (2), 225-232.

Hwang, Y.W. and Tanaka T. (1998) Control of *Microthrix parvicella* foaming in activated sludge. *Water Research,* **5** 1678-1686.

Jenkins, D., Richard, M.G., and Daigger, G.T. (1993) *Manual on the Causes and Control of Activated Sludge Bulking and Foaming, 2nd Edition*. Lewis Publishers, Inc., Chelsea, Michigan.

Lakay, M.T., Hulsman, A., Ketley, D., Warburton, C., de Villiers, M., Casey, T.G., Wentzel, M.C., and Ekama, G.A. (1999) Filamentous organism bulking in nutrient removal activated sludge systems. Paper 7: Exploratory experimental investigations. *Water S. A.,* **25** (4), 383-396.

Madoni, P., Davoli, D., and Gibin, G. (2000) Survey of filamentous microorganisms from bulking and foaming activated-sludge plants in Italy. *Water Research,* **34** (6), 1767-1772.

Mannervik, B. and Danielson, U.H. (1988) Glutathione trasferases - structure and catalytic activity. *CRC Critical Reviews in Biochemistry,* **23** (3), 283-337.

McCutcheon, Lawrence (2001) Operator, Personal Communication. Peppers Ferry Regional Wastewater Treatment Facility. Radford, Virginia.

McDonnell, G.K. and Russell, A.D. (1999) Antiseptics and disinfectants: activity, action and resistance. *Clinical Microbiology Reviews,* **12** (1), 147-177.

McLaggan, D., Naprstek, J., Buurman, E.T., and Epstein, W. (1994) Interdependence of K^+ and glutamate accumulation during osmotic adaption of *Escherichia coli*. *The Journal of Biological Chemistry,* **269** (3), 1911-1917.

Meury, J., Lebail, S., and Kepes, A. (1980) Opening of potassium channels in *Escherichia coli* membranes by thiol reagents and recovery of potassium tightness. *European Journal of Biochemistry,* **113** (1), 33-38.

Meury, J. and Robin, A. (1990) Glutathione-gated K^+ channels of *Escherichia coli* carry out K^+ efflux controlled by the redox state of the cell. *Archives of Microbiology,* **154** 475-482.

Neethling, J.B., Jenkins, D., and Johnson, K.M. (1985) Chemistry, microbiology, and modeling of chlorination for activated sludge bulking control. *Journal Water Pollution Control Federation,* **57** (8), 882-889.

Novak, J.T., Love, N.G., Smith, M.L., and Wheeler, E.R. (1998) The effect of cationic salt addition on the settling and dewatering properties of an industrial activated sludge. *Water Environment Research,* **70** (5), 984-996.

Pietersen, B., Brözel, V., and Cloete, T. (1996) The response of *Escherichia coli* K12 upon exposure to hypochlorous acid and hydrogen peroxide. *Water SA,* **22** (1), 43-48.

Ramirez, G.W., Alonso, J.L., Villanueva, A., Guardino, R., Basiero, J.A., Bernecer, I., and Morenilla, J. (2000) A rapid, direct method for assessing chlorine effect on filamentous bacteria in activated sludge. *Water Research,* **34** (15), 3894-3898.

Saayman, G.B., Schutte, C.F., and Van Leeuwen, J. (1998) Chemical control of filamentous sludge bulking in a full-scale biological nutrient removal activated sludge plant. *Ozone: Science & Engineering,* **20** (1), 1-16.

Saby, S., Leroy, P., and Block, J.-C. (1999) *Escherichia coli* resistance to chlorine and glutathione synthesis in response to oxygenation and starvation. *Applied and Environmental Microbiology,* **65** (12), 5600-5603.

Thompson, G., Swain, J., Kay, M., and Forster, C.F. (2001) The treatment of pulp and paper mill effluent: A review. *Bioresource Technology,* **77** (3), 275-286.

Tietze, F. (1969) Enzymatic method for quantitation determination of nanogram amounts of total and oxidized glutathione: applications to mammalian blood and other tissues. *Analytical Biochemistry,* **27** (3), 502-522.

Table 1 Effluent VSS values for SBR reactors described in Figures 2 and 3. One standard deviation is provided in parenthesis.

Reactor Condition	Effluent VSS (mg/L) before challenge	Effluent VSS (mg/L) after challenge
POTW #1		
Control	6.0 (1.3)	6.6 (0.8)
NEM	4.2 (1.6)	39.7 (1.0)
4 mg NaOCl as Cl_2/g MLVSS - Challenge I	10.2 (1.9)	13.7 (3.0)
8 mg NaOCl as Cl_2/g MLVSS - Challenge I	8.9 (0.3)	34.1 (0.9)
8 mg NaOCl as Cl_2/g MLVSS - Challenge II	9.1 (1.3)	30.5 (1.4)
POTW #2		
Control	4.7 (0.6)	7.0 (1.1)
NEM	5.0 (0.2)	53.9 (1.8)
4 mg NaOCl as Cl_2/g MLVSS - Challenge I	7.1 (0.9)	14.4 (1.3)
10 mg NaOCl as Cl_2/g MLVSS - Challenge I	7.2 (0.8)	28.2 (0.3)
10 mg NaOCl as Cl_2/g MLVSS - Challenge II	6.0 (1.6)	25.0 (0.3)

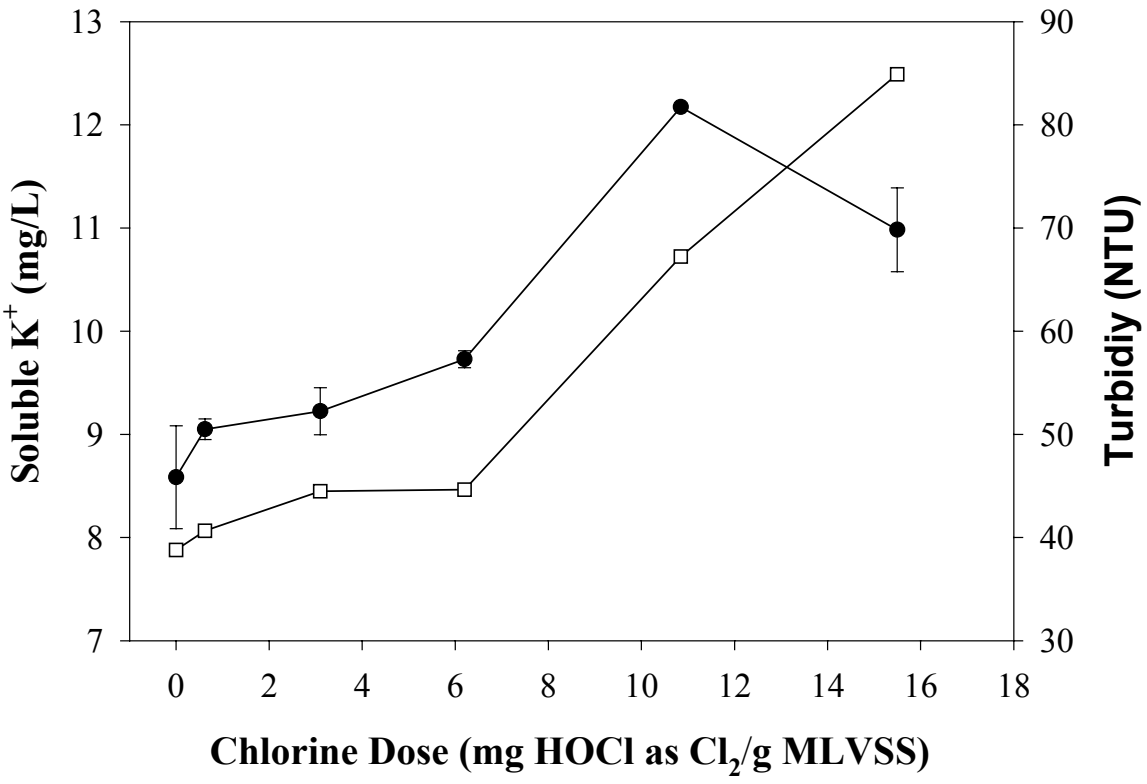

Figure 2-1 Soluble K^+ release and supernatant turbidity of mixed liquor (POTW#1) over various chlorine mass doses. Legend: • represents soluble K^+ values, and □ represents effluent turbidity. Error bars represent one standard deviation and are fully contained within some symbols.

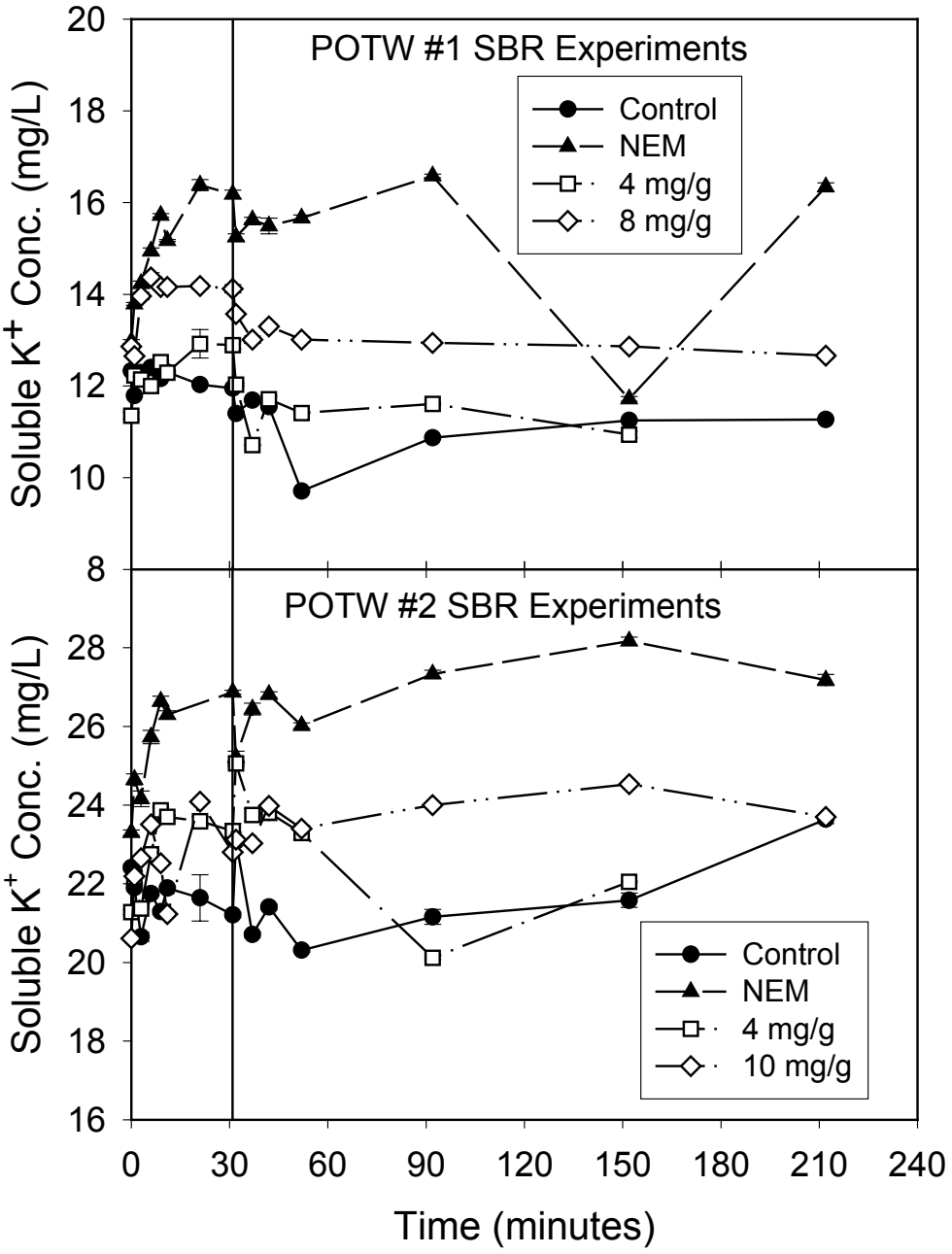

Figure 2-2. **Soluble K^+ concentrations over time during SBR experiments for both POTWs. NaOCl or NEM were added to stressed reactors within the first minute, and primary effluent was added at 31 minutes (designated by the vertical line). Error bars represent one standard deviation and are contained within the symbols in most cases.**

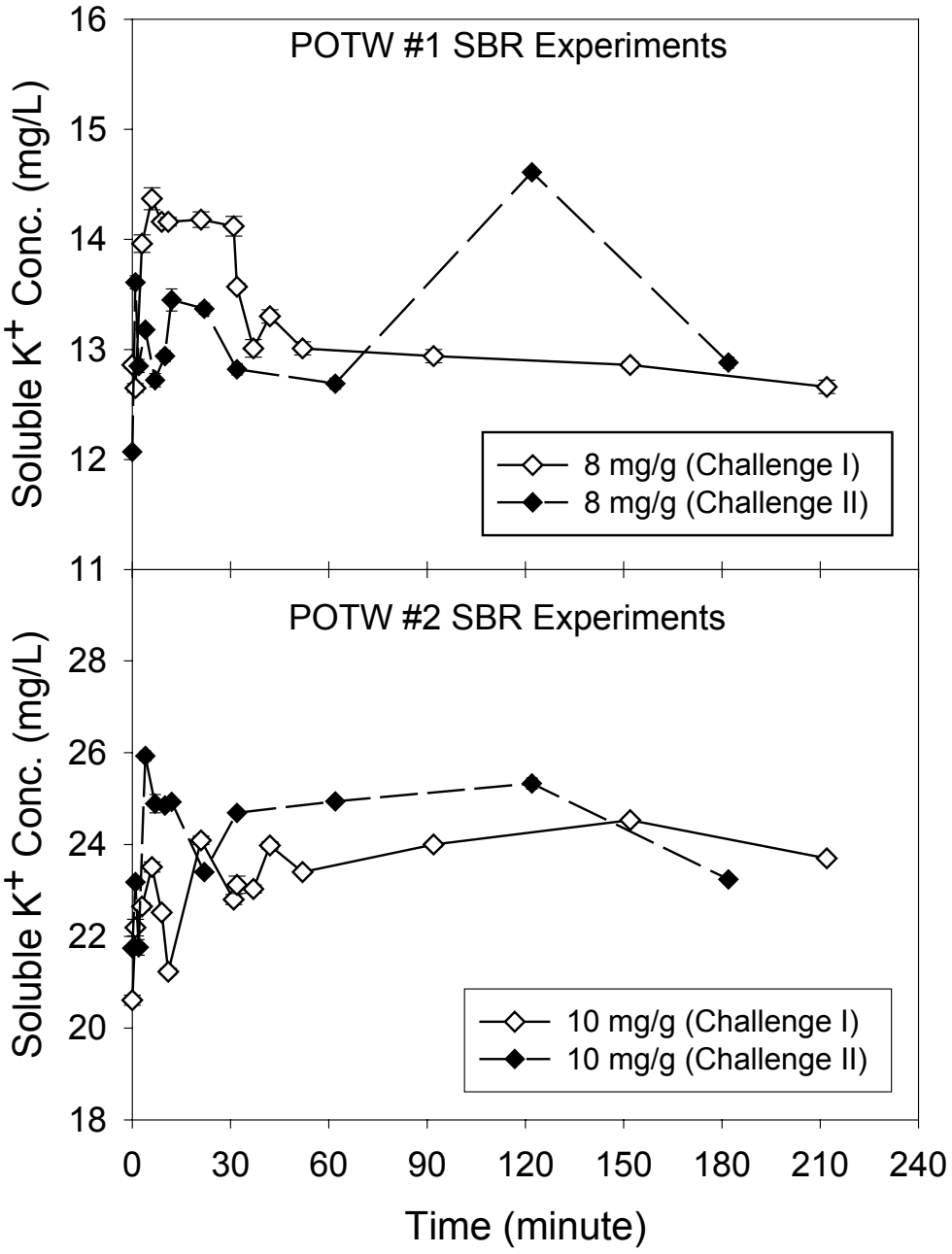

Figure 2-3. **Soluble K^+ efflux from SBRs where NaOCl was added within first minute, and primary effluent was added either 30 minutes later (Challenge I, data repeated from Figure 2) or immediately after NaOCl addition (Challenge II). Error bars represent one standard deviation and are contained within the symbols in most cases.**

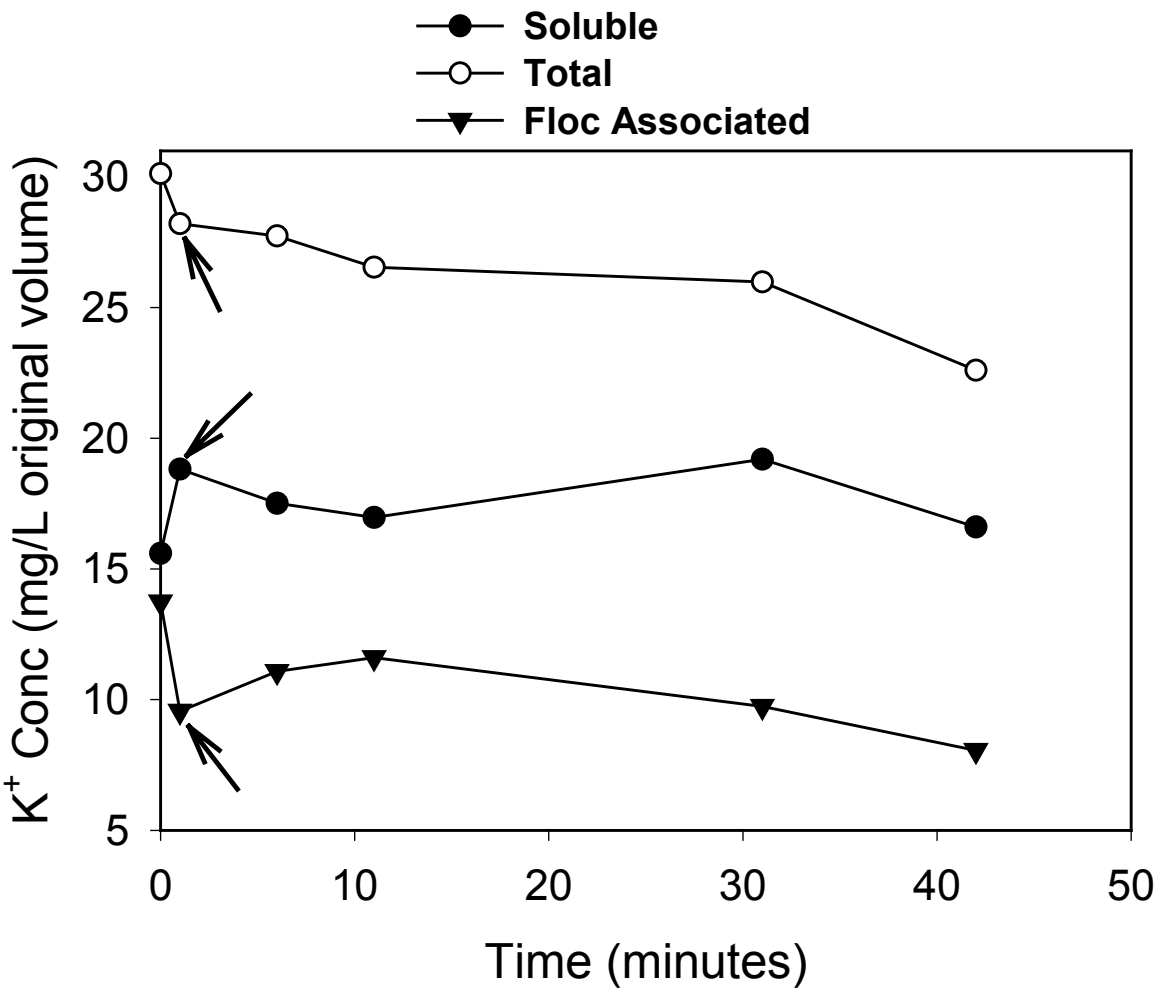

Figure 2-4. **Distribution of K^+ between bulk liquid and floc-associated phases for POTW #1 exposed to 8 mg NaOCl as Cl_2/g MLVSS under Challenge I conditions. Block arrows represent the sample immediately following NaOCl challenge. Error bars represent one standard deviation and are completely contained within the symbols.**

Chapter 4

Engineering Significance

Efficient and effective wastewater treatment systems are integral to protecting the health of receiving waters and the health of citizens. When upset events, such as poor BOD/COD removal, decreased nitrification, deflocculation and many others, occur at wastewater treatment facilities operators are typically forced to react to the effect of the upset with little time to troubleshoot the cause. Reactive responses may only minimize the effect of an upset and the available responses that operators have are limited. If operators are provided with a warning of an impending upset event they may initiate a course of action that may prevent an upset or mitigate the effects of the upset before the effects are quantifiable. The ability to provide an early upset warning device relies upon having both knowledge of the mechanism, biological or chemical, which is the cause of the upset, and upon having the technology to relay this information to the operator. The research conducted in support of this thesis sought to provide information to improve both the mechanistic knowledge and the available technology for the development of upset early warning systems for wastewater operators.

Filamentous bulking impacts the ability of wastewater operators to control the mass of solids in activated sludge systems. The operating maxim that you must "waste what you make" is directly impacted by filamentous bulking. The lack of freedom to control sludge age prevents operators from responding to varied flow and loading conditions, and may impact BOD/COD

removal and nitrification. In the event of a rain event, filamentous bulking may result in the loss of the sludge blanket from the secondary clarifier. Therefore, it is important to prevent and/or control filamentous bulking events.

The ability to control filamentous bulking with chlorine addition allows operators to regain control of the biomass inventory within the system. Chlorine addition is relatively inexpensive, in comparison to commercial polymer addition, is readily available (if effluent chlorination is employed), and typically controls filamentous bulking by selectively killing the filamentous bacteria. It has often been observed that extended chlorination will result in deflocculation and a decrease in final effluent quality. The existence of deflocculation events exemplifies a condition where operators are forced to react to an upset rather than proactively prevent the upset. This reactive situation occurs because the mechanism of chlorine induced deflocculation has not been elucidated. This research hypothesized and supported the idea that the mechanism of chlorine-induced activated sludge deflocculation is the GGKE mechanism. The ability to define the mechanism may allow operators to apply chlorine in a manner so that deflocculation does not occur, but so that filamentous bulking is still controlled. Knowing the mechanism may allow for use of on-line sensors to measure changes in K^+ concentration throughout the system. Alternatively, knowing the mechanism may lead to improved methods for application of chlorine. With this knowledge the ability to operate a wastewater treatment facility in an effective and efficient manner will improve.

The next challenge facing wastewater treatment facilities is the extension of mechanistic knowledge to development of upset early warning technologies. Existing upset early warning

devices (UEWDs) provide an indication of an impending upset but do not identify the source or the mechanism (cause) of the upset. Development of a biosensor to predict chlorine-induced activated sludge deflocculation seeks to fill that void for electrophile-induced deflocculation.

By involving bacteria in the biosensor, the biosensor will be able to predict deflocculation and identify the cause of the deflocculation, GGKE. Without the biological element of the UEWD, the sensor will only indicate that an increase in K has occurred. This may be due to an alteration in influent loading or due to GGKE. Use of a whole cell biosensor pins the increase in K+ to a physiological response indicative of electrophile-induced stress. Without knowing the mechanism, the operator cannot properly react to the information. When the operator is provided with warning of a GGKE event, the influent may be diverted to storage or polymer addition may be initiated. If the operator was provided with information indicating that an increase in K^+ was imminent, they could begin polymer addition until the threat subsided. Since polymer is expensive, use of the biosensor allows operators to minimize their use of polymer to only those situations when it is likely to be needed.

The extension of the knowledge base for chlorine deflocculation mechanisms and the development of a biosensor, which incorporates mechanistic information, will advance wastewater treatment from a reactive enterprise to a proactive one. This advancement will provide more efficient and effective wastewater treatment to the benefit of the environment and the citizens served by the facility.

Appendix 1-a

Data for Chapter #2

Growth curve for K-12 at 20°C for LB media
Cultures were inoculated from a stationary phase culture of LB media to 1e4 cfu/ml based on the assumption that 1e9 cfu/ml is equal to an optical density of 1
Abs is absorbance or optical density at 580 nm

Elapsed Time (hours)	Abs (read)	Dilution	Abs (total)		Abs (read)	Dilution	Abs (total)		Abs (read)	Dilution	Abs (total)		Elapsed Time (hours)	Abs (average)
0	0	1	0		0	1	0		0	1	0		0	0.00
8	0	1	0		0	1	0		0	1	0		8	0.00
10	0.01	1	0.01		0.005	1	0.005		0.005	1	0.005		10	0.01
12	0.02	1	0.02		0.02	1	0.02		0.03	1	0.03		12	0.02
14	0.07	1	0.07		0.09	1	0.09		0.08	1	0.08		14	0.08
16	0.28	1	0.28		0.3	1	0.3		0.3	1	0.3		16	0.29
18	0.7	1	0.7		0.75	1	0.75		0.75	1	0.75		18	0.73
19	0.52	2	1.04		0.54	2	1.08		0.48	2	0.96		19	1.03
20	0.52	3	1.56		0.54	3	1.62		0.48	3	1.44		20	1.54
21	0.49	4	1.96		0.53	4	2.12		0.49	4	1.96		21	2.01
22	0.47	5	2.35		0.52	5	2.6		0.48	5	2.4		22	2.45
23	0.58	5	2.9		0.53	5	2.65		0.51	5	2.55		23	2.70
26	0.43	6	2.58		0.52	6	3.12		0.45	6	2.7		26	2.80
28	0.52	6	3.12		0.49	6	2.94		0.49	6	2.94		28	3.00
30	0.52	6	3.12		0.48	6	2.88		0.54	6	3.24		30	3.08
32	0.47	6	2.82		0.51	6	3.06		0.48	6	2.88		32	2.92

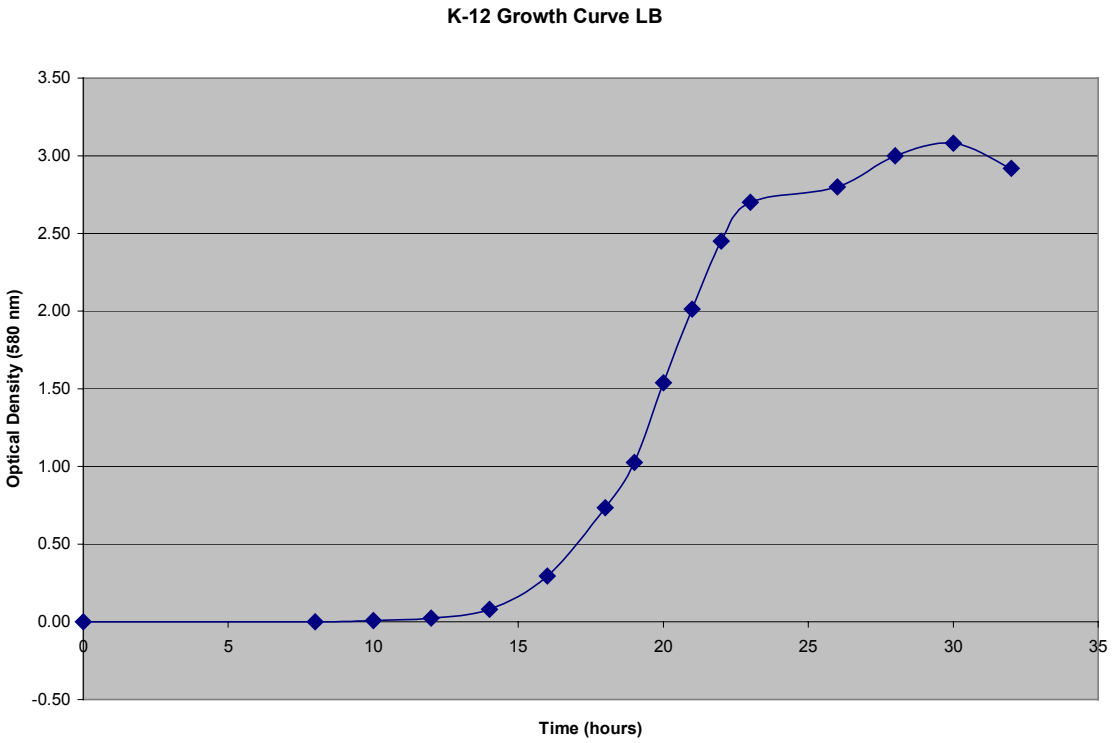
K-12 Growth Curve LB
Optical Density (580 nm)
3.50
3.00
2.50
2.00
1.50
1.00
0.50
0.00
-0.50
0
5
10
15
20
25
30
35
Time (hours)

Appendix 1-b

Growth curves

Cultures were inoculated from a stationary phase culture of the same media to 1e4 cfu/ml based on the assumption that 1e9 cfu/ml is equal to an optical density of 1

	Optical Density (580 nm)	
Time (hr)	M9	M9 LN
88	0.07	
92	0.1	
92		0.005
108	0.33	
110	0.35	
112	0.39	
132		0.02
133	0.8	
138	0.9	
143	1	
145	1.05	
150	1.1	
156		0.155
160	1.12	
160		0.24
165		0.4
170	1.15	
189		0.7
201		0.95
205		1
210		1.05
220		1.1
230		1.1
240		1.12

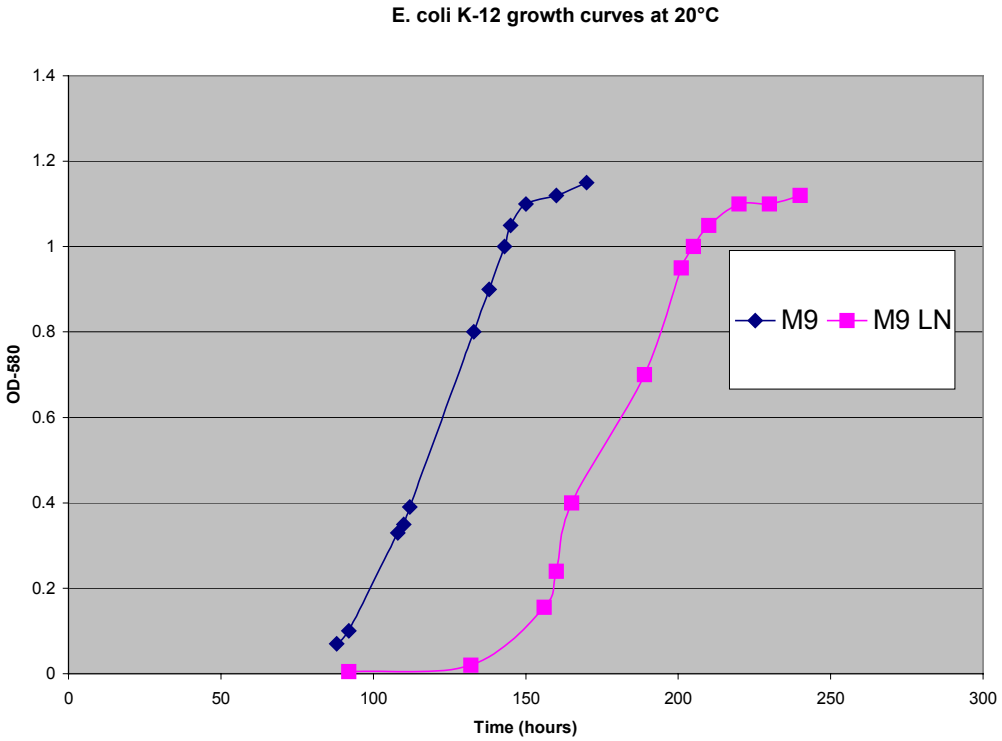
E. coli K-12 growth curves at 20°C
OD-580
Time (hours)
M9
M9 LN
0
0.2
0.4
0.6
0.8
1
1.2
1.4
0
50
100
150
200
250
300

Appendix 1-c

Attachment to polycarbonate plastic in different growth states
threshold is a function in the image analysis program that adjusts image quality
Roman numerals represent replicate pieces of plastic

LB early log	Sample 1					LB stationary						LB late log		late log	LB	
Field	# Live	# Dead	Threshold	%live		Field	# Live	# Dead	Threshold	%live		Field	# Live	# Dead	Threshold	%live
1	72	91	38	44.2		1	83	28	38	74.8		1	137	65	89	67.8
2	80	104	38	43.5		2	72	196	38	26.9		2	53	31	38	63.1
3	62	74	38	45.6		3	139	147	38	48.6		3	90	38	123	70.3
II						II						II				
Field	# Live	# Dead	Threshold	%live		Field	# Live	# Dead	Threshold	%live		Field	# Live	# Dead	Threshold	%live
1	154	307	38	33.4		1	15	6	38	71.4		1	19	5	194	79.2
2	121	280	38	30.2		2	15	16	38	48.4		2	264	105	93	71.5
3	139	115	38	54.7		3	28	12	38	70.0		3	70	145	82	32.6
III						III						III				
Field	# Live	# Dead	Threshold	%live		Field	# Live	# Dead	Threshold	%live		Field	# Live	# Dead	Threshold	%live
1	40	58	38	40.8		1	128	106	38	54.7		1	104	13	113	88.9
2	58	35	38	62.4		2	87	93	38	48.3		2	43	48	65	47.3
3	68	40	38	63.0		3	91	46	38	66.4		3	54	24	74	69.2
	Average	St dev					Average	St dev					Average	St dev		
% live	46.4	11.6				% live	56.6	15.5				% live	65.5	16.7		
live cells	88.2	39.8				live cells	73.1	45.8				live cells	92.7	73.3		

M9LN early log						M9LN stationary						M9LN late log				
Field	# Live	# Dead	Threshold	%live		Field	# Live	# Dead	Threshold	%live		Field	# Live	# Dead	Threshold	%live
1	165	80	108	67.3		1	33	17	156	66.0		1	169	35	74	82.8
2						2	72	27	177	72.7		2	169	71	79	70.4
3	92	122	67	43.0		3	47	13	170	78.3		3	169	46	76	78.6
II						II						II				
Field	# Live	# Dead	Threshold	%live		Field	# Live	# Dead	Threshold	%live		Field	# Live	# Dead	Threshold	%live
1	61	134	94	31.3		1	46	43	141	51.7		1	92	4	128	95.8
2	224	3	99	98.7		2	47	82	155	36.4		2	132	4	88	97.1
3	119	5	81	96.0		3	133	80	106	62.4		3	163	4	138	97.6
III						III						III				
Field	# Live	# Dead	Threshold	%live		Field	# Live	# Dead	Threshold	%live		Field	# Live	# Dead	Threshold	%live
1	204	71	111	74.2		1	85	58	150	59.4		1	4	33	90	10.8
2	165	72	69	69.6		2	8	33	178	19.5		2	33	59	133	35.9
3	147	15	98	90.7		3	36	74	177	32.7		3	164	8	135	95.3
	Average	St dev					Average	St dev					Average	St dev		
% live	147.1	54.8				% live	57.6	40.9				% live	125.4	75.7		
live cells	67.4	19.7				live cells	47.5	21.2				live cells	63.2	31.7		

Growth media and state	**live cells**	**st dev live cells**	**% live cells**	**std dev % live**
LB early log	88.2	39.8	46.4	11.6
LB late log	92.7	73.3	65.5	16.7
LB stationary	73.1	45.8	56.6	15.5
M9 early log	38.8	30.0	40.6	27.7
M9 late log	26.0	28.6	26.6	9.7
M9 stationary	206.6	148.1	70.4	27.6
M9LN early log	147.8	54.8	67.4	19.7
M9LN late log	125.4	75.7	63.2	31.7
M9LN stationary	57.6	40.9	47.5	21.2

M9 early log						M9 stationary						m9 late log				
Field	# Live	# Dead	Threshold	%live		Field	# Live	# Dead	Threshold	%live		Field	# Live	# Dead	Threshold	%live
1	6	74	57	7.5		1	213	112	185	65.5		1	13	68	51	16.0
2	50	23	52	68.5		2	30	306	81	8.9		2	39	122	100	24.2
3	10	186	71	5.1		3	55	12	191	82.1		3	14	38	45	26.9
II						II						II				
Field	# Live	# Dead	Threshold	%live		Field	# Live	# Dead	Threshold	%live		Field	# Live	# Dead	Threshold	%live
1	59	34	61	63.4		1	333	16	115	95.4		1	14	30	80	31.8
2	96	229	65	29.5		2	192	25	109	88.5		2	12	57	70	17.4
3	22	19	90	53.7		3	443	39	138	91.9		3	4	10	73	28.6
III						III						III				
Field	# Live	# Dead	Threshold	%live		Field	# Live	# Dead	Threshold	%live		Field	# Live	# Dead	Threshold	%live
1	38	59	88	39.2		1	344	16	192	95.6		1	99	125	74	44.2
2	53	52	115	50.5		2	113	20	85	85.0		2	24	35	109	40.7
3	15	2	96	88.2		3	136	13	142	91.3		3	15	27	93	35.7
	Average	St dev					Average	St dev					Average	St dev		
% live	38.78	30.03				% live	206.6	148.1				% live	26.0	28.6		
live cells	40.56	27.70				live cells	70.4	27.6				live cells	26.6	9.7		

Appendix 1-d

Field is microscope field
Roman numerals depict replicate pieces of plastic
all conditions were run in triplicate
threshold is a function in the image analysis program that adjusts image quality
***** indicate Scion Image did not accurately count particles and manual count was performed

PETG ammonia							Acrylic Ammonia							Polycarbonate ammonia			
Field	# Live	# Dead	Threshold		Manual count of dead		Field	# Live	# Dead	Threshold		Manual count of dead		Field	# Live	# Dead	Threshold
1	29	3	77				1	8	800	72	*****	4		1	4	1	182
2	1	7	151				2	9	23	71				2	2	800	139
3	6	4	68				3	7	1000	70	*****	4		3	0	2	250
4	3	9	85														
II							II							II			
Field	# Live	# Dead	Threshold		Manual count of dead		Field	# Live	# Dead	Threshold		Manual count of dead		Field	# Live	# Dead	Threshold
1	15	30	108				1	10	3	98				1	36	20	40
2	15	28	83				2	8	1000	48	*****	4		2	30	31	51
3	3	25	88				3	15	1000	55	*****	1		3	17	16	65
4	10	72	100														
5	3	1	130														
III							III							III			
Field	# Live	# Dead	Threshold		Manual count of dead		Field	# Live	# Dead	Threshold		Manual count of dead		Field	# Live	# Dead	Threshold
1	23	11	94				1	57	10	59				1	60	23	70
2	10	2	117				2	72	25	88				2	54	22	83
3	17	3	98				3	65	84	63				3	10	3	93
4	15	2	110														
5	11	1	115														
Average	11.5																

PETG							Acrylic							Polycarbonate			
Field	# Live	# Dead	Threshold		Manual count of dead		Field	# Live	# Dead	Threshold		Manual count of dead		Field	# Live	# Dead	Threshold
1	30	13	43				1	69	46	130	*****	5		1	137	65	89
2	27	9	76				2	36	1	130				2	53	31	38
3	45	2	84				3	57	8	130				3	90	38	123
4	26	5	103				4	18	8	50							
II							II										
Field	# Live	# Dead	Threshold		Manual count of dead		Field	# Live	# Dead	Threshold		Manual count of dead		Field	# Live	# Dead	Threshold
1	35	13	90				1	31	14	61				1	19	5	194
2	10	10	84				2	19	21	61				2	264	105	93
3	17	8	169				3	22	894	54	*****	29		3	70	145	82
4	1	1	100				4	17	52	112							
							III							Field	# Live	# Dead	Threshold
							Field	# Live	# Dead	Threshold		Manual count of dead		1	104	13	113
							1	37	49	82				2	43	48	65
							2	21	7	79				3	54	24	74
							3	10	6	100							

PETG O2							Acrylic O2										
Field	# Live	# Dead	Threshold		Manual count of dead		I							Polycarbonate O2			
1	261	50	74				Field	# Live	# Dead	Threshold		Manual count of dead		Field	# Live	# Dead	Threshold
2	287	60	85				1	23	2	47				1	166	165	62
3	331	40	60				2	32	14	64				2	103	140	69
4	341	250	76	*****	50		3	15	22	55				3	152	11	103
5	414	15	71				4	28	12	39				4	350	126	72
							5	23	19	92				5	113	126	66
II							II										
Field	# Live	# Dead	Threshold		Manual count of dead		Field	# Live	# Dead	Threshold		Manual count of dead		II			
1	351	7	55				1	38	7	40				Field	# Live	# Dead	Threshold
2	332	14	57				2	29	33	47				1	72	15	97
3	314	100	150				3	41	31	54				2	88	37	68
4	422	1	67				4	24	2	59				3	133	11	78
5	409	36	69				5	26	8	80				5	88	18	80
6	223	59	69				6	37	12	63							
														III			
							III							Field	# Live	# Dead	Threshold
III							Field	# Live	# Dead	Threshold		Manual count of dead		1	173	17	121
Field	# Live	# Dead	Threshold		Manual count of dead		1	83	1000	43	****	100		2	188	385	102
1	620	614	39				2	52	31	59				3	83	3	90
2	667	57	32				3	55	54	51				4	135	27	56
3	988	75	41				4	75	3	65				5	223	3	106
4	1112	209	56				5	51	44	106				6	202	67	77
5	923	759	43				6	72	1000	73	*****	53					
6	294	30	35														
7	662	63	52														
8	447	255	63														
	Average # of live cells	St dev															
PC	92.7	73.3															
O2 PC	151.3	72.0															
NH3 PC	23.7	22.6															
AC	30.6	18.2															
O2 AC	41.4	20.2															
NH3 AC	27.9	27.9															
PETG	23.9	14.1															
O2 PETG	494.6	263.0															
NH3 PETG	11.5	8.2															

Appendix 1-e

Photobleaching Experiment
Fluorescent intensity of optode under continuous excitation
Fluorescent intensity determined with the density function of Scion Image

Time (min)	Fluorescent Intensity (*10e6)
0	20.60
1	21.42
2	21.50
3	21.33
4	20.29
5	19.94
10	19.27
15	16.65
20	13.77
25	13.05
30	12.45
35	12.07

Initial Optode standard curve, optode on polyester, befor
Detection of GGKE by E. coli batch culture

K

Standard (mg/L)	Intensity (*10e6)	Intensity	Average	Std dev
1	17.69348	16.45439	17.07	0.88
5		17.99098	17.99	0.00
10	18.98297	18.93553	18.96	0.03
15	19.82337	19.71337	19.77	0.08
20	20.41133	20.3394	20.38	0.05
25	21.19582	21.01867	21.11	0.13

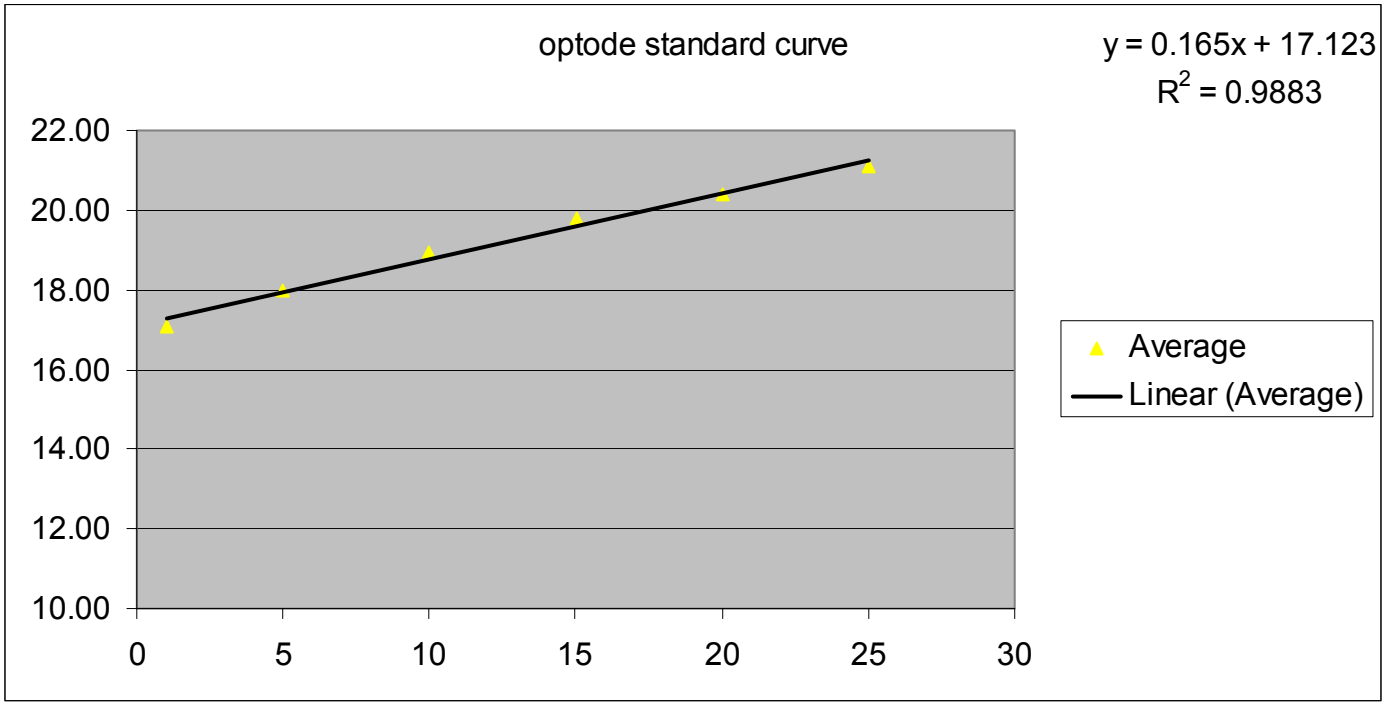

Standards and 10mg/L NEM batch study run on AA

		dilution factor	0.047619			
10 mg/l NEM						
Time	K+	K+	K+	average K+ (mg/L)	after dilution	st dev
0	0.878	0.878	0.877	0.878	18.43	0.01
1	0.844	0.888	0.879	0.870	18.28	0.49
20	1.001	1.02	1.004	1.008	21.18	0.21
Control						
Time	K+	K+	K+	average K+ (mg/L)	after dilution	st dev
0	0.873	0.872	0.867	0.871	18.28	0.07
1	0.844	0.837	0.842	0.841	17.66	0.08
20	0.849	0.847	0.844	0.847	17.78	0.05
Optode Standards						
	K+	K+	K+	average K+ (mg/L)		
5	0.12	0.12	0.12	2.52		
10	0.295	0.296	0.295	6.202		
15	0.426	0.428	0.427	8.967		
20	0.624	0.623	0.624	13.097		

Final Optode standard curve, optode on polyester
Detection of GGKE by E. coli batch culture
This curve uses values for the standards that come from measuring
the standards with AA and is used for quantifying unknown samples with the optode

Original K (mg/L)standard	K Standard (mg/L)	Intensity (*10e6)	Intensity	Average	Std dev		10 mg/L NEM samples	Time (min)	Intensity	Intensity	Average	St dev	Calculated K	st dev
5	2.52		17.99098	17.99	0.00			0	20.75915	20.73704	20.75	0.02	14.13759	0.010656
10	6.202	18.98297	18.93553	18.96	0.03			1	20.81293	20.69826	20.76	0.08	14.17038	0.055358
15	8.967	19.82337	19.71337	19.77	0.08			20	21.23128	21.27326	21.25	0.03	16.34019	0.022823
20	13.097	20.41133	20.3394	20.38	0.05									

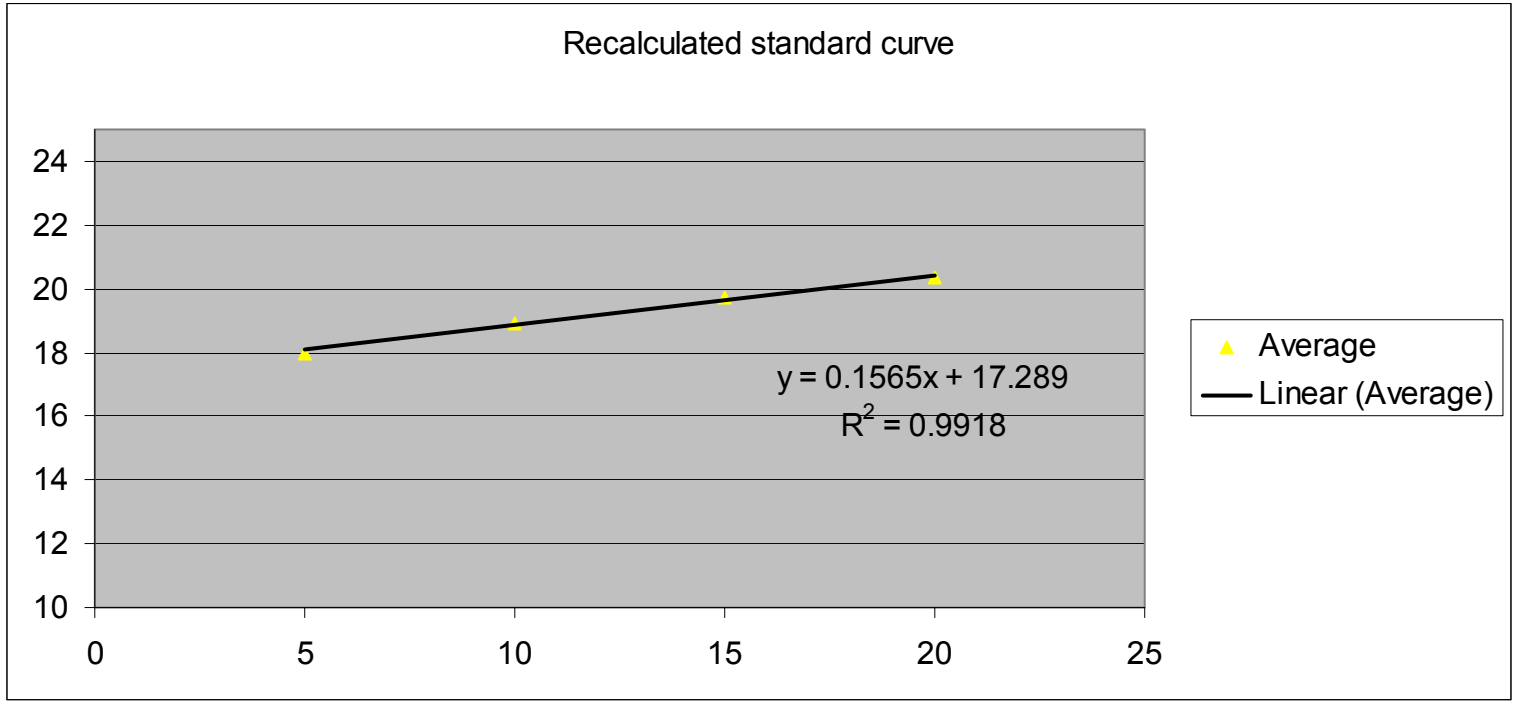

Appendix 2-a

Chapter #3 data

POTW#1
Batch test
HOCl addition with
turbidity and IC
potassium
Average MLVSS
1600 mg/L

	K+ 20 minutes after HOCl addition	
HOCl in reactor (mg Cl2/g MLVSS)	K+ (mg/L)	K+ (mg/L)
0.625	8.23	8.94
3.125	9.06	6.72
3.125	9.39	9.06
6.25	9.67	9.79
10.9	12.19	12.16
15.6	10.70	11.21
50 mg/L NEM	12.18	11.18
	Turbidity after settling	
HOCl in reactor (mg Cl2/g MLVSS)	Turbidity (NTU)	Turbidity (NTU)
0.625	39.5	38.1
3.125	39.8	41.5
3.125	45.5	43.5
6.25	45.3	44
10.9	85.3	84.5
15.6	68	66.5
50 mg/L NEM	44.4	44.5

11/29/01

Using Blacksburg Mixed Liquor and Influent gathered at 3pm
Temp ML = 20°C, influent 20.5°C
pH = 7.33
Fill reactor with 3.5 L of mixed liquor
allow to settle for 30 min
decant 1 L
mix
add HOCl
add 1L of influent

	conductivity (milli ohms)	
	sample #1	sample #2
mixed liquor	0.468	0.458
influent	0.536	0.561

Control

	conductivity (milli ohms)	
time	sample #1	sample #2
after decant	0.468	0.468
5 min after decant	0.472	0.47
after feed	0.491	0.494
5 min after feed	0.484	0.488

	conductivity (milli ohms)	
4mg HOCl / gMLVSS	sample #1	sample #2
after decant	0.475	0.492
5 min after decant	0.468	0.466
after HOCl	0.476	0.466
5 min after HOCl	0.464	0.483
after feed	0.501	0.498
5 min after feed	0.496	0.493

	conductivity (milli ohms)	
8mg HOCl / gMLVSS	sample #1	sample #2
after decant	0.468	0.459
after HOCl	0.499	0.488
5 min after HOCl	0.503	0.502
8 min after HOCl	0.503	0.506
after feed	0.508	0.506
5 min after feed	0.511	0.508

Appendix 2-b

Test of effectiveness of CsCl on Na interference
NaCl stock 5 g/L as Na

K Standard (mg/L)	Volume of standard (ml)	Na added (ml)	Na concentration (mg/L)	AA K+ (mg/L)	AA K+ (mg/L)	K+ with dilution (mg/L)	K+ with dilution (mg/L)
0.9	5	0	0	0.889	0.884	0.889	0.884
0.9	4.9	0.1	100	0.895	0.889	0.913	0.907
0.9	4.8	0.2	200	0.886	0.864	0.923	0.900
0.9	4.7	0.3	300	0.835	0.838	0.888	0.891
0.9	5	0.05	50	0.887	0.879	0.887	0.879

AA K+ are duplicate injections
K+ with dilution is the dilution resulting from the addition of NaCl stock to the K+ standard

Anova: Single Factor comparison of Na spiked vs no Na K+ standards
alpha = 0.05
SUMMARY

Groups	*Count*	*Sum*	*Average*	*Variance*
Column 1	8	7.189112	0.898639008	0.000222
Column 2	2	1.773	0.8865	1.25E-05

ANOVA

Source of Variation	*SS*	*df*	*MS*	*F*	*P-value*	*F crit*
Between Groups	0.000236	1	0.000235769	1.201971	0.304831	5.317645
Within Groups	0.001569	8	0.000196152			
Total	0.001805	9				

Appendix 2-c

Effect of Na on deflocculation with Blacksburg mixed liquor
20 minute settling period
use NaCl

Turbidity (NTU)

Condition	Beginning	End
Control	26.5	25.5
Control II	32.5	33.6
129 mg/L as Na	16	12.8
258 mg/L as Na	12.8	10.6

129 mg/L is 5.6 mM Na
258 mg/L is 11.2 mM Na

Anova: Single Factor between control and treated
alpha 0.05
SUMMARY

Groups	*Count*	*Sum*	*Average*	*Variance*
Column 1	2	59.1	29.55	32.805
Column 2	2	23.4	11.7	2.42

ANOVA

Source of Variation	*SS*	*df*	*MS*	*F*	*P-value*	*F crit*
Between Groups	318.6225	1	318.6225	18.0907	0.051079	18.51276
Within Groups	35.225	2	17.6125			
Total	353.8475	3				

t-Test: Paired Two Sample for Means for treated before and after
alpha =0.05

	Variable 1	*Variable 2*
Mean	14.4	11.7
Variance	5.12	2.42
Observations	2	2
Pearson Correlation	1	
Hypothesized Mean I	0	
df	1	
t Stat	5.4	
P(T<=t) one-tail	0.058286	
t Critical one-tail	6.313749	
P(T<=t) two-tail	0.116572	
t Critical two-tail	12.70615	

Appendix 2-4

IC cations for SBR experiment POTW #1 and #2
11-02 control is POTW #2
11-02 #3 is 10 mg/g HOCl Challenge I POTW #2
11-09 control is POTW #1
11-09 #3 is 10 mg/g HOCl Challenge I POTW #1

Legend
IB = sample immediately before chlorine addition
IAC = sample immediately after chlorine addition
all numerals (2, 5, 8 etc.) correspond to sample time after the addition of chlorine
samples labelled 2a, 5a, 10a etc correspond to sample time after the addition of primary
Roman numeral (II) = duplicate injection

No.	Name	Amount soluble Ca mg/L	Amount soluble K mg/L	Amount soluble Mg mg/L	Amount soluble Na mg/L	Amount soluble NH3 mg/L
1	nanopure	n.a.	0.0770	0.0168	0.0284	0.1408
2	nanopure	n.a.	0.1222	0.0036	0.2874	0.0639
3	1 mg/L std	0.8867	0.6624	0.8591	1.0224	2.7785
4	1 mg/L std	0.3877	0.7460	0.4513	1.0203	2.5397
5	5 mg/L std	4.0584	4.4830	4.1873	4.7854	9.9063
6	5 mg/L std	5.0315	4.1320	4.3652	4.7805	8.6298
7	10 mg/L std	9.8995	8.9776	9.5615	9.8359	14.1245
8	10 mg/L std	9.6082	8.7885	9.5996	9.8413	14.6864
9	20 mg/L std	19.9283	18.5053	21.2330	18.9736	22.1351
10	20 mg/L std	20.5816	18.6060	21.6619	19.5027	21.9602
11	50 mg/L std	n.a.	51.0294	49.7512	50.4217	48.0712
12	50 mg/L std	n.a.	50.7232	49.4171	50.2949	47.6085
13	nanopure	0.2174	0.0565	0.1145	0.0883	0.2626
14	nanopure	n.a.	0.0631	n.a.	0.0355	0.1102
15	11-02 control IB	16.0309	17.6180	7.9766	432.6567	n.a.
16	11-02 control IB II	17.7753	18.1341	9.3192	432.8917	n.a.
17	11-02 control IAC	19.3440	13.6850	7.1846	318.2957	n.a.
18	11-02 control IAC II	19.4544	13.7781	7.5846	318.1115	n.a.
19	11-02 Control 2	21.3765	15.6694	n.a.	351.5703	n.a.
20	11-02 control 2 II	20.6489	15.4710	9.2692	352.9248	n.a.
21	11-02 control 5	21.1752	19.8835	11.1434	469.3277	n.a.
22	11-02 control 5II	20.9982	19.6050	11.4033	469.7958	n.a.
23	11-02 control 8	18.7873	12.9814	7.8690	303.6995	n.a.
24	11-02 control 8 II	18.1192	13.0882	6.8141	304.6303	n.a.
25	11-02 control 10	21.4944	16.8932	10.1360	394.3815	n.a.
26	11-02 control 10II	21.7086	17.2177	10.9969	395.9050	n.a.
27	11-02 control 20	16.4094	14.4581	7.3347	345.9220	n.a.
28	11-02 control 20 II	17.8224	14.8915	8.2134	346.4543	n.a.
29	11-02 control 30	22.0040	14.7203	9.5221	330.0154	n.a.
30	11-02 control 30 II	21.8214	15.0011	9.3773	330.5788	n.a.
31	11-02 control IAF	15.6691	13.5972	7.1987	318.6347	7.6927
32	11-02 control IAF II	18.7154	14.2119	8.5823	319.4530	8.5720
33	11-02 control 5a	19.5395	17.3813	10.3758	397.0600	9.1854
34	11-02 control 5a II	17.0724	17.0967	9.2533	399.5816	9.1433
35	11-02 control 10a	23.5716	20.8925	14.0802	511.2051	n.a.
36	11-02 control 10a II	23.3031	20.9483	13.5342	509.7514	n.a.
37	11-02 control 20a	22.6091	21.3095	13.9481	510.8399	n.a.
38	11-02 control 20a II	n.a.	0.0141	n.a.	0.0491	1.4702
39	11-02 control 60a	19.1455	17.5934	9.6964	419.7016	n.a.
40	11-02 control 60a II	19.5477	17.5739	9.5187	420.4951	n.a.
41	11-02 control 120a	20.5084	19.8708	10.7904	465.5804	n.a.
42	11-02 control 120a II	21.0049	20.0346	10.3933	471.5187	n.a.
43	11-02 control 180a	23.7685	16.4812	10.1767	363.0057	n.a.
44	11-02 control 180a II	14.8792	16.4590	7.9547	361.7389	n.a.

45	11-02 #3 IB	23.5990	17.0701	10.4100	372.0349	n.a.
46	11-02 #3 IB II	16.9028	16.9301	8.0789	369.8347	n.a.
47	11-02 #3 5	14.1411	17.7569	7.5021	326.0966	n.a.
48	11-02 #3 5 II	16.0656	18.0770	8.0201	326.9752	n.a.
49	11-02 #3 IAC	12.8176	17.5506	6.4024	325.6113	n.a.
50	11-02 #3 IAC II	5.4408	6.6025	2.6380	127.0084	n.a.
51	11-02 #3 2	27.6320	22.8802	13.2408	422.0495	n.a.
52	11-02 #3 2 II	26.4040	22.7252	12.9544	421.3187	n.a.
53	11-02 #3 8	15.2546	22.8405	9.5192	446.0913	n.a.
54	11-02 #3 8 II	18.4654	23.1411	12.1076	444.7416	n.a.
55	11-02 #3 10	14.8815	18.5538	8.2653	344.5750	n.a.
56	11-02 #3 10 II	14.5495	18.7651	8.1135	344.7658	n.a.
57	11-02 #3 20	15.6125	21.0898	9.1868	396.0400	n.a.
58	11-02 #3 20 II	15.5857	20.4822	9.0214	394.9650	n.a.
59	11-02 #3 30	14.5626	20.9713	8.9285	423.6317	8.9940
60	11-02 #3 30 II	14.1887	21.1015	9.7631	425.1828	7.8164
61	11-02 #3 IAF	15.0492	21.5367	9.2060	420.8043	8.9523
62	11-02 #3 IAF II	15.3277	21.5616	8.5319	421.3920	7.5562
63	11-02 #3 5a	14.3127	20.4785	9.7951	398.6100	8.8727
64	11-02 #3 5a II	16.2725	20.4259	11.1754	398.1344	8.0184
65	11-02 #3 10a	15.1908	20.2645	9.2958	399.2994	7.5729
66	11-02 #3 10a II	14.0045	19.8798	9.0820	399.6961	5.9666
67	11-02 #3 20a	14.3053	21.2948	9.9188	435.1383	n.a.
68	11-02 #3 20a II	14.5990	21.3575	9.3178	436.5267	n.a.
69	11-02 #3 60a	26.7964	23.2954	13.7700	454.4540	n.a.
70	11-02 #3 60a II	27.3772	23.6958	14.0651	457.0097	n.a.
71	11-02 #3 120a	20.6910	20.5170	11.0202	402.4291	n.a.
72	11-02 #3 120a II	19.6522	19.9719	10.2513	401.6315	n.a.
73	11-02 #3 180a	24.7209	24.7286	13.2892	552.4774	22.3794
74	11-02 #3 180a II	25.3795	24.9278	13.7212	554.6233	25.2732
75	11-02 influent	25.7684	12.0898	11.9921	83.3670	2.9218
76	11-02 influent II	23.3790	12.6078	10.2421	82.7374	1.4248
77	11-09 control IAC	21.5582	10.8756	9.3408	70.9001	0.1998
78	11-09 control IAC	22.1802	11.3717	9.8464	71.1402	0.2062
79	11-09 control 2	23.7542	12.0521	10.9015	78.5959	0.2585
80	11-09 control 2 II	24.1083	12.0998	11.3789	78.6319	0.0611
81	11-09 control 5	20.7692	9.2751	8.1765	60.8236	0.9537
82	11-09 control 5II	16.2215	9.8375	6.4522	61.5029	0.9623
83	11-09 control 8	4.1117	0.3217	1.0083	2.4717	0.3058
84	11-09 control 8II	10.6664	10.6526	4.9728	69.1284	1.1853
85	11-09 control 10	24.6234	12.5121	11.6072	82.7957	0.3522
86	11-09 control 10II	21.8637	12.4619	10.2281	82.6241	0.0233
87	11-09 control 20	18.7973	10.4235	7.6380	67.9402	0.1426
88	11-09 control 20 II	21.2370	10.4097	8.8349	68.0844	0.2083
89	11-09 control 30	20.2888	10.8510	8.1407	70.1273	0.3259
90	11-09 control 30II	23.0575	10.8276	9.5730	70.2494	0.1693
91	11-09 control IAF	19.9512	9.3141	6.8156	63.1873	7.8051
92	11-09 control IAF II	22.6223	9.3208	7.8575	63.3419	8.0994
93	11-09 control 5a	24.0487	11.1164	10.7100	78.0507	9.2376
94	11-09 control 5a II	23.9722	11.1848	10.7609	78.5845	8.2401
95	11-09 control 10a	21.4372	10.1436	8.9737	69.0812	6.9154
96	11-09 control 10a II	19.5265	10.2240	7.5780	69.2591	6.9387
97	11-09 control 20a	25.3387	10.7075	11.1338	76.9851	6.5151
98	11-09 control 20a II	24.7467	10.7150	10.8853	77.1592	5.6451
99	11-09 control 60a	24.1013	9.7821	9.2229	66.8626	0.0103
100	11-09 control 60a II	21.1349	9.6919	7.2084	67.7256	n.a.
101	11-09 control 120a	21.5449	11.7103	9.7285	82.5485	n.a.
102	11-09 control 120a II	24.0359	11.6839	11.2781	82.5265	n.a.
103	11-09 control 180a	23.3912	10.9566	10.7236	80.0108	0.0542
104	11-09 control 180 a II	23.3460	11.3487	10.9890	80.2103	0.0508
105	11-09 influent II	20.1978	10.4370	10.6789	80.5862	22.0552
106	11-09 influent II	20.5925	10.6167	10.0457	80.8481	21.1180

107	nanopure	19.2335	9.9045	9.4063	72.6914	21.4559
108	nanopure	0.0128	0.1073	0.0425	0.2332	0.4451
109	11-09 #3 IB	23.9988	13.3145	11.9137	84.4320	0.7830
110	11-09 #3 IB II	24.8325	13.0945	12.2186	84.8314	0.8194
111	11-09 #3 IAC	23.7003	13.8905	11.5952	94.8696	2.1449
112	11-09 #3 IAC II	21.9832	13.9724	10.9625	94.6058	1.4135
113	11-09 #3 2	17.2463	15.0986	9.4044	95.4409	0.4187
114	11-09 #3 2 II	22.4759	15.5536	11.8084	96.1311	0.6885
115	11-09 #3 5	22.5486	15.2799	11.6781	95.8084	0.8254
116	11-09 #3 5 II	23.7895	15.4707	12.0780	95.8618	1.0483
117	11-09 #3 8	22.0436	14.6126	11.1101	91.3029	0.5291
118	11-09 #3 8II	22.0705	14.8736	11.2713	90.9497	0.2789
119	11-09 #3 10	22.0534	14.5974	11.3264	90.7373	0.4838
120	11-09 #3 10 II	0.2023	0.0723	0.0680	0.3369	0.1007
121	11-09 #3 20	26.2179	15.1335	12.6327	95.1295	1.7248
122	11-09 #3 20 II	21.3804	15.0959	11.2448	94.5791	1.8970
123	11-09 #3 30	16.9401	15.2057	9.7390	94.9272	n.a.
124	11-09 #3 30 II	21.5337	15.3557	11.7643	95.1158	n.a.
125	nanopure	20.4543	16.6428	11.4040	94.8768	12.4093

Appendix 2-d

Blacksburg is POTW #1
Legend
N = 50mg/L NEM
phi = control
1 = 4mg/g HOCl challenge I
2 = 4 mg/g HOCl challenge II
3 = 10 mg/g HOCl challenge I
4 = 10 mg/g HOCl chllenge II

Eff 1 = Effluent solids at Time 0
Eff 2 = Effluent solids following challenge

Pan Label	Tare g	Sample	Volume Ml	103C wt g	TSS mg/L	550C wt g	VSS mg/L
17-	1.1353	N EFF 1	450	1.1382	6.4	1.1360	4.9
6-	1.1294	N EFF 1	450	1.1315	4.7	1.1292	5.1
35	1.1347	N EFF 2	125	1.1439	73.6	1.1370	55.2
9-	1.1113	N EFF 2	150	1.1425	208.0	1.1346	52.7
30-	1.1357	N MLSS 1	10	1.1770	4130.0	1.1441	3290.0
14	1.1377	N MLSS 1	10	1.1801	4240.0	1.1463	3380.0
16-	1.1132	N MLSS 2	10	1.1666	5340.0	1.1414	2520.0
1-	1.1423	N MLSS 2	10	1.1727	3040.0	1.1485	2420.0
11E1	1.1241	1 EFF 1	450	1.1494	56.2	1.1465	6.4
3-	1.1221	1 EFF 1	450	1.1482	58.0	1.1447	7.8
20-	1.1153	2 EFF 1	450	1.1412	57.6	1.1380	7.1
11-	1.1174	2 EFF 1	450	1.1423	55.3	1.1393	6.7
26-	1.1389	3 EFF 1	450	1.1422	7.3	1.1387	7.8
27-	1.1366	3 EFF 1	450	1.1394	6.2	1.1364	6.7
7-	1.1305	4 EFF 1	450	1.1329	5.3	1.1307	4.9
24-	1.1143	4 EFF 1	450	1.1403	57.8	1.1371	7.1
13-	1.1376	Φ EFF 1	450	1.1404	6.2	1.1381	5.1
34-	1.1363	Φ EFF 1	450	1.1392	6.4	1.1373	4.2
19-	1.1156	Φ EFF 2	450	1.1410	56.4	1.1375	7.8
18E1	1.1215	Φ EFF 2	450	1.1467	56.0	1.1439	6.2
28-	1.1388	Φ MLSS 1	10	1.1800	4120.0	1.1475	3250.0
A3	1.1355	Φ MLSS 1	10	1.1764	6260.0	1.1440	3240.0
36-	1.1138	Φ MLSS 2	10	1.1751	6130.0	1.1430	3210.0
38-	1.1162	Φ MLSS 2	10	1.1773	6110.0	1.1533	2400.0
23-	1.1139	1 EFF 2	450	1.1442	67.3	1.1373	15.3
10-	1.1142	1 EFF 2	450	1.1435	65.1	1.1374	13.6
15-	1.1126	2 EFF 2	450	1.1423	66.0	1.1360	14.0
25-	1.1118	2 EFF 2	450	1.1420	67.1	1.1354	14.7
8-	1.1336	3 EFF 2	250	1.1420	33.6	1.1349	28.4
18	1.1370	3 EFF 2	250	1.1448	31.2	1.1378	28.0
A10	1.1086	4 EFF 2	250	1.1162	30.4	1.1100	24.8
A11	1.1062	4 EFF 2	250	1.1134	28.8	1.1071	25.2
2-	1.1453	1 MLSS 1	10	1.1864	4110.0	1.1535	3290.0
12-	1.1378	1 MLSS 1	10	1.1789	4110.0	1.1469	3200.0
32-	1.1321	2 MLSS 1	10	1.1741	4200.0	1.1487	2540.0
31-	1.1333	2 MLSS 1	10	1.1681	3480.0	1.1485	1960.0
29-	1.1142	3 MLSS 1	10	1.1751	6090.0	1.1450	3010.0
21-	1.1154	3 MLSS 1	10	1.1752	5980.0	1.1456	2960.0
A2	1.1378	4 MLSS 1	10	1.1763	3850.0	1.1461	3020.0
A9	1.1094	4 MLSS 1	10	1.1463	3690.0	1.1162	3010.0
37-	1.1172	1 MLSS 2	10	1.1782	6100.0	1.1162	6200.0
5-	1.1083	1 MLSS 2	10	1.1683	6000.0	1.1162	5210.0
A1	1.1316	2 MLSS 2	10	1.1726	4100.0	1.1162	5640.0
A8	1.1068	2 MLSS 2	10	1.1432	3640.0	1.1162	2700.0
4-	1.1313	3 MLSS 2	10	1.1660	3470.0	1.1379	2810.0
A7	1.1054	3 MLSS 2	10	1.1415	3610.0	1.1127	2880.0
A5	1.1052	4 MLSS 2	10	1.1412	3600.0	1.1122	2900.0
A6	1.1052	4 MLSS 2	10	1.1420	3680.0	1.1127	2930.0
A1	1.1346	PFB1 MLSS	10	1.1755	4090.0	1.1438	3170.0
A2	1.1317	PFB1 MLSS	10	1.1725	4080.0	1.1409	3160.0
27	1.135	PFB2 MLSS	10	1.1608	2580.0	1.1411	1970.0
*** 26	1.1363	PFB2 MLSS	10	1.6946	55830.0	1.1426	55200.0

Measurement of HOCl stock
DPD chlorine titration
FAS Normality 0.05
Std Methods
Normality 0.00282
Multiplication
factor 17.723

Assay #	Bleach added (ml)	Total sample volume (ml)	FAS start	FAS end	Delta	HOCl (mg Cl2/ml)
1	1	100	2.32	2.68	0.36	638.028
2	1	100	2.68	3.06	0.38	673.474
3	1	100	3.02	3.38	0.36	638.028
					Average HOCl	649.843333

note: Standard methods utilizes a FAS with normality of 0.00282. The DPD titration was performed with FAS with a Normality of 0.05 requiring the multiplication factor of 17.723

Control Reactor Challenge I
AA analysis
Sample volume refers to sample that had been centrifuged and then filtered through 0.45µm filter
Acid is volume of digestion acid added to sample

				AA determined K				K+ (mg/L) after dilution calculation						
Sample (minutes after chlorine challenge or addition of primary	Minutes after start of experiment	Acid (ml)	Sample volume (ml)	K	K	K	K	Calc K	Calc K	Calc K	Calc K	Average K+ (mg/L)	St dev	Sample
Before Cl2	0	10	1	1.229	1.237	1.232	1.244	12.29	12.37	12.32	12.44	12.33	0.04	Before Cl2
After Cl2	1	10	1	1.179	1.173	1.184	1.183	11.79	11.73	11.84	11.83	11.79	0.06	After Cl2
+2	3	10	1	1.226	1.226	1.234	1.232	12.26	12.26	12.34	12.32	12.29	0.05	+2
+5	6	10	1	1.23	1.241	1.248	1.245	12.3	12.41	12.48	12.45	12.40	0.09	+5
+8	9	10	1	1.208	1.215	1.224	1.221	12.08	12.15	12.24	12.21	12.16	0.08	+8
+10	11	10	1	1.224	1.231	1.235	1.238	12.24	12.31	12.35	12.38	12.30	0.06	+10
+20	21	10	1	1.201	1.204	1.203	1.208	12.01	12.04	12.03	12.08	12.03	0.02	+20
+30	31	10	1	1.19	1.2	1.196	1.199	11.9	12	11.96	11.99	11.95	0.05	+30
After feed	32	10	1	1.137	1.141	1.143	1.144	11.37	11.41	11.43	11.44	11.40	0.03	After feed
+5	37	10	1	1.159	1.176	1.173	1.166	11.59	11.76	11.73	11.66	11.69	0.09	+5
+10	42	10	1	1.151	1.157	1.158	1.166	11.51	11.57	11.58	11.66	11.55	0.04	+10
+20	52	10	1	0.97	0.974	0.968	0.971	9.7	9.74	9.68	9.71	9.71	0.03	+20
+60	92	10	1	1.085	1.086	1.089	1.087	10.85	10.86	10.89	10.87	10.87	0.02	+60
+120	152	10	1	1.12	1.129	1.127	1.147	11.2	11.29	11.27	11.47	11.25	0.05	+120
+180	212	10	1	1.12	1.133	1.129	1.132	11.2	11.33	11.29	11.32	11.27	0.07	+180

50 mg/L NEM Reactor Challenge I
AA analysis
Sample volume refers to sample that had been centrifuged and then filtered through 0.45µm filter
Acid is volume of digestion acid added to sample

				AA determined K				K+ (mg/L) after dilution calculation						
Sample (minutes after chlorine challenge or addition of primary	Minutes after start of experiment	Acid (ml)	Sample volume (ml)	K	K	K	K	Calc K	Calc K	Calc K	Calc K	Average K+ (mg/L)	St dev	Sample
Before Cl2	0	10	1	1.293	1.296	1.302	1.298	12.93	12.96	13.02	12.98	12.97	0.04	Before Cl2
After Cl2	1	10	1	1.382	1.38	1.374	1.38	13.82	13.8	13.74	13.8	13.79	0.03	After Cl2
+2	3	10	1	1.414	1.427	1.424	1.427	14.14	14.27	14.24	14.27	14.23	0.06	+2
+5	6	10	1	1.485	1.494	1.493	1.503	14.85	14.94	14.93	15.03	14.94	0.07	+5
+8	9	10	1	1.566	1.575	1.57	1.575	15.66	15.75	15.7	15.75	15.72	0.04	+8
+10	11	10	1	1.515	1.515	1.517	1.519	15.15	15.15	15.17	15.19	15.17	0.02	+10
+20	21	10	1	1.629	1.631	1.636	1.655	16.29	16.31	16.36	16.55	16.38	0.12	+20
+30	31	10	1	1.608	1.614	1.626	1.625	16.08	16.14	16.26	16.25	16.18	0.09	+30
After feed	32	10	1	1.515	1.529	1.528	1.529	15.15	15.29	15.28	15.29	15.25	0.07	After feed
+5	37	10	1	1.566	1.569	1.557	1.557	15.66	15.69	15.57	15.57	15.62	0.06	+5
+10	42	10	1	1.534	1.538	1.552	1.572	15.34	15.38	15.52	15.72	15.49	0.17	+10
+20	52	10	1	1.562	1.559	1.574	1.569	15.62	15.59	15.74	15.69	15.66	0.07	+20
+60	92	10	1	1.653	1.663	1.658	1.658	16.53	16.63	16.58	16.58	16.58	0.04	+60
+120	152	10	1	1.166	1.172	1.173	1.178	11.66	11.72	11.73	11.78	11.72	0.05	+120
+180	212	10	1	1.621	1.634	1.639	1.641	16.21	16.34	16.39	16.41	16.34	0.09	+180

4mg/g HOCl Reactor Challenge I
AA analysis
Sample volume refers to sample that had been centrifuged and then filtered through 0.45µm filter
Acid is volume of digestion acid added to sample

				AA determined K				K+ (mg/L) after dilution calculation						
Sample (minutes after chlorine challenge or addition of primary	Minutes after start of experiment	Acid (ml)	Sample volume (ml)	K	K	K	K	Calc K	Calc K	Calc K	Calc K	Average K+ (mg/L)	St dev	Sample
Before Cl2	0	10	1	1.125	1.139	1.142	1.135	11.25	11.39	11.42	11.35	11.35	0.07	Before Cl2
After Cl2	1	10	1	1.216	1.224	1.224	1.226	12.16	12.24	12.24	12.26	12.23	0.04	After Cl2
+2	3	10	1	1.206	1.213	1.221	1.214	12.06	12.13	12.21	12.14	12.14	0.06	+2
+5	6	10	1	1.199	1.199	1.2	1.202	11.99	11.99	12	12.02	12.00	0.01	+5
+8	9	10	1	1.248	1.254	1.253	1.258	12.48	12.54	12.53	12.58	12.52	0.03	+8
+10	11	10	1	1.221	1.229	1.231	1.234	12.21	12.29	12.31	12.34	12.29	0.06	+10
+20	21	10	1	1.258	1.302	1.317	1.286	12.58	13.02	13.17	12.86	12.92	0.31	+20
+30	31	10	1	1.279	1.286	1.294	1.295	12.79	12.86	12.94	12.95	12.89	0.08	+30
After feed	32	10	1	1.201	1.202	1.206	1.203	12.01	12.02	12.06	12.03	12.03	0.03	After feed
+5	37	10	1	1.07	1.071	1.071	1.078	10.7	10.71	10.71	10.78	10.71	0.01	+5
+10	42	10	1	1.164	1.173	1.177	1.177	11.64	11.73	11.77	11.77	11.71	0.07	+10
+20	52	10	1	1.139	1.143	1.142	1.141	11.39	11.43	11.42	11.41	11.41	0.02	+20
+60	92	10	1	1.159	1.162	1.163	1.161	11.59	11.62	11.63	11.61	11.61	0.02	+60
+120	152	10	1	1.088	1.093	1.101	1.104	10.88	10.93	11.01	11.04	10.94	0.07	+120

4mg/g HOCl Reactor Challenge II
AA analysis
Sample volume refers to sample that had been centrifuged and then filtered through 0.45µm filter
Acid is volume of digestion acid added to sample

				AA determined K				K+ (mg/L) after dilution calculation						
Sample (minutes after chlorine challenge or addition of primary	Minutes after start of experiment	Acid (ml)	Sample volume (ml)	K	K	K	K	Calc K	Calc K	Calc K	Calc K	Average K+ (mg/L)	St dev	Sample
Before Cl2	0.01	10	1	1.566	1.563	1.574	1.574	15.66	15.63	15.74	15.74	15.69	0.06	Before Cl2
After Cl2	1.01	10	1	1.234	1.239	1.247	1.25	12.34	12.39	12.47	12.5	12.43	0.07	After Cl2
After feed	2	10	1	1.226	1.23	1.235	1.234	12.26	12.3	12.35	12.34	12.31	0.04	After feed
+2	4	10	1	1.189	1.196	1.195	1.198	11.89	11.96	11.95	11.98	11.95	0.04	+2
+5	7	10	1	1.24	1.247	1.245	1.25	12.4	12.47	12.45	12.5	12.46	0.04	+5
+8	10	10	1	1.21	1.216	1.215	1.213	12.1	12.16	12.15	12.13	12.14	0.03	+8
+10	12	10	1	1.194	1.185	1.191	1.189	11.94	11.85	11.91	11.89	11.90	0.04	+10
+20	22	10	1	1.166	1.172	1.18	1.185	11.66	11.72	11.8	11.85	11.76	0.08	+20
+30	32.01	10	1	1.206	1.204	1.213	1.219	12.06	12.04	12.13	12.19	12.11	0.07	+30
+60	62	10	1	1.184	1.199	1.2	1.2	11.84	11.99	12	12	11.96	0.08	+60
+120	122	10	1	1.16	1.168	1.167	1.17	11.6	11.68	11.67	11.7	11.66	0.04	+120
+180	182	10	1	1.221	1.223	1.227	1.224	12.21	12.23	12.27	12.24	12.24	0.02	+180

8 mg/g HOCl Reactor Challenge I
AA analysis
Sample volume refers to sample that had been centrifuged and then filtered through 0.45µm filter
Acid is volume of digestion acid added to sample

				AA determined K				K+ (mg/L) after dilution calculation						
Sample (minutes after chlorine challenge or addition of primary	Minutes after start of experiment	Acid (ml)	Sample volume (ml)	K	K	K	K	Calc K	Calc K	Calc K	Calc K	Average K+ (mg/L)	St dev	Sample
Before Cl2	0	10	1	1.29	1.287	1.284	1.282	12.9	12.87	12.84	12.82	12.86	0.03	Before Cl2
After Cl2	1	10	1	1.262	1.264	1.263	1.27	12.62	12.64	12.63	12.7	12.65	0.04	After Cl2
+2	3	10	1	1.385	1.394	1.401	1.403	13.85	13.94	14.01	14.03	13.96	0.08	+2
+5	6	10	1	1.429	1.431	1.438	1.451	14.29	14.31	14.38	14.51	14.37	0.10	+5
+8	9	10	1	1.417	1.42	1.414	1.414	14.17	14.2	14.14	14.14	14.16	0.03	+8
+10	11	10	1	1.412	1.415	1.415	1.422	14.12	14.15	14.15	14.22	14.16	0.04	+10
+20	21	10	1	1.412	1.412	1.422	1.425	14.12	14.12	14.22	14.25	14.18	0.07	+20
+30	31	10	1	1.399	1.415	1.419	1.414	13.99	14.15	14.19	14.14	14.12	0.09	+30
After feed	32	10	1	1.355	1.358	1.354	1.36	13.55	13.58	13.54	13.6	13.57	0.03	After feed
+5	37	10	1	1.289	1.304	1.305	1.305	12.89	13.04	13.05	13.05	13.01	0.08	+5
+10	42	10	1	1.321	1.331	1.333	1.335	13.21	13.31	13.33	13.35	13.30	0.06	+10
+20	52	10	1	1.296	1.296	1.301	1.309	12.96	12.96	13.01	13.09	13.01	0.06	+20
+60	92	10	1	1.287	1.29	1.3	1.297	12.87	12.9	13	12.97	12.94	0.06	+60
+120	152	10	1	1.284	1.286	1.289	1.283	12.84	12.86	12.89	12.83	12.86	0.03	+120
+180	212	10	1	1.26	1.26	1.271	1.271	12.6	12.6	12.71	12.71	12.66	0.06	+180
Influent		**10**	**1**	**1.077**	**1.082**	**1.085**	**1.084**	**10.77**	**10.82**	**10.85**	**10.84**	**10.82**	**0.04**	

8 mg/g HOCl Reactor Challenge II
AA analysis
Sample volume refers to sample that had been centrifuged and then filtered through 0.45µm filter
Acid is volume of digestion acid added to sample

				AA determined K				K+ (mg/L) after dilution calculation						
Sample (minutes after chlorine challenge or addition of primary	Minutes after start of experiment	Acid (ml)	Sample volume (ml)	K	K	K	K	Calc K	Calc K	Calc K	Calc K	Average K+ (mg/L)	St dev	Sample
Before Cl2	0	10	1	1.205	1.205	1.21	1.213	12.05	12.05	12.1	12.13	12.07	0.03	Before Cl2
After Cl2	1	10	1	1.352	1.363	1.366	1.362	13.52	13.63	13.66	13.62	13.61	0.06	After Cl2
After feed	2	10	1	1.278	1.286	1.29	1.287	12.78	12.86	12.9	12.87	12.85	0.06	After feed
+2	4	10	1	1.317	1.315	1.322	1.322	13.17	13.15	13.22	13.22	13.18	0.04	+2
+5	7	10	1	1.266	1.275	1.276	1.277	12.66	12.75	12.76	12.77	12.72	0.06	+5
+8	10	10	1	1.289	1.298	1.296	1.297	12.89	12.98	12.96	12.97	12.94	0.05	+8
+10	12	10	1	1.338	1.34	1.357	1.359	13.38	13.4	13.57	13.59	13.45	0.10	+10
+20	22	10	1	1.337	1.332	1.341	1.337	13.37	13.32	13.41	13.37	13.37	0.05	+20
+30	32	10	1	1.277	1.283	1.286	1.281	12.77	12.83	12.86	12.81	12.82	0.05	+30
+60	62	10	1	1.265	1.274	1.268	1.273	12.65	12.74	12.68	12.73	12.69	0.05	+60
+120	122	10	1	1.461	1.463	1.458	1.474	14.61	14.63	14.58	14.74	14.61	0.03	+120
+180	182	10	1	1.286	1.284	1.293	1.296	12.86	12.84	12.93	12.96	12.88	0.05	+180

K mass balance
control challenge I
Acid is total dilution acid

Floc associated calculation is AA value times dilution factor
divided by original sample volume (1.3 ml)

MLSS	5190	mg/L	1513 mg/L
MLVSS	3245	mg/L	7 mg/L

MLSS/MLVSS standard deviation (n=2)

Soluble

			AA determined K				K+ (mg/L) after dilution calculation					
Sample	Minutes after start of experiment	Acid (ml)	K	K	K	K	Calc K	Calc K	Calc K	Calc K	Average K (mg/L)	St dev
Before HOCl	0	18					0.00	0.00	0.00		0.00	0.00
After HOCl	1	18	1.29	1.331	1.34		24.51	25.29	25.46		25.09	0.51
5	6	18	1.219	1.253	1.271		23.16	23.81	24.15		23.71	0.50
10	11	18	1.248	1.26	1.2		23.71	23.94	22.80		23.48	0.60
30	31	18	1.158	1.094	1.169	1.186	22.00	20.79	22.21	22.53	21.88	0.76
10 min after primary	42	18	1.299	1.308	1.344		24.68	24.85	25.54		25.02	0.45

Measured Total

			AA determined K				K+ (mg/L) after dilution calculation					
Sample	Minutes after start of experiment	Acid (ml)	K	K	K		Calc K	Calc K	Calc K		Average K (Mg/L)	St dev
Before HOCl	0	18	1.975	1.974	1.966		37.53	37.51	37.35		37.46	0.09
After HOCl	1	18	2.165	2.107	2.091		41.14	40.03	39.73		40.30	0.74
5	6	18	2.029	1.989	2.007		38.55	37.79	38.13		38.16	0.38
10	11	18	1.94	1.965	1.962		36.86	37.34	37.28		37.16	0.26
30	31	18	1.928	1.92	1.92		36.63	36.48	36.48		36.53	0.09
10 min after primary	42	18	1.608	1.641	1.624		30.55	31.18	30.86		30.86	0.31

Floc Associated

			AA determined K				K+ (mg/L) after dilution calculation					
Sample	Minutes after start of experiment	Acid (ml)	K	K	K	K	Calc K	Calc K	Calc K	Calc K	Average K (Mg/L)	St dev
Before HOCl	0	10	1.209	1.206	1.212	1.208	10.23	10.20	10.26	10.22	10.23	0.02
After HOCl	1	5	1.124	1.122	1.134		8.65	5.18	5.23		6.35	1.99
5	6	10										
10	11	10	1.723	1.729	1.724	1.723	14.58	14.63	14.59	14.58	14.60	0.03
30	31	10	1.66	1.659	1.653	1.657	14.05	14.04	13.99	14.02	14.02	0.03
10 min after primary	42	10	1.094	1.087	1.087	1.092	9.26	9.20	9.20	9.24	9.22	0.03

Calculated total (soluble + floc associated)	difference from measured total	% recovery
31.44	-8.86	71.8
23.71	-14.45	39.0
38.08	0.93	97.6
35.91	-0.62	98.3
34.24	3.38	90.1

K mass balance
50 mg/L NEM challenge I
Acid is total dilution acid

Floc associated calculation is AA value times dilution factor
divided by original sample volume (1.3 ml)

MLSS	4185	mg/L	78 mg/L
MLVSS	3335	mg/L	64 mg/L

MLSS/MLVSS standard deviation (n=2)

Soluble			AA determined K					K+ (mg/L) after dilution calculation						
Sample	Minutes after start of experiment	Acid (ml)	K	K	K	K	K	Calc K	Calc K	Calc K	Calc K	Calc K	Average K (mg/L)	St dev
Before HOCl	0	10	1.551	1.541	1.529	1.529		17.06	16.95	16.82	16.82		16.91	0.12
After HOCl	1	10	0.912	0.913	0.916			22.57	22.60	22.67			22.61	0.05
5	6	15	1.191	1.194	1.194	1.19	1.192	19.06	19.10	19.10	19.04	19.07	19.08	0.03
10	11	15	1.278	1.279	1.272	1.275	1.277	20.45	20.46	20.35	20.40	20.43	20.42	0.04
30	31	15	1.444	1.447	1.446	1.449	1.45	23.10	23.15	23.14	23.18	23.20	23.16	0.04
10 min after primary	42	10	1.702	1.701	1.7	1.688		18.72	18.71	18.70	18.57		18.68	0.07

Measured Total			AA determined K					K+ (mg/L) after dilution calculation						
Sample	Minutes after start of experiment	Acid (ml)	K	K	K	K	K	Calc K	Calc K	Calc K	Calc K	Calc K	Average K (mg/L)	St dev
Before HOCl	0	15	1.614	1.604	1.614	1.621	1.631	25.82	25.66	25.82	25.94	26.10	25.87	0.16
After HOCl	1	15	1.598	1.591	1.593	1.598	1.597	25.57	25.46	25.49	25.57	25.55	25.53	0.05
5	6	15	1.596	1.599	1.599	1.593	1.599	25.54	25.58	25.58	25.49	25.58	25.56	0.04
10	11	15	1.645	1.612	1.613	1.616	1.615	26.32	25.79	25.81	25.86	25.84	25.92	0.22
30	31	15	1.647	1.644	1.646	1.652	1.653	26.35	26.30	26.34	26.43	26.45	26.37	0.06
10 min after primary	42	15	1.33	1.335	1.342	1.336	1.338	21.28	21.36	21.47	21.38	21.41	21.38	0.07

Floc Associated			AA determined K					K+ (mg/L) after dilution calculation						
Sample	Minutes after start of experiment	Acid (ml)	K	K	K	K		Calc K	Calc K	Calc K	Calc K		Average K (mg/L)	St dev
Before HOCl	0	10	1.691	1.685	1.673	1.671		14.31	14.26	14.16	14.14		14.22	0.08
After HOCl	1	10	0.777	0.774	0.776	0.777		6.57	6.55	6.57	6.57		6.57	0.01
5	6	10	1.297	1.301	1.303	1.298		10.97	11.01	11.03	10.98		11.00	0.02
10	11	10	0.933	0.929	0.925	0.929		7.89	7.86	7.83	7.86		7.86	0.03
30	31	10												
10 min after primary	42	10	0.718	0.72	0.722	0.719		6.08	6.09	6.11	6.08		6.09	0.01

Calculated total (soluble + floc associated)	difference from measured total	% recovery
31.13	5.26	83.1
29.18	3.65	87.5
30.07	4.52	85.0
28.28	2.36	91.7
23.16	-3.22	86.1

K mass balance
4 mg/g HOCl challenge I
Acid is total dilution acid

Floc associated calculation is AA value times dilution factor divided by original sample volume (1.3 ml)

MLSS	4110	mg/L	0	mg/L
MLVSS	3245	mg/L	64	mg/L

MLSS/MLVSS standard deviation (n=2)

Soluble

Sample	Minutes after start of experiment	Acid (ml)	AA determined K					K+ (mg/L) after dilution calculation					Average K (mg/L)	St dev
			K	K	K	K		Calc K	Calc K	Calc K	Calc K			
Before HOCl	0	10	1.356	1.346	1.35	1.35		14.92	14.81	14.85	14.85		14.86	0.05
After HOCl	1	10	1.338	1.353	1.355	1.355		14.72	14.88	14.91	14.91		14.85	0.09
5	6	10	1.322	1.321	1.318	1.327		14.54	14.53	14.50	14.60		14.54	0.04
10	11	10	1.364	1.367	1.37	1.37		15.00	15.04	15.07	15.07		15.05	0.03
30	31	10	1.32	1.314	1.321	1.322		14.52	14.45	14.53	14.54		14.51	0.04
10 min after primary	42	10	1.527	1.545	1.527	1.542		16.80	17.00	16.80	16.96		16.89	0.11

Measured Total

Sample	Minutes after start of experiment	Acid (ml)	AA determined K					K+ (mg/L) after dilution calculation					Average K (mg/L)	St dev
			K	K	K	K	K	Calc K	Calc K	Calc K	Calc K	Calc K		
Before HOCl	0	15	1.623	1.633	1.642	1.633	1.634	25.97	26.13	26.27	26.13	26.14	26.13	0.11
After HOCl	1	15	1.401	1.41	1.402	1.404	1.409	22.42	22.56	22.43	22.46	22.54	22.48	0.07
5	6	15	1.559	1.549	1.556	1.558	1.565	24.94	24.78	24.90	24.93	25.04	24.92	0.09
10	11	15	1.579	1.585	1.578	1.582	1.567	25.26	25.36	25.25	25.31	25.07	25.25	0.11
30	31	15	1.565	1.558	1.569	1.568	1.565	25.04	24.93	25.10	25.09	25.04	25.04	0.07
10 min after primary	42	15	1.309	1.305	1.312	1.314	1.318	20.94	20.88	20.99	21.02	21.09	20.99	0.08

Floc Associated

Sample	Minutes after start of experiment	Acid (ml)	AA determined K					K+ (mg/L) after dilution calculation					Average K (mg/L)	St dev
			K	K	K	K		Calc K	Calc K	Calc K	Calc K			
Before HOCl	0	10	1.485	1.483	1.474	1.468		12.57	12.55	12.47	12.42		12.50	0.07
After HOCl	1	10	1.45	1.447	1.435	1.443		12.27	12.24	12.14	12.21		12.22	0.06
5	6	10	1.537	1.542	1.559	1.54		13.01	13.05	13.19	13.03		13.07	0.08
10	11	10	1.583	1.577	1.572	1.57		13.39	13.34	13.30	13.28		13.33	0.05
30	31	10	1.591	1.597	1.592	1.615		13.46	13.51	13.47	13.67		13.53	0.09
10 min after primary	42	10	0.993	0.995	0.995	1.001		8.40	8.42	8.42	8.47		8.43	0.03

Calculated total (soluble + floc associated)	difference from measured total	% recovery
27.36	1.23	95.5
27.07	4.59	83.1
27.61	2.69	90.2
28.38	3.13	89.0
28.04	3.00	89.3
25.32	4.33	82.9

Floc associated calculation is AA value times dilution factor divided by original sample volume (1.3 ml)

				MLSS/MLVSS standard deviation (n=2)	
MLSS	3840	mg/L		509	mg/L
MLVSS	2250	mg/L		410	mg/L

AA determined K					K+ (mg/L) after dilution calculation						
K	K	K	K		Calc K	Calc K	Calc K	Calc K		Average K (mg/L)	St dev
1.359	1.363	1.366	1.349		14.95	14.99	15.03	14.84		14.99	0.04
1.733	1.735	1.731	1.773		19.06	19.09	19.04	19.50		19.06	0.02
1.614	1.626	1.623	1.63		17.75	17.89	17.85	17.93		17.83	0.07
1.38	1.325	1.33	1.336		15.18	14.58	14.63	14.70		14.80	0.33
1.32	1.316	1.326	1.33		14.52	14.48	14.59	14.63		14.53	0.06
1.299	1.311	1.316	1.319		14.29	14.42	14.48	14.51		14.40	0.10

AA determined K					K+ (mg/L) after dilution calculation						
K	K	K	K	K	Calc K	Calc K	Calc K	Calc K	Calc K	Average K (mg/L)	St dev
1.765	1.757	1.758	1.76	1.758	28.24	28.11	28.13	28.16	28.13	28.16	0.07
1.897	1.898	1.898	1.917	1.897	30.35	30.37	30.37	30.67	30.35	30.36	0.01
1.386	1.382	1.397	1.402	1.398	22.18	22.11	22.35	22.43	22.37	22.21	0.12
1.492	1.493	1.477	1.474	1.477	23.87	23.89	23.63	23.58	23.63	23.80	0.14
1.464	1.467	1.459	1.476	1.464	23.42	23.47	23.34	23.62	23.42	23.41	0.06
1.42	1.424	1.436	1.451	1.442	22.72	22.78	22.98	23.22	23.07	22.83	0.13

AA determined K					K+ (mg/L) after dilution calculation						
K	K	K	K		Calc K	Calc K	Calc K	Calc K		Average K (mg/L)	St dev
1.642	1.641	1.637	1.659		13.89	13.89	13.85	14.04		13.92	0.08
0.919	0.912	0.924	0.922		7.78	7.72	7.82	7.80		7.78	0.04
0.857	0.862	0.861	0.863		7.25	7.29	7.29	7.30		7.28	0.02
1.133	1.131	1.134			9.59	9.57	9.60			9.58	0.01
1.162	1.144	1.149	1.158		9.83	9.68	9.72	9.80		9.76	0.07
1.239	1.235	1.242	1.25		10.48	10.45	10.51	10.58		10.51	0.05

K mass balance
8 mg/g HOCl challenge I
Acid is total dilution acid

Floc associated calculation is AA value times dilution factor divided by original sample volume (1.3 ml)

			MLSS/MLVSS standard deviation (n=2)	
MLSS	6035	mg/L	78	mg/L
MLVSS	2985	mg/L	35	mg/L

Soluble

			AA determined K					K+ (mg/L) after dilution calculation						
Time	Minutes after start of experiment	Acid (ml)	K	K	K	K	K	Calc K	Calc K	Calc K	Calc K	Calc K	Average K (mg/L)	St dev
Before HOCl	0	10	1.425	1.419	1.415	1.415		15.68	15.61	15.57	15.57		15.60	0.05
After HOCl	1	15	1.17	1.173	1.178	1.176	1.183	18.72	18.77	18.85	18.82	18.93	18.82	0.08
5	6	15	1.088	1.095	1.096	1.095	1.098	17.41	17.52	17.54	17.52	17.57	17.51	0.06
10	11	15	1.056	1.066	1.058	1.059	1.064	16.90	17.06	16.93	16.94	17.02	16.97	0.07
30	31	15	1.203	1.192	1.197	1.202	1.207	19.25	19.07	19.15	19.23	19.31	19.20	0.09
10 min after primary	42	10	1.508	1.505	1.513	1.513		16.59	16.56	16.64	16.64		16.61	0.04

Measured Total

			AA determined K					K+ (mg/L) after dilution calculation						
Time	Minutes after start of experiment	Acid (ml)	K	K	K	K	K	Calc K	Calc K	Calc K	Calc K	Calc K	Average K (mg/L)	St dev
Before HOCl	0	15	1.883	1.889	1.88	1.884	1.881	30.13	30.22	30.08	30.14	30.10	30.13	0.06
After HOCl	1	15	1.762	1.757	1.763	1.773	1.76	28.19	28.11	28.21	28.37	28.16	28.21	0.10
5	6	15	1.721	1.729	1.74	1.736	1.743	27.54	27.66	27.84	27.78	27.89	27.74	0.14
10	11	15	1.649	1.656	1.66	1.664	1.668	26.38	26.50	26.56	26.62	26.69	26.55	0.12
30	31	15	1.621	1.624	1.621	1.625	1.629	25.94	25.98	25.94	26.00	26.06	25.98	0.05
10 min after primary	42	15	1.41	1.411	1.409	1.413	1.42	22.56	22.58	22.54	22.61	22.72	22.60	0.07

Floc Associated

			AA determined K					K+ (mg/L) after dilution calculation						
Time	Minutes after start of experiment	Acid (ml)	K	K	K	K		Calc K	Calc K	Calc K	Calc K		Average K (mg/L)	St dev
Before HOCl	0	10	1.622	1.626	1.629	1.618		13.72	13.76	13.78	13.69		13.74	0.04
After HOCl	1	10	1.13	1.132	1.127	1.132		9.56	9.58	9.54	9.58		9.56	0.02
5	6	10	1.31	1.31	1.307	1.31		11.08	11.08	11.06	11.08		11.08	0.01
10	11	10	1.373	1.371	1.372	1.371		11.62	11.60	11.61	11.60		11.61	0.01
30	31	10	1.153	1.151	1.149	1.152		9.76	9.74	9.72	9.75		9.74	0.01
10 min after primary	42	10	0.952	0.954	0.953	0.953		8.06	8.07	8.06	8.06		8.06	0.01

Calculated total (soluble + floc associated)	difference from measured total	% recovery
29.34	-0.79	97.3
28.38	0.17	99.4
28.59	0.85	97.0
28.58	2.03	92.9

K mass balance
8 mg/g HOCl challenge II
Acid is total dilution acid

Floc associated calculation is AA value times dilution factor
divided by original sample volume (1.3 ml)

MLSS	3770	mg/L	113 mg/L
MLVSS	3015	mg/L	7 mg/L

MLSS/MLVSS standard deviation (n=2)

Soluble

			AA determined K					K+ (mg/L) after dilution calculation						
Time	Minutes after start of experiment	Acid (ml)	K	K	K	K		Calc K	Calc K	Calc K	Calc K		Average K (mg/L)	St dev
Before HOCl	0	10	1.493	1.496	1.494	1.488		16.42	16.46	16.43	16.37		16.42	0.04
After HOCl	1	10	1.651	1.65	1.66	1.659		18.16	18.15	18.26	18.25		18.21	0.06
5	2	10	1.594	1.599	1.59	1.593		17.53	17.59	17.49	17.52		17.53	0.04
10	7	10	1.524	1.524	1.525	1.524		16.76	16.76	16.78	16.76		16.77	0.01
30	12	10	1.523	1.526	1.538	1.533		16.75	16.79	16.92	16.86		16.83	0.07
10 min after primary	32	10	1.5	1.491	1.49	1.488		16.50	16.40	16.39	16.37		16.41	0.06

Measured Total

			AA determined K					K+ (mg/L) after dilution calculation						
Time	Minutes after start of experiment	Acid (ml)	K	K	K	K	K	Calc K	Calc K	Calc K	Calc K	Calc K	Average K (mg/L)	St dev
Before HOCl	0	15	1.674	1.673	1.669	1.679	1.685	26.78	26.77	26.70	26.86	26.96	26.82	0.10
After HOCl	1	15	1.942	1.949	1.961	1.957	1.971	31.07	31.18	31.38	31.31	31.54	31.30	0.18
5	2	15	1.342	1.352	1.353	1.356	1.352	21.47	21.63	21.65	21.70	21.63	21.62	0.08
10	7	15	1.398	1.401	1.402	1.406	1.406	22.37	22.42	22.43	22.50	22.50	22.44	0.05
30	12	15	1.43	1.435	1.438	1.447	1.44	22.88	22.96	23.01	23.15	23.04	23.01	0.10
10 min after primary	32	15	1.506	1.512	1.516	1.528	1.517	24.10	24.19	24.26	24.45	24.27	24.25	0.13

Floc Associated

			AA determined K					K+ (mg/L) after dilution calculation						
Time	Minutes after start of experiment	Acid (ml)	K	K	K	K		Calc K	Calc K	Calc K	Calc K		Average K (mg/L)	St dev
Before HOCl	0	10	1.637	1.658	1.659	1.664		13.85	14.03	14.04	14.08		14.00	0.10
After HOCl	1	10	1.249	1.245	1.244	1.248		10.57	10.53	10.53	10.56		10.55	0.02
5	2	10	0.819	0.822	0.825	0.824		6.93	6.96	6.98	6.97		6.96	0.02
10	7	10	0.851	0.854	0.854	0.857		7.20	7.23	7.23	7.25		7.23	0.02
30	12	10	0.78	0.776	0.78	0.772		6.60	6.57	6.60	6.53		6.57	0.03
10 min after primary	32	10	0.888	0.891	0.888	0.887		7.51	7.54	7.51	7.51		7.52	0.01

Calculated total (soluble + floc associated)	difference from measured total	% recovery
30.42	3.60	88.2
28.75	-2.54	91.2
24.49	2.88	88.3
23.99	1.55	93.5
23.40	0.40	98.3

SOUR data (mg O2/min-g MLVSS)
Challenge I configuration
HOCl added mg/g

	control	1mg/g	3mg/g	6mg/g	8mg/g	10 mg/g
our	-0.49	-0.64	-0.61	-0.66	-0.65	-0.64
our	-0.63	-0.68	-0.67	-0.69	-0.67	-0.57
average	-0.63	-0.66	-0.64	-0.67	-0.66	-0.60
st dev	0.00	0.02	0.05	0.03	0.02	0.04
sour	0.39	0.41	0.39	0.45	0.43	0.38
sour st dev	0.02	0.02	0.03	0.05	0.05	0.05

Statistics

	HOCl Challenge	SOUR	control
sour	1mg/g	-0.41	-0.39
	3mg/g	-0.39	
	6mg/g	-0.45	
	8mg/g	-0.43	
	10 mg/g	-0.38	

Anova: Single Factor
alpha = 0.05
SUMMARY

Groups	*Count*	*Sum*	*Average*	*Variance*
Column 1	5	-2.05597	-0.41119	0.000722
Column 2	1	-0.38891	-0.38891	#DIV/0!

ANOVA

Source of Varia	*SS*	*df*	*MS*	*F*	*P-value*	*F crit*
Between Groups	0.000414	1	0.000414	0.573427	0.491058	7.70865
Within Groups	0.002888	4	0.000722			
Total	0.003302	5				

t-Test: Two-Sample Assuming Equal Variances
alpha = 0.05

	Variable 1	*Variable 2*
Mean	-0.41119	-0.38891
Variance	0.000722	#DIV/0!
Observations	5	1
Pooled Variance	0.000722	
Hypothesized Mean Difference	0	
df	4	
t Stat	-0.75725	
P(T<=t) one-tail	0.245529	
t Critical one-tail	2.131846	
P(T<=t) two-tail	0.491058	
t Critical two-tail	2.776451	

Appendix 2-e

Pepper's Ferry is POTW #2
Legend

N = 50mg/L NEM
phi = control
1 = 4mg/g HOCl challenge I
2 = 4 mg/g HOCl challenge II
3 = 10 mg/g HOCl challenge I
4 = 10 mg/g HOCl chllenge II

Eff 1 = Effluent solids at Time 0
Eff 2 = Effluent solids following challenge

Pan Label	Tare g	Sample	Volume Ml	103C wt g	TSS mg/L	550C wt g	VSS mg/L
17-	1.1353	N EFF 1	450	1.1382	6.4	1.1360	4.9
6-	1.1294	N EFF 1	450	1.1315	4.7	1.1292	5.1
35	1.1347	N EFF 2	125	1.1439	73.6	1.1370	55.2
9-	1.1113	N EFF 2	150	1.1425	208.0	1.1346	52.7
30-	1.1357	N MLSS 1	10	1.1770	4130.0	1.1441	3290.0
14	1.1377	N MLSS 1	10	1.1801	4240.0	1.1463	3380.0
16-	1.1132	N MLSS 2	10	1.1666	5340.0	1.1414	2520.0
1-	1.1423	N MLSS 2	10	1.1727	3040.0	1.1485	2420.0
11E1	1.1241	1 EFF 1	450	1.1494	56.2	1.1465	6.4
3-	1.1221	1 EFF 1	450	1.1482	58.0	1.1447	7.8
20-	1.1153	2 EFF 1	450	1.1412	57.6	1.1380	7.1
11-	1.1174	2 EFF 1	450	1.1423	55.3	1.1393	6.7
26-	1.1389	3 EFF 1	450	1.1422	7.3	1.1387	7.8
27-	1.1366	3 EFF 1	450	1.1394	6.2	1.1364	6.7
7-	1.1305	4 EFF 1	450	1.1329	5.3	1.1307	4.9
24-	1.1143	4 EFF 1	450	1.1403	57.8	1.1371	7.1
13-	1.1376	Φ EFF 1	450	1.1404	6.2	1.1381	5.1
34-	1.1363	Φ EFF 1	450	1.1392	6.4	1.1373	4.2
19-	1.1156	Φ EFF 2	450	1.1410	56.4	1.1375	7.8
18E1	1.1215	Φ EFF 2	450	1.1467	56.0	1.1439	6.2
28-	1.1388	Φ MLSS 1	10	1.1800	4120.0	1.1475	3250.0
A3	1.1355	Φ MLSS 1	10	1.1764	6260.0	1.1440	3240.0
36-	1.1138	Φ MLSS 2	10	1.1751	6130.0	1.1430	3210.0
38-	1.1162	Φ MLSS 2	10	1.1773	6110.0	1.1533	2400.0
23-	1.1139	1 EFF 2	450	1.1442	67.3	1.1373	15.3
10-	1.1142	1 EFF 2	450	1.1435	65.1	1.1374	13.6
15-	1.1126	2 EFF 2	450	1.1423	66.0	1.1360	14.0
25-	1.1118	2 EFF 2	450	1.1420	67.1	1.1354	14.7
8-	1.1336	3 EFF 2	250	1.1420	33.6	1.1349	28.4
18	1.1370	3 EFF 2	250	1.1448	31.2	1.1378	28.0
A10	1.1086	4 EFF 2	250	1.1162	30.4	1.1100	24.8
A11	1.1062	4 EFF 2	250	1.1134	28.8	1.1071	25.2
2-	1.1453	1 MLSS 1	10	1.1864	4110.0	1.1535	3290.0
12-	1.1378	1 MLSS 1	10	1.1789	4110.0	1.1469	3200.0
32-	1.1321	2 MLSS 1	10	1.1741	4200.0	1.1487	2540.0
31-	1.1333	2 MLSS 1	10	1.1681	3480.0	1.1485	1960.0
29-	1.1142	3 MLSS 1	10	1.1751	6090.0	1.1450	3010.0
21-	1.1154	3 MLSS 1	10	1.1752	5980.0	1.1456	2960.0
A2	1.1378	4 MLSS 1	10	1.1763	3850.0	1.1461	3020.0
A9	1.1094	4 MLSS 1	10	1.1463	3690.0	1.1162	3010.0
37-	1.1172	1 MLSS 2	10	1.1782	6100.0	1.1162	6200.0
5-	1.1083	1 MLSS 2	10	1.1683	6000.0	1.1162	5210.0
A1	1.1316	2 MLSS 2	10	1.1726	4100.0	1.1162	5640.0
A8	1.1068	2 MLSS 2	10	1.1432	3640.0	1.1162	2700.0
4-	1.1313	3 MLSS 2	10	1.1660	3470.0	1.1379	2810.0
A7	1.1054	3 MLSS 2	10	1.1415	3610.0	1.1127	2880.0
A5	1.1052	4 MLSS 2	10	1.1412	3600.0	1.1122	2900.0
A6	1.1052	4 MLSS 2	10	1.1420	3680.0	1.1127	2930.0
A1	1.1346	PFB1 MLSS	10	1.1755	4090.0	1.1438	3170.0
A2	1.1317	PFB1 MLSS	10	1.1725	4080.0	1.1409	3160.0
27	1.135	PFB2 MLSS	10	1.1608	2580.0	1.1411	1970.0
*** 26	1.1363	PFB2 MLSS	10	1.6946	55830.0	1.1426	55200.0

Measurement of HOCl stock
DPD chlorine titration
FAS Normality 0.05
Std Methods
Normality 0.00282
Multiplication
factor 17.723

Assay #	Bleach added (ml)	Total sample volume (ml)	FAS start	FAS end	Delta	HOCl (mg Cl2/ml)
1	1	100	2.32	2.68	0.36	0.10152
2	1	100	2.68	3.06	0.38	0.10716
3	1	100	3.02	3.38	0.36	0.10152
					Average HOCl	0.1034

note: Standard methods utilizes a FAS with normality of 0.00282. The DPD titration was performed with FAS with a Normality of 0.05 requiring the multiplication factor of 17.723

Control Reactor Challenge I
AA analysis
Sample volume refers to sample that had been centrifuged and then filtered through 0.45µm filter
Acid is digestion acid added to sample

				AA determined K			K+ (mg/L) after dilution calculation					
Sample (minutes after chlorine challenge or addition of primary	Minutes after start of experiment	Acid (ml)	Sample volume (ml)	K	K	K	Calc K	Calc K	Calc K	Average K+ (mg/L)	St dev	Condition
Before Cl2	0	10	0.55	1.228	1.234	1.235	22.33	22.44	22.45	22.41	0.07	Before Cl2
After Cl2	1	10	0.55	1.199	1.207	1.207	21.80	21.95	21.95	21.90	0.08	After Cl2
+2	3	10	0.55	1.132	1.143	1.133	20.58	20.78	20.60	20.65	0.11	+2
+5	6	10	0.55	1.193	1.198	1.198	21.69	21.78	21.78	21.75	0.05	+5
+8	9	10	0.55	1.168	1.175	1.17	21.24	21.36	21.27	21.29	0.07	+8
+10	11	10	0.55	1.207	1.201	1.204	21.95	21.84	21.89	21.89	0.05	+10
+20	21	10	0.55	1.153	1.209	1.209	20.96	21.98	21.98	21.64	0.59	+20
+30	31	10	0.55	1.163	1.166	1.171	21.15	21.20	21.29	21.21	0.07	+30
After feed	32	10	0.55	1.271	1.265	1.273	23.11	23.00	23.15	23.08	0.08	After feed
+5	37	10	0.55	1.135	1.142	1.14	20.64	20.76	20.73	20.71	0.07	+5
+10	42	10	0.55	1.175	1.176	1.182	21.36	21.38	21.49	21.41	0.07	+10
+20	52	10	0.55	1.12	1.117	1.114	20.36	20.31	20.25	20.31	0.05	+20
+60	92	10	0.55	1.169	1.171	1.152	21.25	21.29	20.95	21.16	0.19	+60
+120	152	10	0.55	1.184	1.179	1.198	21.53	21.44	21.78	21.58	0.18	+120
+180	212	10	0.55	1.302	1.293	1.305	23.67	23.51	23.73	23.64	0.11	+180

50 mg/L NEM reactor Challenge I
AA analysis
Sample volume refers to sample that had been centrifuged and then filtered through 0.45µm filter
Acid is digestion acid added to sample

				AA determined K				K+ (mg/L) after dilution calculation						
Sample (minutes after chlorine challenge or addition of primary	Minutes after start of experiment	Acid (ml)	Sample volume (ml)	K	K	K	K	Calc K	Calc K	Calc K	Calc K	Average K+ (mg/L)	St dev	Sample
Before Cl2	0	10	0.55	1.276	1.282	1.285	1.284	23.20	23.31	23.36	23.35	23.30	0.07	Before Cl2
After Cl2	1	10	0.55	1.346	1.358	1.354	1.364	24.47	24.69	24.62	24.80	24.65	0.14	After Cl2
+2	3	10	0.55	1.322	1.318	1.333	1.342	24.04	23.96	24.24	24.40	24.16	0.20	+2
+5	6	10	0.55	1.406	1.412	1.414	1.428	25.56	25.67	25.71	25.96	25.73	0.17	+5
+8	9	10	0.55	1.458	1.472	1.466		26.51	26.76	26.65		26.64	0.13	+8
+10	11	10	0.55	1.438	1.449	1.447	1.451	26.15	26.35	26.31	26.38	26.30	0.10	+10
+30	31	10	0.55	1.476	1.476	1.481	1.492	26.84	26.84	26.93	27.13	26.87	0.05	+30
After feed	32	10	0.55	1.377	1.394	1.389	1.393	25.04	25.35	25.25	25.33	25.21	0.16	After feed
+5	37	10	0.55	1.448	1.451	1.464	1.477	26.33	26.38	26.62	26.85	26.44	0.15	+5
+10	42	10	0.55	1.472	1.473	1.479	1.488	26.76	26.78	26.89	27.05	26.81	0.07	+10
+20	52	10	0.55	1.432	1.434	1.427	1.432	26.04	26.07	25.95	26.04	26.02	0.07	+20
+60	92	10	0.55	1.499	1.501	1.509	1.494	27.25	27.29	27.44	27.16	27.33	0.10	+60
+120	152	10	0.55	1.544	1.549	1.555	1.546	28.07	28.16	28.27	28.11	28.17	0.10	+120
+180	212	10	0.55	1.502	1.487	1.495	1.495	27.31	27.04	27.18	27.18	27.18	0.14	+180

4 mg/g HOCl reactor Challenge I
AA analysis
Sample volume refers to sample that had been centrifuged and then filtered through 0.45µm filter
Acid is digestion acid added to sample

				AA determined K				K+ (mg/L) after dilution calculation						
Sample (minutes after chlorine challenge or addition of primary	Minutes after start of experiment	Acid (ml)	Sample volume (ml)	K	K	K	K	Calc K	Calc K	Calc K	Calc K	Average K+ (mg/L)	St dev	Sample
Before Cl2	0	10	0.55	1.167	1.168	1.173	1.173	21.22	21.24	21.33	21.33	21.28	0.06	Before Cl2
After Cl2	1	10	0.55	1.208	1.222	1.223	1.224	21.96	22.22	22.24	22.25	22.17	0.14	After Cl2
+2	3	10	0.55	1.175	1.174	1.176	1.177	21.36	21.35	21.38	21.40	21.37	0.02	+2
+5	6	10	0.55	1.248	1.246	1.253	1.258	22.69	22.65	22.78	22.87	22.75	0.10	+5
+8	9	10	0.55	1.315	1.308	1.316	1.309	23.91	23.78	23.93	23.80	23.87	0.08	+8
+10	11	10	0.55	1.307	1.301	1.304	1.303	23.76	23.65	23.71	23.69	23.70	0.05	+10
+20	21	10	0.55	1.29	1.3	1.303	1.3	23.45	23.64	23.69	23.64	23.59	0.12	+20
+30	31	10	0.55	1.269	1.284	1.288	1.294	23.07	23.35	23.42	23.53	23.34	0.19	+30
After feed	32	10	0.55	1.378	1.375	1.382	1.393	25.05	25.00	25.13	25.33	25.06	0.06	After feed
+5	37	10	0.55	1.298	1.305	1.315	1.314	23.60	23.73	23.91	23.89	23.75	0.16	+5
+10	42	10	0.55	1.299	1.309	1.321	1.316	23.62	23.80	24.02	23.93	23.81	0.20	+10
+20	52	10	0.55	1.268	1.284	1.283	1.289	23.05	23.35	23.33	23.44	23.29	0.16	+20
+60	92	10	0.55	1.104	1.106	1.109	1.107	20.07	20.11	20.16	20.13	20.12	0.05	+60
+120	152	10	0.55	1.212	1.214	1.212	1.214	22.04	22.07	22.04	22.07	22.05	0.02	+120

4 mg/g HOCl reactor Challenge II
AA analysis
Sample volume refers to sample that had been centrifuged and then filtered through 0.45µm filter
Acid is digestion acid added to sample

				AA determined K				K+ (mg/L) after dilution calculation						
Sample (minutes after chlorine challenge or addition of primary	Minutes after start of experiment	Acid (ml)	Sample volume (ml)	K	K	K	K	Calc K	Calc K	Calc K	Calc K	Average K+ (mg/L)	St dev	Sample
Before Cl2	0.01	10	0.55	1.051	1.054	1.057	1.043	19.11	19.16	19.22	18.96	19.11	0.11	Before Cl2
After Cl2	1.01	10	0.55	1.111	1.11	1.115	1.117	20.20	20.18	20.27	20.31	20.24	0.06	After Cl2
After feed	2	10	0.55	1.159	1.169	1.174	1.185	21.07	21.25	21.35	21.55	21.30	0.20	After feed
+2	4	10	0.55	1.228	1.262	1.285	1.244	22.33	22.95	23.36	22.62	22.81	0.45	+2
+5	7	10	0.55	1.178	1.182	1.193	1.196	21.42	21.49	21.69	21.75	21.59	0.16	+5
+10	12	10	0.55	1.287	1.281	1.292	1.293	23.40	23.29	23.49	23.51	23.42	0.10	+10
+20	22	10	0.55	1.24	1.251	1.26	1.257	22.55	22.75	22.91	22.85	22.76	0.16	+20
+30	32	10	0.55	1.193	1.195	1.204	1.218	21.69	21.73	21.89	22.15	21.77	0.11	+30
+60	62.01	10	0.55	1.245	1.243	1.255	1.254	22.64	22.60	22.82	22.80	22.71	0.11	+60
+120	122	10	0.55	1.202	1.203	1.205	1.211	21.85	21.87	21.91	22.02	21.91	0.07	+120
+180	182	10	0.55	1.168	1.183	1.181	1.185	21.24	21.51	21.47	21.55	21.41	0.15	+180

10 mg/g HOCl reactor Challenge I
AA analysis
Sample volume refers to sample that had been centrifuged and then filtered through 0.45µm filter
Acid is digestion acid added to sample

				AA determined K				K+ (mg/L) after dilution calculation						
Sample (minutes after chlorine challenge or addition of primary	Minutes after start of experiment	Acid (ml)	Sample volume (ml)	K	K	K	K	Calc K	Calc K	Calc K	Calc K	Average K+ (mg/L)	St dev	Sample
Before Cl2	0	10	0.55	1.142	1.133	1.128	1.132	20.76	20.60	20.51	20.58	20.61	0.11	Before Cl2
After Cl2	1	10	0.55	1.211	1.213	1.225	1.232	22.02	22.05	22.27	22.40	22.19	0.18	After Cl2
+2	3	10	0.55	1.245	1.241	1.247	1.251	22.64	22.56	22.67	22.75	22.65	0.08	+2
+5	6	10	0.55	1.297	1.284	1.297	1.295	23.58	23.35	23.58	23.55	23.51	0.11	+5
+8	9	10	0.55	1.241	1.235	1.239	1.245	22.56	22.45	22.53	22.64	22.52	0.06	+8
+10	11	10	0.55	1.164	1.164	1.17	1.172	21.16	21.16	21.27	21.31	21.23	0.07	+10
+20	21	10	0.55	1.319	1.331	1.323	1.326	23.98	24.20	24.05	24.11	24.09	0.09	+20
+30	31	10	0.55	1.252	1.25	1.25	1.263	22.76	22.73	22.73	22.96	22.80	0.11	+30
After feed	32	10	0.55	1.258	1.268	1.279	1.281	22.87	23.05	23.25	23.29	23.12	0.19	After feed
+5	37	10	0.55	1.26	1.267	1.268	1.272	22.91	23.04	23.05	23.13	23.03	0.09	+5
+10	42	10	0.55	1.317	1.314	1.322	1.323	23.95	23.89	24.04	24.05	23.98	0.08	+10
+20	52	10	0.55	1.283	1.288	1.289	1.288	23.33	23.42	23.44	23.42	23.40	0.05	+20
+60	92	10	0.55	1.317	1.319	1.32	1.325	23.95	23.98	24.00	24.09	24.00	0.06	+60
+120	152	10	0.55	1.348	1.347	1.351	1.35	24.51	24.49	24.56	24.55	24.53	0.03	+120
+180	212	10	0.55	1.301	1.302	1.306	1.305	23.65	23.67	23.75	23.73	23.70	0.04	+180
Influent		**10**	**0.55**	**1.262**	**1.251**	**1.253**	**1.265**	**22.95**	**22.75**	**22.78**	**23.00**	**22.87**	**0.12**	

10 mg/g HOCl reactor Challenge II
AA analysis
Sample volume refers to sample that had been centrifuged and then filtered through 0.45µm filter
Acid is digestion acid added to sample

				AA determined K				K+ (mg/L) after dilution calculation						
Sample (minutes after chlorine challenge or addition of primary	Minutes after start of experiment	Acid (ml)	Sample volume (ml)	K	K	K	K	Calc K	Calc K	Calc K	Calc K	Average K+ (mg/L)	St dev	Sample
Before Cl2	0	10	0.55	1.193	1.199	1.197	1.193	21.69	21.80	21.76	21.69	21.74	0.05	Before Cl2
After Cl2	1	10	0.55	1.277	1.27	1.277	1.276	23.22	23.09	23.22	23.20	23.18	0.06	After Cl2
After feed	2	10	0.55	1.186	1.201	1.203		21.56	21.84	21.87		21.76	0.17	After feed
+2	4	10	0.55	1.423	1.424	1.422	1.435	25.87	25.89	25.85	26.09	25.93	0.11	+2
+5	7	10	0.55	1.358	1.361	1.379	1.377	24.69	24.75	25.07	25.04	24.89	0.20	+5
+8	10	10	0.55	1.366	1.373	1.364	1.365	24.84	24.96	24.80	24.82	24.85	0.07	+8
+10	12	10	0.55	1.371	1.368	1.373	1.373	24.93	24.87	24.96	24.96	24.93	0.04	+10
+20	22	10	0.55	1.288	1.28	1.291	1.288	23.42	23.27	23.47	23.42	23.40	0.09	+20
+30	32	10	0.55	1.353	1.362	1.359		24.60	24.76	24.71		24.69	0.08	+30
+60	62	10	0.55	1.375	1.37	1.373	1.368	25.00	24.91	24.96	24.87	24.94	0.06	+60
+120	122	10	0.55	1.392	1.385	1.396	1.4	25.31	25.18	25.38	25.45	25.33	0.12	+120
+180	182	10	0.55	1.277	1.272	1.28	1.283	23.22	23.13	23.27	23.33	23.24	0.09	+180

SOUR data (mg O2/min-g MLVSS)
Challenge I configuration
HOCl added mg/g

	control	1 mg/g	3 mg/g	6mg/g	8mg/g	10 mg/g
our	-0.66	-0.83	-1.00	-0.93	-0.93	-1.52
our	-0.80	-0.46	-0.92	-0.89	-0.92	-1.80
average	-0.80	-0.65	-0.96	-0.91	-0.93	-1.66
st dev	0.00	0.26	0.05	0.02	0.01	0.20
sour	0.23	0.17	0.24	0.25	0.25	0.39
sour st dev	0.01	0.07	0.02	0.03	0.00	0.05

Statistics
Anova: Single Factor between control and challenged
alpha = 0.05
SUMMARY

Groups	*Count*	*Sum*	*Average*	*Variance*
Column 1	5	-1.29358	-0.25872	0.006383
Column 2	1	-0.22514	-0.22514	#DIV/0!

ANOVA

Source of Variation	*SS*	*df*	*MS*	*F*	*P-value*	*F crit*
Between Groups	0.00094	1	0.00094	0.147219	0.720729	7.70865
Within Groups	0.025531	4	0.006383			
Total	0.02647	5				

Robert F. Wimmer

2533 Paso Fino Dr.
Finksburg, MD 21048
(410) 871-2847
rwimmer@vt.edu

EMPLOYMENT

Design Engineer, Water and Wastewater
JMT Engineering
72 Loveton Circle
Baltimore, MD 21152

EDUCATION

Master of Science; Environmental Engineering, December 2001
Virginia Polytechnic Institute and State University, Blacksburg, VA.
Thesis; Development and Characterization of a Biosensor to Predict Deflocculation. **Advisor:** Dr. Nancy Love

Bachelor of Science; Dairy Science, May 1996
Virginia Polytechnic Institute and State University, Blacksburg, VA
Biotechnology Option

RELATED EXPERIENCE

Research Assistant February 1998 to August 2000
Sybron Chemicals Inc. Salem, VA

- Chemical analysis of wastewater samples
- General and applied microbiology
- Study design and implementation
- GC and HPLC method development and analysis
- Oral and written presentations of results and scientific meetings
- Training of distributors and salesmen
- Written and oral reports to clients
- Advising salesmen on applications

Laboratory Technician January 1997 to January 1998
TechLab Inc. Blacksburg, VA

COMPUTER SKILLS

Software: AutoCAD short course, SSSP, Lab View, Visual Basic

CERTIFICATION

Engineer in Training, Virginia

AWARDS

Best Student Paper, Virginia Water Environment Association Annual Conference, May 2001.

PROFESSIONAL ORGANIZATIONS WEF, IAWQ, ASCE